PERCEIVING THE FUTURE:

Predictive processing from the eyes to the brain

Tao He

PERCEIVING THE FUTURE:

Predictive processing from the eyes to the brain

Tao He

ISBN:

978-94-6284-272-4

Design and layout:

Wendy Bour-van Telgen, Gildeprint | www.gildeprint.nl

Print:

Gildeprint | www.gildeprint.nl

PERCEIVING THE FUTURE:

Predictive processing from the eyes to the brain

Proefschrift

ter verkrijging van de graad van doctor

aan de Radboud Universiteit Nijmegen

op gezag van de rector magnificus prof. dr. J.H.J.M. van Krieken,

volgens besluit van het college van decanen

in het openbaar te verdedigen op woensdag 2 september 2020

om 15.30 uur precies

door

Tao He

geboren op 5 september 1991

te Anhui, China

Promotor:

Prof. dr. F.P. de Lange

Manuscriptcommissie:

Prof. dr. W.P. Medendorp

Prof. dr. Li Zhaoping (Eberhard Karls Universität Tübingen, Duitsland)

Prof. dr. S. van der Stigchel (Universiteit Utrecht)

PERCEIVING THE FUTURE:

Predictive processing from the eyes to the brain

Doctoral Thesis

to obtain the degree of doctor

from Radboud University Nijmegen

on the authority of the Rector Magnificus prof. dr. J.H.J.M. van Krieken,

according to the decision of the Council of Deans

to be defended in public on Wednesday, September 2, 2020

at 15.30 hours

by

Tao He

born on September 5, 1991

in Anhui, China

TABLE OF CONTENTS

CHAPTER 1

INTRODUCTION

Visual input is the most essential information for humans. While other animals, such as dogs, primarily rely on their sense of smell, humans are undoubtedly visual beings. When we open our eyes, we are constantly bombarded with an enormous amount of visual information flowing from the eyes to the brain. However, when experiencing exactly the same physical visual stimuli in the world, people may still perceive them differently. Although the camera is commonly taken as a metaphor for human vision, there is an essential difference: our visual perception is selective and subjective whereas a camera is not. In fact, one of the most intriguing facets of visual perception is its subjective nature. By definition, visual perception is the process by which our brain rapidly makes sense of the surrounding environment from the light that is reflected by or emitted from the objects within our visual field. However, visual perception not only depends on the sensory input but also on the internal state of the brain.

Predictions are one important source that determines one's internal brain state and they reflect prior information about what is likely to occur in the environment (Summerfield & Egner, 2009). For instance, when waiting for a friend in a crowded street, we have prior knowledge about the friend's features. This type of foreknowledge can strongly modulate visual perception in many different ways. As our sensory information is often inherently ambiguous due to occlusion, different viewpoints etc., predictions can bias our perception of the world and thus disambiguate the interpretation of visual inputs (Chalk et al., 2010; Kok et al., 2013; Sterzer et al., 2008). For example, the interpretation of a given percept ('Is this a hair dryer or a drill?') can be guided by contextual probabilities ('Am I in the bathroom or in the garage?'). Accordingly, visual perception has also evolved to take advantage of these conditional probabilities via statistical learning of scene information (Fiser & Aslin, 2001).

Predictive processing is also relevant in the context of eye movements. When preparing an eye movement toward a location we are interested in, our brain must already know the vector of this saccade (e.g., direction, length) before its execution. In order to support visual stability across saccades, predictions about the eye movement and the target based on the perception of the future saccadic targets is used (Melcher, 2011). Figuratively speaking, our brain has been likened to a 'prediction machine' that actively constructs internal models to interpret incoming visual inputs with the help of top-down predictions (Clark, 2013; de Lange et al., 2018). In this

thesis, I will mainly investigate two different forms of predictability that are exploited by the visual system to aid perception. Specifically, I will focus on predictive remapping across eye movements in order to maintain visual stability and on prior context that arises from conditional probabilities.

1

BIOPHYSICS OF VISUAL PERCEPTION

How does our brain reconstruct the visual world? This process starts with the input that arrives in the eyes (**Figure 1.1**). When light passes through the pupil, the lens focuses the incoming light onto the retina. The retina is a sheet of photoreceptor cells at the back of our eyes. The photoreceptors are sensitive to light and transform it into electrochemical signals. There are two main types of photoreceptors: while cones are color sensitive, rods are sensitive to light-dark differences. These photoreceptors are packed most densely at the center of the retina, which is termed the fovea. Although the fovea occupies only a very small area of the retina (1.5 mm in diameter, corresponding to ~ 5 degrees in visual angle), it has the highest visual accuracy. This is due to the densely packed photoreceptors at the fovea. With distances further away from the center of the fovea, that is in the periphery, detail decreases progressively. Therefore, in order to clearly see the world around us, we need to keep moving our eyes. This allows us to direct the fovea toward the part of the environment we are most interested in, a process called saccades.

The optic nerve connects the eyes to the lateral geniculate nucleus (LGN) in the brain. On the way from the eyes to the brain, the visual signals also need to go through the optic chiasm. The optic chiasm is an X-shaped structure formed by the crossing of the optic nerves in the brain. At the optic chiasm, the nerve fibers from the nasal half of each retina cross over to the opposite side of the brain. Therefore, the input from the left visual field travels via the right thalamus to the right primary visual cortex (V1), and vice versa. Because of this crossing, each brain hemisphere receives visual signals from both eyes.

The fibers of the optic nerve end in the thalamus at the LGN. The LGN is a central relay station in the visual pathway from the retina to the cortex and from there the visual information is conveyed to the occipital cortex, particularly to V1. V1 performs the first step of cortical processing of visual information and is also the most studied visual area in the brain. The key function of V1 is to process visual information coming from the LGN, transform it, and then transmit the outcomes to higher visual areas (e.g., areas V2, V3, MT, MST, FEF; Maunsell & Newsome, 1987; Felleman & Van Essen, 1991) and subcortical structures (e.g., LGN, thalamic reticular nucleus, superior colliculus, pulvinar, pons). It is also believed that V1 is selective to a number of basic visual features, such as orientation, motion direction, depth, and color (Hubel & Wiesel, 1977; Livingstone & Hubel, 1988, 1987).

After V1 has processed the information it received from LGN, the processed signals leave V1 and travel via two streams to a number of areas collectively known as the extrastriate cortex. The two streams are the 'what' and the 'where' stream (Goodale, 1995; Mishkin et al., 1983; Mishkin & Ungerleider, 1982). The 'what' stream travels ventrally to the inferotemporal cortex and is responsible for object identification, whereas the 'where' stream travels dorsally to the posterior parietal cortex and is involved in locating objects in the world and in interacting with them. Moreover, the two streams are also closely connected and interact to process information in multiple brain regions.
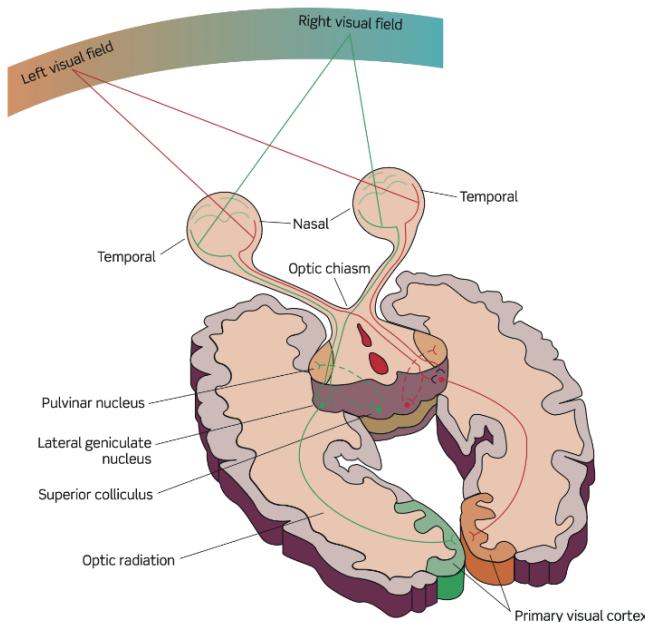

Figure 1.1. The visual pathway from the eyes to the primary visual cortex (V1). Visual information travels from the eyes via the optic chiasm to the lateral geniculate nucleus (LGN) and from there the information is passed on to V1. V1 is located at the rear end of the brain, as far away from the eyes as possible. Adapted from Snowden et al. (2011).

VISUAL STABILITY AND PREDICTIVE REMAPPING

The goal of visual perception is to yield accurate information about the world around us in order to guide our actions. Yet, our sensation is often incomplete due to eye movements. Humans normally make about 150,000 saccades every day, meaning around three saccades per second (Fafrowicz et al., 2012; Rayner, 1998). Saccades can direct the most sensitive part of the retina, the fovea, toward the locations we are most interested in, but at the same time visual objects in the world dramatically change their position on the retina after each saccade. Nevertheless, our perception of the world is stable and continuous and we rarely feel disoriented. This gives rise to a very important question: How do we perceive a stable visual world despite the constantly changing inputs from the visual system? Or put differently: how do we keep track of objects across eye movements in order to maintain spatial constancy?

At the moment, there are mainly two broad categories of hypotheses concerning this question. The first set of hypotheses posits a spatiotopic map within the brain that is updated after every eye movement. Specifically, they assume that our brain uses a world-centered instead of an eye-centered representation for visual perception and action. This world-centered map is located at higher areas in the brain. With every saccade, the changed retinal image is integrated into this map and thus our perception of the visual world remains stable across eye movements (Melcher & Morrone, 2003). However, the existence of such a spatiotopic map for continuity in perception has been challenged (e.g., Wurtz, 2008). First, a world-centered map as well as the eye position signal required for updating this map have not been identified in the brain. Second, results from change blindness studies argue against the existence of a world-centered map. If there was a world-centered map of the whole visual field, that was independent of the current retinal image and available at all times, then why would salient changes still be missed (O'Regan & Noë, 2001; Simons & Rensink, 2005)?

The second group of hypotheses does not posit a higher-order spatial map in the brain. Instead, the representation of the visual world always remains in retinotopic coordinates. One of the famous theories under these hypotheses is the *shifting receptive fields theory*. In their landmark study, Duhamel et al. (1992) showed that neurons in the parietal cortex had the remarkable property of shifting the location of their visual sensitivity in anticipation of the

upcoming saccade. As an example and illustrated in **Figure 1.2**: when you are initially looking at the kite in the figure and we record from a neuron in your brain, then this neuron is only sensitive to a small region around the kite, called its receptive field (RF, **Figure 1.2**). Next, you are planning to move your eyes from the kite to the boy's head, which will then become the RF after the eye movement. Thus it is called the future field (FF, **Figure 1.2**). Intriguingly, even before saccade onset, the sensitivity of the recorded neuron in FF already increases simply because you are planning a saccade toward its location. In other words, neurons can not only respond to stimuli in their current RF during fixation, but also to stimuli in their FF when you are planning an eye movement. This anticipatory change has been referred to as shifting receptive fields. To do so, these neurons must have information about the amplitude and direction of the impending saccade. However, the term shifting receptive field seems to be somewhat misleading as it suggests that the neurons shift their RF from one location to another. According to our understanding, it is only the response activity rather than the RF that is transferred between the current and future fields.
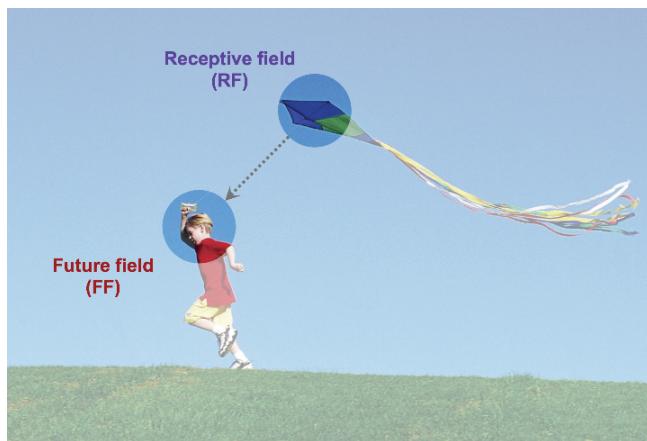
Figure 1.2. The logic of shifting receptive fields. Receptive field (RF) and future field (FF) around the onset of an eye movement. The dashed arrow indicates the saccade direction. The neural sensitivity in FF, where the RF will be after the saccade, increases even before we move our eyes, which is considered as the shifting receptive field.

It has also been proposed that visual stability is achieved by predictive remapping of attention rather than the shifting of receptive fields (Cavanagh et al., 2010a). Here, predictive remapping means that the so-called 'attentional pointer' is updated across saccades. The

attentional pointer can be understood as the activity in priority maps, comprised of the lateral intraparietal area (LIP), the frontal eye fields (FEF) as well as the superior colliculus (SC). The priority map is a top layer that is organized in the visual system. It integrates bottom-up saliency with the current top-down behavioral relevance of the scene, thus tightly linked to the preparation of goal-directed eye movements (Fecteau & Munoz, 2006). Right before we make a saccade, the target location becomes more salient in the priority map. Then a feedback signal is sent back from the priority maps to the lower feature maps, consisting of V1 - V4 and middle temporal (MT) areas, guiding spatial attention. Therefore, under this account attention instead of features becomes the most important information for tracking objects and maintaining visual stability (Rolfs, 2015). However, it is still an ongoing debate whether and how feature information of visual objects is remapped across saccades. I focus on this question in **Chapter 2**.

VISUAL WORKING MEMORY

Visual working memory (VWM) refers to the ability to temporarily maintain relevant information that is no longer present in the sensorium. Working memory's two key properties are its flexibility and limited capacity. It is flexible enough to represent novel combinations of visual features but limited in storage to only a few chunks of information at once (Adam & Serences, 2019). Many researchers have shown that VWM information is represented in higher-order brain regions, including parietal (Christophel et al., 2015; Ester et al., 2015; Bettencourt & Xu, 2016) and prefrontal cortex (Durstewitz et al., 2000), as well as in early visual areas (Albers et al., 2013; Ester et al., 2009; Harrison & Tong, 2009; Rademaker et al., 2019). More specifically, detailed feature information of visual objects (e.g., orientation) can be read out from early visual cortex using functional magnetic resonance imaging (fMRI) and multivariate pattern analysis (MVPA), pointing to an important role of this region in representing WM contents. Recent studies, however, provided evidence against the central role of early visual cortex in VWM storage in the human brain (Bettencourt & Xu, 2016), as they found impaired decoding accuracy in early visual cortex when distractors were presented during the delay period. Therefore, this remains a topic of active debate.

As described in the previous paragraph, our visual system can not only process incoming sensory information that is present in our visual field, but may also be relevant for maintaining information in VWM. In our daily life, VWM is typically dynamic and fragile: we often need to keep an item in mind, while at the same time receiving new visual input from the environment. For instance, when you look for a key in your apartment, you need to maintain a mental image of the key while simultaneously and continuously moving your eyes toward different search locations. Currently, the impact of eye movements on VWM representations in early visual areas and beyond is unclear. On the one hand, VWM contents could be remapped predictively before making an eye movement, using the same mechanism as for the predictive remapping of attention or features of visual objects. On the other hand, given that the function of VWM is to temporarily store information, working memory information might not be remapped following eye movements. In **Chapter 3**, I look into this question using fMRI and MVPA.

1

PREDICTIONS IN VISUAL COGNITION

Visual perception is an active process. Our brain not only passively receives information from the environment, but also actively predicts future input by extracting statistical regularities in its inputs. Statistical regularities in our environment are ubiquitous (de Lange et al., 2018; Girshick et al., 2011). For instance, cardinally oriented (i.e., horizontal and vertical) lines are more prevalent than oblique ones or a thunder always follows a flash of lightning. These relatively stable physical features of the world allow us to form prior expectations. However, although our environment is full of these temporal as well as spatial statistical regularities, learning is often an implicit process – we rarely have the feeling that we are explicitly learning these statistical regularities.

As human agents implicitly learn and extract structure from the environment, this implicit knowledge allows to predict future sensory input. These predictions play an important role in modulating sensory representations. At the neural level, a number of studies have demonstrated that predictions can reduce the blood-oxygen-level-dependent (BOLD) response in early sensory areas (Egner et al., 2010; Kok et al., 2012; Summerfield et al., 2008; Summerfield & de Lange, 2014) as well as the amplitudes of event related fields (ERFs) and gamma band power (Todorovic et al., 2011), although the specific nature of these effects is still under debate. In particular, under the 'sharpening' hypothesis, expected stimuli lead to attenuated neural activity because our brain only uses the more efficient and selective neurons to represent the current stimulus. Thus, a sharpened representation occurs for expected stimuli, although the overall neural activity is reduced (Kok et al., 2012). Alternatively, the reduced neural activity could be caused by less surprise for expected compared to unexpected stimuli, as our brain filters out the expected components of sensory inputs, which is referred to as the 'dampening account' (Kumar et al., 2017).

Although many studies have shed light on the role of predictions and the learning of *temporal* statistical regularities, few studies have examined statistical learning across *space*, especially at the neural level. It is known that different sensory modalities can bias processing toward different aspects of the forthcoming input. For instance, vision is inherently organized in a spatial manner (i.e., retinotopically), while audition deals with extracting meaning from

temporally organized inputs (Kubovy, 1988). Hence, for visual stimuli, we would expect that spatial expectations are stronger compared to temporal expectations. In **Chapter 4**, I investigate this question in detail.

1

OUTLINE OF THE THESIS

In this thesis, I examined how different forms of predictability are exploited by the visual system to facilitate vision and visual cognition.

In **Chapter 2**, I focused on visual predictions of future input that are thought to be generated automatically in anticipation of eye movements (i.e., predictive saccadic remapping). I investigated whether and how feature information of visual objects was remapped across saccades. Specifically, I used the tilt aftereffect (TAE), where prolonged exposure to a stimulus (the adaptor) results in a perceptual shift of a test stimulus away from the adaptor. This is a sensitive method to address the question of feature remapping. Earlier research proposed that only the attentional pointers and not the feature information itself can be predictively remapped across saccades (Rolfs et al., 2011). By linking the attentional pointers at the current and future retinotopic locations around the time of an eye movement, the feature information at these two distinct locations is pooled together in a hierarchically higher priority map. Furthermore, I examined whether the stimulus or the adaptation itself is predictively remapped. Although several previous studies have demonstrated the predictive feature remapping effect, it is still unclear what is supposed to be remapped prior to an eye movement: the adaptor (the state of adaptation), the test stimulus, or both. Finally, I explored whether predictive remapping of features also occurs for stimuli outside of the saccadic target. This allowed us to differentiate between different forms of remapping (i.e., forward versus convergent remapping), as earlier research has provided opposite results concerning this point.

In **Chapter 3**, I also examined remapping – not of anticipated visual input but instead of internally stored visual working memory representations. We have demonstrated that feature information of visual objects can be remapped across eye movements (**Chapter 2**). However, it is still unclear whether saccadic remapping also occurs for stimuli that are not present in our visual field but maintained in working memory. This is also a common situation in daily life. For instance, we have to keep a friend's appearance in mind while constantly moving our eyes toward different locations when looking for the friend at a train station. Moreover, I asked whether eye movements degrade VWM representations in visual cortex. Previous studies showed that WM content can be robustly maintained in higher brain areas (parietal cortex), but distractors

during the working memory period significantly interfere with storage in early visual cortex. However, it is unknown whether eye movements would also impair the WM representations in early visual cortex. To this end, I directly compared the content of VWM between saccade and no-saccade conditions using MVPA of the delay-related response measured with fMRI.

In **Chapter 4**, I investigated the effects of a different form of predictability on visual processing, namely prior context. Context can be defined both temporally (e.g., the red light is followed by the green light in a traffic light) and spatially (e.g., a table lamp is next to a computer monitor on the desk). In this chapter, I directly investigated the effects of spatial and temporal context on perception. Although we already know that expectations can modulate neural responses in the brain with expected stimuli leading to an attenuated neural response, this expectation suppression has not yet been studied at the neural level for spatial regularities. Almost all previous studies used temporal regularities to investigate expectation suppression. More specifically, researchers often present successive stimuli, where a certain leading stimulus is followed by a specific trailing stimulus, thus leading to temporal expectations. Nevertheless, for visual conditions, participants appeared to best extract statistical patterns when the input was presented in a spatial rather than a temporal context. In this chapter, I set out to explore the existence and the characteristics of spatial expectation suppression. I indeed found that there is significant spatial expectation suppression throughout the ventral visual stream. Moreover, the regions exhibiting spatial expectation suppression partly overlap with those showing an effect of temporal violations, suggesting commonalities in the underlying neural codes for temporal and spatial expectation suppression.

Finally, in **Chapter 5**, I summarized all the empirical findings and discuss their relevance for our understanding of predictions in the brain. The thesis finally concludes with a general discussion about the implications of the presented research.

CHAPTER 2

PREDICTIVE REMAPPING OF VISUAL FEATURES

BEYOND SACCADIC TARGETS

ABSTRACT

Visual stability is thought to be mediated by predictive remapping of the relevant object information from its current, pre-saccadic locations to its future, post-saccadic location on the retina. However, it is heavily debated whether and what feature information is predictively remapped during the pre-saccadic interval. Here, we examined the spatial and featural properties of predictive remapping in a set of three psychophysical studies. We made use of an orientation adaptation paradigm, in which we induced a tilt aftereffect (TAE) by prolonged exposure to an oriented adaptor stimulus. Following this adaptation phase, a test stimulus was presented shortly before saccade onset. We found strong evidence for predictive remapping of the features of this test stimulus presented shortly before saccade onset, evidenced by a large TAE elicited when the adaptor was positioned at the post-saccadic retinal location of the test stimulus. Conversely, the adaptation state itself, caused by the exposure to the adaptor stimulus, was not predictively remapped. Furthermore, we establish that predictive remapping also occurs for stimuli that are not saccade targets, pointing toward a 'forward remapping' process operating across the whole visual field. Together, our findings suggest that predictive feature remapping of object information plays an important role in mediating visual stability.

This chapter has been published as:

INTRODUCTION

Each time we move our eyes, the image of objects in the world shifts its position on the retina, yet our perception is remarkably stable. Previous research revealed that predictive remapping could contribute to this visual stability. Predictive remapping refers to the phenomenon that neurons become active in response to stimuli outside their receptive fields (RFs) shortly before a saccade moves their receptive fields onto the stimulated regions (Duhamel et al., 1992). Predictive remapping has been demonstrated in many cortical regions, such as the lateral intraparietal area (LIP) (Duhamel et al., 1992), the frontal eye field (FEF) (Goldberg & Bruce, 1990; Umeno & Goldberg, 1997), superior colliculus (SC) (Walker et al., 1995), and early visual cortex including V2, V3 and V3a (Nakamura & Colby, 2002) and has been shown to depend on the intention to execute eye movements rather than shifting covert attention alone (Colby, 1996). Predictively increasing activity of visually responsive neurons in these areas according to postsaccadic stimulus information could facilitate the processing of visual information across saccades, which is crucial for achieving perceptual stability.

Although predictive remapping has been widely studied, there is an ongoing debate regarding the issue whether and how feature information of visual objects is remapped during this process (Cavanagh et al., 2010b; Ezzati et al., 2008; Harrison et al., 2013; He et al., 2017; Lescroart et al., 2016; Mayo & Sommer, 2010; Melcher, 2005, 2007, 2010; Pelli & Cavanagh, 2013; Zimmermann et al., 2017; Zirnsak & Moore, 2014). On the one hand, several psychophysical studies suggest that visual feature information, such as orientation and letter information, is transmitted around the time of a saccade (Harrison et al., 2013; He et al., 2017; Melcher, 2007). Furthermore, previous studies suggest that foveal and peripheral feature information are integrated across saccades in a statistically optimal manner, which might rely on predictive feature remapping (Ganmor et al., 2015; Hübner & Schütz, 2017; Wolf & Schütz, 2015). More specifically, it is suggested that relevant features of a test stimulus, which are extracted before the saccade, are transferred to their postsaccadic retinal location based on the computation of the saccade vector. On the other hand, Rolfs et al., (2011) proposed that it is merely the attentional pointers, but not the feature information, that are predictively remapped across saccades. By linking the attentional pointers at the current and future retinotopic locations together, the feature

information at these two distinct locations is combined at higher processing stages.

The tilt aftereffect (TAE), in which prolonged exposure to a stimulus (the adaptor) results in a perceptual shift of a test stimulus away from the adaptor is a sensitive method to address the question of feature remapping (Knapen et al., 2010; Melcher, 2007). Namely, orientation feature integration between the pre- and post-saccadic location can be inferred from observing a TAE. There has been considerable confusion however concerning *what* is supposedly remapped prior to executing a saccade. Specifically, it is unclear whether the adaptor (or the state of adaptation, induced by the adaptor stimulus), the test stimulus, or both, is remapped (see **Figure 2.1C** and **2.1D**). Moreover, the spatial properties of remapping are a current topic of debate. In particular, it is not clear whether receptive fields are shifted to their postsaccadic location (forward remapping; Biber & Ilg, 2011; Dorr & Bex, 2013; Duhamel et al., 1992; Melcher, 2007), or toward the saccade target (convergent remapping; Zirnsak & Moore, 2014; Zirnsak, et al., 2014). Since in most of the previous studies the probe location coincided with the saccade target location, these previous studies are unable to differentiate between convergent and forward remapping effects, and more recent studies that aimed to dissociate these effects provided conflicting results (Neupane et al., 2016a; Zirnsak et al., 2014). Interestingly, in a behavioral study by Zirnsak et al. (2011), in which probe and saccade target location were dissociated, the authors reported evidence for convergent remapping and no evidence for forward remapping. However, this result was based on a small sample (N=3), which limits the inferences that can be drawn (Button et al., 2013), and the test location for forward remapping was located far in the periphery of the visual field, potentially abolishing a forward remapping effect. Consequently, further investigations about the presence of forward and/or convergent remapping effects are necessary.

In the current study, we investigated whether stimulus orientation is predictively remapped, and whether adaptation itself is remapped, as has been suggested before. Further, we examined whether presaccadic remapping also occurs for non-saccade targets, in order to distinguish between forward and convergent remapping. To this end, we made use of the orientation adaptation paradigm to test the TAE at each critical location, e.g., the initial fixation location, the saccade target location and the future retinotopic location of the adaptor. To

preview, we found predictive feature remapping of the test stimulus when presented shortly before a saccade, in line with Melcher (2007). Remapping occurred irrespective of whether they are a saccade goal, suggesting that the visual system employs forward predictive remapping of features.
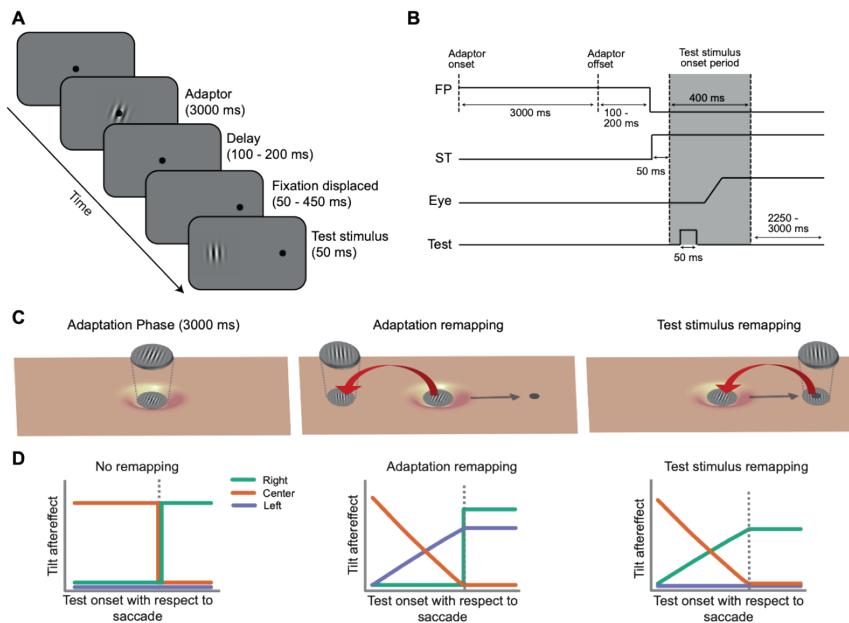

Figure 2.1. Experimental design and hypotheses. A) Experimental design. An adaptor was first presented at the initial fixation location for 3 s. After a random delay period, participants were asked to make a horizontal eye movement to the saccade target following the shift of fixation (black dot). Immediately after the presentation of test stimulus, participants were asked to report whether the test stimulus was tilted to the left or right relative to vertical. The test stimulus could appear at one of three locations (left, center, or right) and could appear before or after saccade onset. **B)** Time course of a trial. The grey area denotes the time period during which a test stimulus could be presented (before, during or after a saccade). Trials on which a test stimulus was presented during the saccade were removed prior to the analysis. FP, fixation point; ST, saccade target. **C)** Left: Adaptation effect. After a prolonged exposure to the adaptor, the neural population that is sensitive to the location of the adaptor becomes adapted (the "hole" in the figure). Middle**:** Adaptation remapping hypothesis. Upon preparing a rightward saccade (grey arrow), the adaptation is remapped to its anticipated postsaccadic location. As a consequence, in this example a TAE is expected at the left location. Right**:** Test stimulus remapping hypothesis. Upon preparing a rightward saccade (grey arrow), the test stimulus is remapped to its anticipated postsaccadic location. As a consequence, in this example a TAE is expected at the right location. **D)** The expected pattern of results under conditions of no remapping (left column), adaptation remapping (middle column) and test stimulus remapping (right column).

METHODS

The current study consisted of three experiments. In the first experiment we tested whether predictive feature remapping occurs for stimuli that are saccade targets and whether adaptation itself would remap. In the second experiment we tested whether predictive feature remapping similarly occurs for peripheral stimuli that are not saccade targets. The third experiment acted as a control experiment to further corroborate the results of Experiment 1 and 2.

Participants

A total of 72 subjects participated in three experiments, engaging in a total of 82,080 trials. Each experiment had 24 subjects (Exp.1: 11 females, mean age 23.6 years, range from 19 to 43 years; Exp.2: 16 females, mean age 22.8 years, range from 18 to 30 years; Exp.3: 15 females, mean age 24.4 years, range from 20 to 34 years). The sample size was based on an a priori power calculation, computing the required sample size to achieve a power of 0.80 to detect an effect size of Cohen's $d \geq 0.6$, at alpha $= 0.05$ for a within-subject comparison. All participants reported normal or corrected-to-normal vision, and were naive with respect to the purposes of the study. Participants were recruited from the institute's subject pool in exchange for either monetary compensation or study credits. The experiments were approved by the Radboud University Institutional Review Board and were carried out in accordance with the guidelines expressed in the Declaration of Helsinki. Written informed consent was obtained from all participants prior to the start of the study.

Apparatus

All stimuli were generated with custom scripts written in Python (Python Software Foundation. Version 2.7. Available at http://www.python.org) and were presented on a 24-inch flat panel display (BenQ XL2420T, resolution 1920 x 1080, refresh rate: 60Hz). The visible area of the display measured $48° \times 27°$ visual degrees at a viewing distance of about 64 cm. The participants' head position was stabilized with a chin rest. Eye movements were monitored by an Eyelink 1000 plus (SR Research®) eye-tracker, sampling at 1000 Hz. Only the right eye was recorded. Saccade initiation was detected online, with a velocity threshold of 30°/s and an

acceleration threshold of 8000°/s². A 9-point calibration and validation procedure was conducted at the beginning of each block.

Stimuli and Experimental Design

Experiment 1. Participants were tested in a quiet and dimly lit laboratory. Each trial began with the presentation of a fixation dot at the center of the screen. This fixation dot also served as the drift-correction target and remained visible until the participant's gaze was within 1 visual degrees of it and the space bar was pressed. The sequence of events and time course in a single trial is illustrated in **Figure 2.1A** and **2.1B**.

After the initiation of the trial a black fixation dot (diameter = 0.4°) and an oriented Gabor patch (oriented +20° or -20° relative to vertical) were presented at the center of the screen against a uniform mid-gray background for 3 seconds. The Gabor patch consisted of a sinusoidal wave grating (spatial frequency = 2 cycles/°; phase = 0.25; contrast = 1.0), windowed by a Gaussian envelope (SD 1.67°). Participants were asked to fixate the dot until it disappeared. After 3 seconds, the Gabor patch disappeared and participants continued maintaining fixation at the central dot for a 100 – 200 ms delay. After the delay, the fixation dot was horizontally displaced to the left or right side of the screen (8 visual degrees), which served as a cue for participant to make a saccade to the new fixation location. A test stimulus (Gabor stimulus with one of five orientations: -2°, -1°, 0°, 1°, 2°) was then flashed briefly at one of three locations (left, center or right) for 50 ms. In the subsequent data analysis, we pooled the data for left- and rightward saccades (no difference, all p > 0.12), expressing all data in the reference frame of the rightward saccade condition. In this reference frame, the right test stimulus location corresponds to the saccade target location, the center test stimulus location corresponds to the initial fixation location and the left test stimulus location corresponds to the future, postsaccadic retinotopic location of the adaptor. Crucially, the onset of the test stimulus varied in the range of 50 – 350 ms after the displacement of the fixation dot, such that it could occur either before or after the onset of the saccade, given that human saccade latency is estimated to lie around 200 ms (Robinson, 1964). The participant's task was to indicate whether the test stimulus was tilted to left or right with respect to vertical, regardless of its location.

Participants completed 3 sessions of the task, comprising a total of 1260 trials. There were 210 trials for each combination of the two adaptor tilt orientations and three test stimulus locations. If the participant's gaze deviated more than 2° from the central fixation dot during the adaptation period, or landed at a location that was more than 2° away from the saccade target, auditory and visual feedback was given and the trial was aborted. All aborted trials were discarded and retested in a random order, until all trials were completed successfully.

Experiment 2. In order to test whether predictive feature remapping also occurs for stimuli that are not saccade targets, we repeated Experiment 1, but presented both adaptor and test stimulus 4° above fixation. Consequently, the test stimulus was never a saccade target. In addition, as Experiment 1 yielded no evidence of adaptor remapping prior to a saccade, we did not test for remapping at the future retinotopic location of the adaptor in this experiment.

The trial sequence in Experiment 2 was identical to Experiment 1. Each trial began with the presentation of an oriented Gabor patch 4° above central fixation. Participants were next asked to move their eyes to the periphery following the shift of the fixation dot. The test stimulus was flashed 4° above the initial fixation location or the saccade target location to measure transfer of feature information between these two locations. Experiment 2 consisted of 2 sessions. For each combination of the two test stimulus locations and adaptor tilt orientations 270 trials were collected, resulting in a total of 1080 trials.

Experiment 3. In Experiment 3, the task was similar to Experiment 1, except that two oppositely oriented adaptors were presented simultaneously at the two peripheral locations. In a given trial, participants initially fixated at the center of the screen, while two oppositely oriented Gabor patches (either +20°/-20° or -20°/+20° from vertical) were presented simultaneously for 3 seconds, 8° left and right of the center of the screen. Next participants were prompted to move their eyes to the left or right peripheral location, following the shift of the fixation dot. The test stimulus was either flashed at the initial fixation location or at the saccade target location. Experiment 3 consisted of 2 sessions. For each combination of the two test stimulus locations and adaptor tilt orientations 270 trials were collected, resulting in a total of 1080 trials.

The logic behind Experiment 3 is as follows. Imagine a trial in which the participant performs a saccade from the center to the right peripheral location. Under the forward remapping hypothesis, receptive fields are expected to shift in the rightward direction, parallel to the saccade vector. Note that this is equivalent to remapping feature information in the direction opposite to the saccade vector. Therefore, a test stimulus that is centrally presented prior to the saccade would be remapped to the left peripheral location. Under the convergent remapping hypothesis, receptive fields are remapped towards the saccade target. Therefore, a test stimulus that is centrally presented, far away from the saccade target, would not be remapped to the left peripheral location, and no TAE is expected.

Data Analysis

All data analyses were performed with MATLAB (R2016a. Natick, Massachusetts: The MathWorks Inc., 2016.) using the Palamedes Matlab toolbox for fitting psychophysical data (Prins & Kingdom, 2018). The significance threshold was set to 0.05. All data and code are available from Donders Institute for Brain, Cognition and Behavior Repository at https://hdl. handle.net/11633/di.dccn.DSC_3018034.01_694.

Outlier Criteria

Experiment 1. A total of 37,114 trials were obtained for experiment 1. Only successfully completed trials were considered in the further analyses. We excluded a trial from the analyses if a) fixation was broken before fixation displacement (7.75% of all trials), or b) the participant did not execute the required eye movements or missed the displaced fixation dot by more than 2° (10.87% of all trials). In the remaining trials, saccade latency was defined as the temporal distance between the onset of the fixation dot displacement and the initiation of the saccade that followed. Trials with saccade latencies shorter than 90 ms (0.23%) or longer than 500 ms (1.04%) were excluded. We also excluded trials whose response time was < 200 ms (0.3%) or more than 3 standard deviations above the subject's mean response time (1.27%). Finally, trials in which the test stimulus was presented during the execution of the saccade were also excluded (15.71%). In total, 24,692 (81.55%) trials were included in the analysis.

Experiment 2. A total of 34,770 trials were obtained for Experiment 2. We excluded trials from further analyses if a) fixation was broken before fixation displacement (9.62%), or b) the participant did not execute the required eye movements or missed the displaced fixation dot by more than 2° (16.19%). Of the remaining trials, trials in which the saccade latency was < 90 ms (0.07%) or > 500 ms (1.04%) were excluded. We also excluded trials in which the button response time was < 200 ms (1.34%) or more than 3 standard deviations above the subject's mean response time (1.08%). Finally, the trials in which test stimulus was presented during the saccade period were also excluded (16.75%). Together, 20,593 (79.83%) trials were included in the analysis.

Experiment 3. A total of 32,792 trials were obtained for Experiment 3. We excluded trials from the analyses if a) fixation was broken before fixation displacement (11.47% of all trials), or b) the participant did not execute the required eye movements or missed the displaced fixation dot by more than 2° (9.42% of all trials). Of the remaining trials, trials with saccade latencies shorter than 90 ms (0.07%) or longer than 500 ms (1.90%) were excluded. We also excluded trials whose response time was < 200 ms (5.32%) or more than 3 standard deviations higher than the subject's mean response time (0.78%). Finally, trials in which test stimulus was presented during the execution of the saccade were also excluded (14.87%). In total, 20,820 (80.26%) trials were included in the analysis.

Quantification of Time Bins

To plot the TAE magnitude as the function of time, we first separated all trials into two bins at the group level: one bin contained all trials in which the test stimulus was presented before saccade onset, whereas the other bin contained all trials in which the test stimulus was presented after saccade offset. Trials in which the test stimulus was presented during the saccade were removed. For both bins, the trials were then further subdivided into two time bins by a median split with respect to the test stimulus onset times, respectively. Trials with an onset time that was equal to the median were assigned to the later time bin. This resulted in a total of four time bins. We used four time bins to maximize the trials numbers in each time point and condition to be able to reliably fit the psychometric functions. In Experiment 1, the total number of trials were 5715, 5801, 6531, and 6582 in each time bin. Mean test stimulus onset time with

respect to saccade onset (for pre-saccadic trials) or saccade offset (for post-saccadic trials) was -133 ms (SD 73 ms), -31 ms (SD 17 ms), 36 ms (SD 21 ms), and 115 ms (SD 28 ms) for each time bin, respectively. In Experiment 2, the total number of trials was 5016, 5075, 5213, and 5289 in each time bin. Mean test stimulus onset time was -117 ms (SD 63 ms), -29 ms (SD 17 ms), 32 ms (SD 18 ms), and 104 ms (SD 26 ms) for each time bin, respectively. In Experiment 3, the total number of trials was 6049, 6089, 4320, and 4362 in each time bin. Mean test stimulus onset time was -156 ms (SD 68 ms), -38 ms (SD 22 ms), 29 ms (SD 17 ms), and 97 ms (SD 26 ms) for each time bin, respectively.

In order to follow up on the time course of pre-saccadic predictive remapping, we further split the trials with test stimuli presented before saccade onset into four narrower time bins to quantify the time course of remapping in more detail. For this analysis, we took the three quartiles instead of the median for defining the boundaries of the time bins. As a result, in Experiment 1, the total number of trials were 2850, 2865, 2916, and 2885 in each time bin. Mean test stimulus onset time with respect to saccade onset was -189 ms (SD 66 ms), -77 ms (SD 11 ms), -45 ms (SD 9 ms), and -16 ms (SD 9 ms) for each time bin, respectively. In Experiment 2, the total number of trials was 2484, 2532, 2530, and 2545 in each time bin. Mean test stimulus onset time was -159 ms (SD 67 ms), -75 ms (SD 10 ms), -44 ms (SD 8 ms), and -15 ms (SD 8 ms) for each time bin, respectively. In Experiment 3, the total number of trials was 3029, 3020, 2981, and 3108 in each time bin. Mean test stimulus onset time was -210 ms (SD 58 ms), -103 ms (SD 18 ms), -58 ms (SD 11 ms), and -20 ms (SD 11 ms) for each time bin, respectively.

Quantification of Tilt Aftereffect

In order to quantify TAE magnitude, we fitted psychometric functions to the pooled group data. Fitting the pooled group data was preferred over fitting single subject data due to the limited amount of trials per condition in each subject. First, for each test stimulus location x adaptor tilt combination in each time bin, we expressed the proportion of "rightward" responses as a function of the test stimulus orientation with respect to vertical. For convenience, the leftward saccade trials were first collapsed with rightward saccade trials in each bin. Subsequently, we fitted cumulative normal distribution functions to this data. The point of subjective equality (PSE) was defined as the midpoint of the psychometric function, at which the test stimulus was

perceived equally often as tilted to the right and left. The magnitude of TAE was then measured as half of the difference between the PSE of the leftward and rightward tilted adaptor conditions, for each time bin and each test stimulus location separately. In experiment 3, two adaptors were presented simultaneously. The TAE for test stimuli presented at the initial fixation location (center) was always calculated with respect to the orientation of the adaptor that was opposite of the saccade target, whereas the TAE for test stimuli presented at the saccade target location was calculated based on the adaptor at the saccade target location.

Statistical Analyses

We used permutation tests to statistically compare: 1) differences of TAEs between time bins (before saccade), and 2) the interaction effect between locations (incorporating the initial fixation and the future saccade target location only) and the time bins (two time bins before eye movement) at the group level. First, to test for differences in TAEs between time bins, the condition labels of the first and second time bin of each participant were randomly shuffled. The resulting permutation group data was fitted with cumulative normal functions and was used to compute the difference in TAE between the time bins. This procedure was repeated 10,000 times. As p-values we report the proportion of permutations that led to an equal or more extreme TAE difference than the one we observed in the experiment. The exchangeability requirement for permutation tests is met, because under the null hypothesis of no difference in TAE between the first and second time bin, the condition labels are exchangeable. Second, in order to test for an interaction effect between locations and time bins, we first computed the differences of TAEs between initial fixation and saccade target location at each time bin, and then randomly shuffled the time bin labels of those differences for each participant. The exchangeability requirement for permutation tests is met, because under the null hypothesis of no interaction effect between locations and time bins, the TAE differences between locations should not be influenced by the time bin factor, and therefore the time bin labels are exchangeable. Again, this procedure was repeated for 10,000 times. As p-values we report the proportion of permutations that led to an equal or more extreme outcome than the one we observed in the experiment.

RESULTS

We collected psychophysical data in a series of three experiments, each employing 24 human participants. In total, we recruited a sample of 72 participants and 82,080 trials.

Selective remapping of future target stimuli but not adaptation

Our first aim was to test whether the test stimulus or adaptation is remapped. To this end, we compared the temporal profile of the TAE for test stimuli presented at the saccade target location, initial fixation location and future, postsaccadic retinotopic location of the adaptor. Specifically, when a test stimulus was presented well before the saccade initiation (**Figure 2.2**, first column), we found that the perceived orientation of the test stimulus at each location was systematically biased away from the adaptor stimulus that was previously presented at the center of the screen (**Figure 2.2**). This repulsive bias, which is well known as the tilt-aftereffect (TAE) in orientation perception, was quantified as the difference in the point of subjective equality (PSE) between a left-tilted and right-tilted adaptor (illustrated as the black bar between the psychometric curves). It was strongest when the test stimulus was presented at the initial fixation (center) location (middle row), where the adaptor had been presented, and markedly reduced but still present at the other two locations. We next investigated if, when, and where the TAE was transferred shortly before subjects initiated a saccade. We found that shortly before an eye movement, the TAE was significantly reduced at the future retinotopic location of the adaptor (**Figure 2.2**, "FRA" location, violet lines, comparison between first and second time point: $p = 0.0165$). Also at the initial fixation location, the TAE was reduced before an eye movement (**Figure 2.2**, "IF" location, orange lines, comparison between first and second time point: $p = 0.0039$). However, the TAE at the future saccade target location was significantly enhanced before the onset of the saccade (**Figure 2.2**, "ST" location, green lines, comparison between first and second time point: $p < 0.0001$). This opposite behavior over time between the locations resulted in a significant ($p = 0.0002$) interaction between target location (initial vs. future saccade location) and time (first vs. second time bin), showing that TAE increased at the future saccade target location and decreased at the initial location.
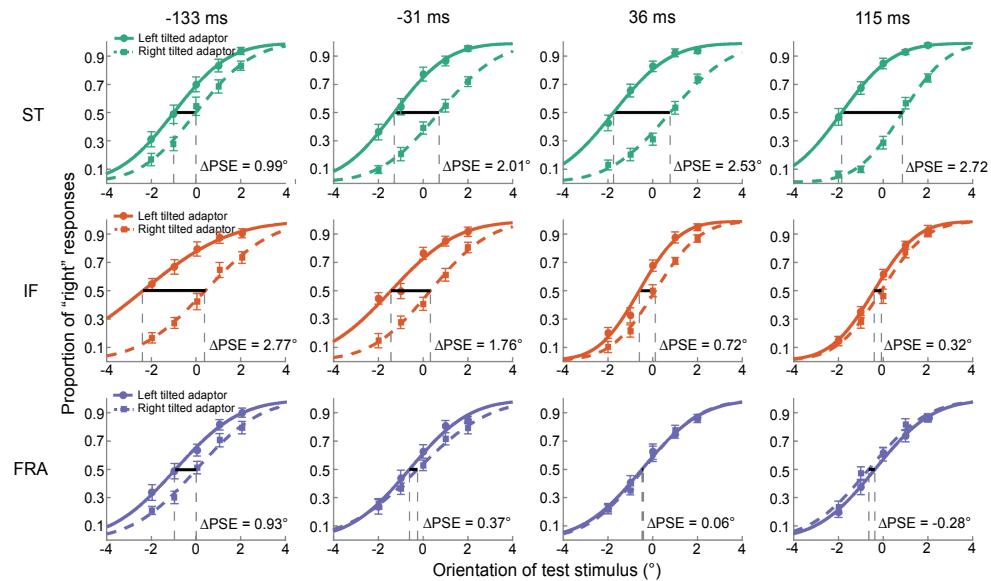
Figure 2.2. Psychometric curves for orientation judgements in Experiment 1. The number above each column represents the mean test stimulus onset relative to saccade onset (first and second columns) or offset (third and fourth columns) for each time bin. The labels of "ST", "IF" and "FRA" in the left of each row represent the three different test stimulus locations. ST: Saccadic target location, IF: Initial fixation location, FRA: Future retinotopic location of adaptor. For each panel, we plotted the percentage of a "right" response (y axis) as a function of the orientation of a test stimulus (x axis) for each time bin and location. the positive x values mean the test stimulus was tilted more clockwise while the negative x values mean more countclockwise relative to vertical. The black lines indicate that the difference between the point of subjective equality (PSE, the angle in which participants judge a test stimulus was oriented left or right equally) of the leftward (solid line) and rightward (dashed line) tilted adaptor conditions, the value of tilt aftereffect (TAE) was defined as the half of ∆ PSE.

These results are consistent with, and extend, those reported by Melcher (2007). When the test stimulus was presented at the saccadic target location, the features of the test stimulus were predictively remapped to the presaccadic foveal location, that was previously adapted. Importantly, however, we found no TAE at the future postsaccadic location of the adaptor, to which the adaptation would be hypothetically remapped. Put simply, it is the orientation feature information of a stimulus that is presented shortly before the saccade, but not a previously seen adaptor and its consequences, that is predictively remapped before saccade onset.

Selective remapping of non-saccade targets

In Experiment 1, we observed predictive feature remapping of the test stimulus towards its post-saccadic location. However, since in this crucial condition the test stimulus was always a saccade target, we cannot differentiate between a mechanism that remaps stimuli towards the saccade target (convergent remapping) and one that more generally remaps stimuli across the visual field to their post-saccadic locations (forward remapping). In order to test whether remapping also occurs for non-saccade targets, we flashed both the adaptor and test stimulus 4° vertically above fixation. The idea behind this design is straightforward: If predictive remapping only occurs for saccade targets, we would expect no TAE when the test stimulus is presented 4° above the fixation target. However, if predictive remapping also occurs for stimuli that are not saccade targets, an increase of TAE for peripherally presented test stimuli should be observable during the pre-saccadic period.

Despite the fact that different locations were used for the adaptor and the test stimulus, we found a similar pattern of results as in Experiment 1. Specifically, before an eye movement, the TAE was significantly increased at the future target location (**Figure 2.3**, "PT" location, green lines, comparison between first and second time point: $p = 0.0068$). However, the TAE at the adaptor stimulus location was decreased for the second compared to the first time bin (**Figure 2.3**, "AS" location, orange lines, comparison between first and second time point: $p = 0.0197$). This opposite behavior over time between the locations also resulted in a significant ($p = 0.0019$) interaction between test stimulus location (adaptor stimulus vs. future target location) and time (first vs. second time bin). This result suggests that predictive remapping likewise occurs for stimuli that are not saccade targets, consistent with a forward remapping account.
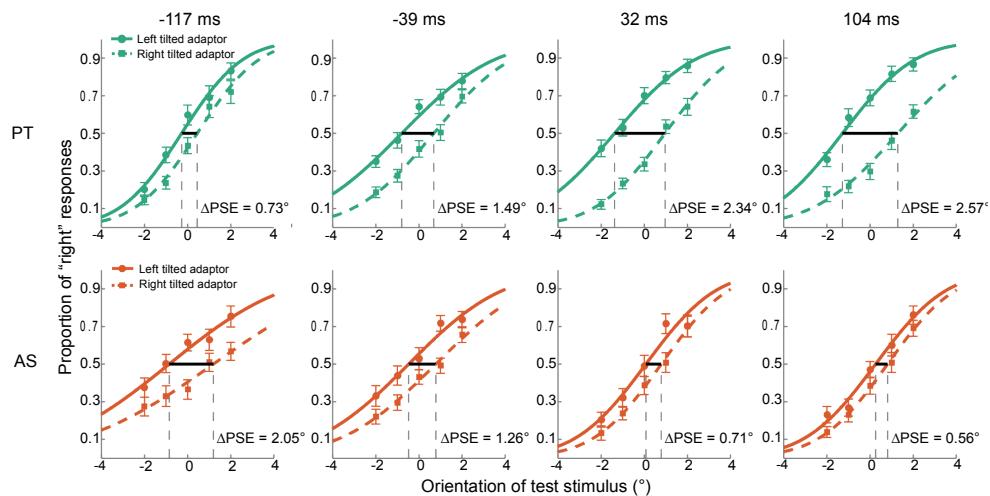
Figure 2.3. Psychometric curves for orientation judgements in Experiment 2. Same conventions as in **Figure 2.2** but only peripheral target (PT) and adaptor stimulus (AS) locations were tested, while both the adaptor and test stimulus were presented 4° above fixation.

The results of Experiment 1 and 2 indicate that predictive remapping of orientation occurs, irrespective of whether the stimulus is a saccade target. However, due to the short spatial distance between the test stimulus and saccade target location, and between the adaptor location and foveal fixation (both 4°), one may still argue that the findings in Experiment 2 could be explained by remapping of stimuli close to the fixation target or the fovea. To more directly contrast the convergent remapping and forward remapping hypotheses, we designed Experiment 3, in which two oppositely oriented adaptors were presented simultaneously at peripheral locations while the test stimulus was flashed at the initial fixation location or saccade target location.

Forward remapping hypothesizes a remapping of receptive fields in the same direction as the saccade. Therefore, a test stimulus presented at the initial fixation location (center) will, just prior to making a rightward saccade, be remapped to the left, opposite of the saccade vector. Convergent remapping, on the other hand, hypothesizes a remapping of receptive fields towards the future saccade location. In this case, no TAE would be predicted for a stimulus presented at the initial fixation location, because no receptive fields are remapped to this location (see Methods section for more details).

The results indicated a positive TAE for stimuli presented at the initial fixation location, just before participants made a saccade (**Figure 2.4**, "IF" location, orange lines, second column: $p = 0.0337$), in line with forward remapping. Conversely, the TAE for stimuli presented at the saccade target location was significantly decreased before saccade onset (**Figure 2.4**, "ST" location, green lines, comparison between first and second time point: $p < 0.0001$). Further, there was a significant ($p = 0.0001$) interaction between test stimulus location (initial fixation vs. saccade target) and time (first vs. second time bin). This pattern of results suggests that the test stimulus was predictively forward remapped prior to the eye movement. Furthermore, this result provides further evidence against adaptation remapping, in line with Experiment 1. If the information of the adaptor at the saccade target would have been remapped towards the initial fixation location, one should observe an attractive TAE (expressed in relation to the opposite adaptor) for test stimuli presented at initial fixation. Instead we observed a repulsive TAE, thus further corroborating the absence of adaptation remapping.
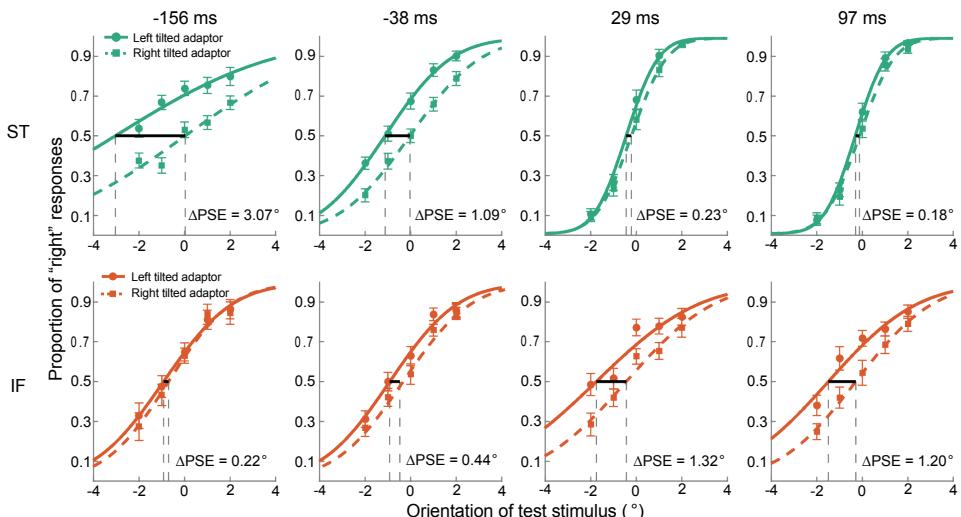
Figure 2.4. Psychometric curves for orientation judgements in Experiment 3. Same conventions as in **Figure 2.2** but only saccade target (ST) and initial fixation (IF) locations were tested while two oppositely oriented adaptors were presented in the periphery before saccade target onset. The TAE at the initial fixation location was calculated with respect to the orientation of the adaptor that was opposite of the saccade target.

Comparison of Tilt aftereffect (TAE) across experiments

As illustrated by **Figure 2.5**, a direct comparison of the three experiments confirm that the orientation information of the test stimulus, instead of the adaptor or its consequences, was predictively remapped to its future retinotopic location shortly before an eye movement (**Figure 2.5A**). This effect also occurs when the test stimulus was presented above saccade target (**Figure 2.5B**) or at peripheral location (**Figure 2.5C**), which is a non-saccade target location, suggesting that the visual system employs forward predictive remapping of features across the whole visual field.
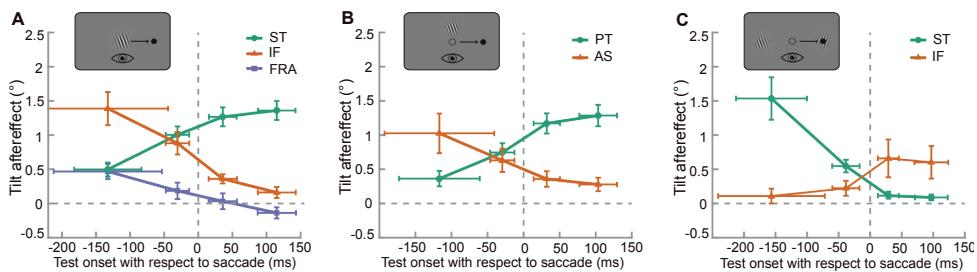

Figure 2.5. Comparison of Tilt aftereffect (TAE) across experiments. A) Experiment 1: the adaptor was shown at initial fixation location. For analysis, leftward saccade trials were collapsed into rightward saccade trials. The vertical dashed line indicates the onset/offset of a saccade. **ST**: Saccadic target location, **IF**: Initial fixation location, **FRA**: Future retinotopic location of adaptor. **B)** Experiment 2: the adaptor was shown 4° above fixation. Only initial fixation and saccade target location were probed. Other parameters were identical to Experiment 1. **PT**: Peripheral target location, **AS**: Adaptor stimulus location. **C)** Experiment 3: two oppositely oriented adaptors were presented at peripheral location. The test stimulus was presented at the initial fixation location or saccade target location. **ST**: Saccadic target location, **IF**: Initial fixation location. All vertical error bars represent one SD of the bootstrapped distribution. All horizontal error bars represent one SD of the distribution of test onset times within the respective time bin.

In order to follow up on the time period of test stimulus remapping, we further split all trials with test stimuli presented before saccade onset into four narrower time bins to quantify the time course of remapping in more detail (**Figure 2.6**). In these analyses, we found that while the TAE at each location did not change much up to 80 ms before saccade onset, a dramatic change occurred within the 50 ms before saccade onset, suggesting that predictive remapping occurred very close to the saccade onset in our experiment. This result is consistent with that of Duhamel et al. (1992) who shown that the LIP neurons start responding to the visual stimuli in their future field 80 ms before the saccade onset, suggesting that the feature remapping

we observe more likely represents a predictive oculomotor effect instead of the pre-saccadic attention shift, which presumably occurs much earlier.
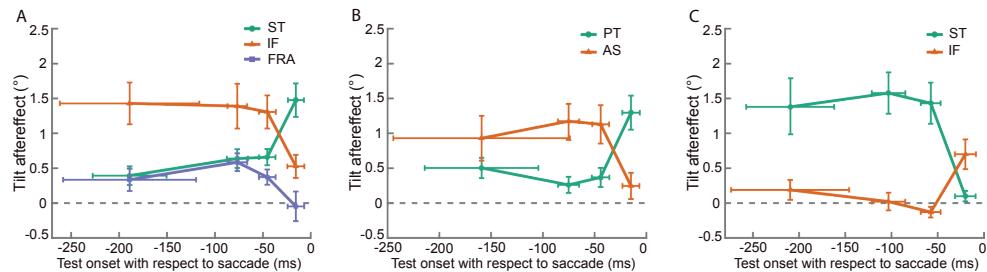
Figure 2.6. Tilt aftereffect (TAE) in finer time bins before saccade onset in Experiment 1, 2 and 3. A) In Experiment 1, while the TAE at each location did not change much up to 80 ms before saccade onset, a dramatic change occurred within 50 ms before saccade onset, suggesting that predictive remapping occurred very close to the saccade onset in our experiment. **ST**: Saccadic target location, **IF**: Initial fixation location, **FRA**: Future retinotopic location of adaptor. **B)** A similar pattern to the one of Experiment 1 was observed in Experiment 2. **PT**: Peripheral target location, **AS**: Adaptor stimulus location. **C)** Similar to Experiment 1 and 2, feature remapping occurred close to the saccade onset in Experiment 3. **ST**: Saccadic target location, **IF**: Initial fixation location. All vertical error bars denote one SD of the bootstrapped distribution. All horizontal error bars denote one SD of the distribution of test onset times within the respective time bin.

DISCUSSION

We used an orientation adaptation paradigm to investigate whether and how feature information is predictively remapped prior to saccades. In Experiment 1 (see **Figure 2.5A**), and consistent with the results reported in Melcher (2007), we found strong evidence for predictive remapping of visual information that is presented shortly before saccade onset, but no remapping of adaptation, as had been previously hypothesized (Melcher, 2007; Rolfs et al., 2011). Notably, predictive feature remapping occurred very shortly before saccade onset (i.e., < 80 ms before saccade onset, see **Figure 2.6**). In Experiment 2 and 3 (see **Figure 2.5B** and **Figure 2.5C**), we provided evidence that pre-saccadic remapping of features also occurs for stimuli that are not a saccade target, consistent with forward remapping, which further underscores the generality of this mechanism (Neupane et al., 2016a, 2016b).

No predictive remapping of adaptation

The results of Experiment 1 and 3 indicate that while features of stimuli presented shortly before the impending saccade are remapped to their future retinal location, the adaptation effect itself is not remapped during this time period. While there is also a significant TAE at the saccade target (ST) location and future retinotopic location of the adaptor (FRA) at the first time bin in Experiment 1 of our study (**Figure 2.5A**), this reflect a spatially unspecific tilt-aftereffect that spreads across the whole visual field (Knapen et al., 2010). In our experiments, the adaptor stimulus is presented during an initial fixation period, long before participants are instructed to prepare a saccade. Therefore, at the time participants could prepare a specific saccade plan, the adaptor stimulus had already disappeared. Since the saccade preparation occurred after the adaptor stimulus offset, any processing of the adaptor stimulus is likely finished by the time participants prepare the saccade. As the remapping dynamics also clearly show, only stimulus information that is presented very shortly before the saccade is remapped. This is also in line with the notion that adaptation occurs in a retinotopic reference frame (Knapen et al., 2010; Wenderoth & Wiese, 2008), possibly due to a reduction of excitability of the adapted neurons. It is unlikely that such a reduction of neuronal excitability can be 'remapped' by the planning of a saccade.

Contrary to our results, a recent paper by He et al. (2017) did observe predictive feature remapping of adaptation. In their study, however, participants were required to make the same saccade on every trial and the test stimulus always appeared at the same location (i.e., the future retinotopic location of the adaptor). Since the saccade plan was known to the participant already at the beginning of each trial it seems likely that participants could build up a spatiotopic representation of the adaptor, even before they saw the cue to execute the saccade. In line with this, Zimmermann et al. (2013) found that post-saccadic spatiotopic effects of the TAE are not immediately present after the eye movement but require substantial time to build up (Zimmermann et al., 2013). In contrast, in our experiment the saccade direction on a given trial was only known to the participant at the time of the fixation dot displacement, leaving little time to transform the adaptor information into a spatiotopic representation before and after the saccade.

Importantly, while the study by Zimmermann et al. (2013) is broadly consistent with our finding that there is no pre-saccadic remapping of adaptation, when the preview duration of the saccade target is short, Zimmerman et al. presented the test stimulus always after the saccade, thus measuring post-saccadic TAEs in their study. Given that pre- and post-saccadic remapping may not share the same properties, the current study complements the previous research on post-saccadic spatiotopic adaptation effects. Furthermore, the evidence for pre-saccadic remapping of the test stimulus in our study suggests that predictive remapping of feature information can occur even for short saccade target preview durations, and thus predictive feature remapping as such is not dependent on an extended saccade planning time.

Remapping of features or attentional pointers?

The question whether feature information is involved in the predictive remapping process has been extensively debated in the recent decade. Rolfs et al. (2011) found that visual performance was gradually enhanced at the future retinotopic location even before the onset of eye movements. Since the target was very difficult to detect and required a high degree of attention toward the particular location, the authors proposed that attention, rather than feature information is predictively remapped prior to a saccade. This hypothesis was further supported by several subsequent studies (e.g., Harrison et al., 2013; Hunt & Cavanagh, 2011; Jonikaitis

et al., 2013; Puntiroli et al., 2015). However, in recent years a number of studies provide evidence that feature information, in addition to the attentional pointers alone, is also involved in transsaccadic remapping (Cha & Chong, 2013; Demeyer et al., 2009, 2010, 2011; Eccelpoel et al., 2008; Edwards et al., 2017; Fracasso et al., 2010; Gordon et al., 2008; Habtegiorgis et al., 2018; Harrison & Bex, 2014; Hayhoe et al., 1991; He et al., 2017; Herwig & Schneider, 2014; Koller & Rafal, 2018; Melcher, 2007; Nakashima & Sugita, 2017; Wijdenes et al., 2015; Paeye et al., 2017; Prime et al., 2006, 2011; Sligte et al., 2017; Wittenberg et al., 2008; Wolfe & Whitney, 2015; Zimmermann et al., 2013, 2016, 2017; Zirnsak et al., 2011). Our study is in line with these studies, and further extends the findings by showing that orientation features of an actively processed stimulus, rather than the adaptation effects due to previous stimulation, are remapped.

Notably, several fMRI studies have also shown evidence for predictive feature remapping (but see Dunkley et al., 2016; Fairhall et al., 2017). Zimmermann et al., (2016) found that visual feature information was dynamically remapped from a retinotopic coordinate into a spatiotopic coordinate system in ventral visual areas V3, V4, and VO. Merriam et al., (2007) found remapping of information associated with the execution of eye movements not only in higher-order extrastriate areas (areas V3A, hV4) but also in V1 and V2, although smaller in magnitude, consistent with an earlier study in non-human primates (Nakamura & Colby, 2002). How is this feature information transferred within the visual system? A possible explanation for this might be that feature remapping is the effect of the combination of corollary discharge and bottom-up information. Activity elicited by the test stimulus could be remapped under the guidance of corollary discharge signals (Rao et al., 2016; Sommer & Wurtz, 2006; Sperry, 1950). The basic idea of corollary discharge is that when the motor system generates a movement command for muscles to produce a movement, a copy or corollary of this command will also be sent to other regions of the brain to inform them about the impending movement. Thus when a saccade is prepared by the oculomotor system, a corollary discharge signal containing information about the onset and target location of the imminent eye movement could be used to redirect the flow of feature information in visual cortex (Fries, 1984; Tolias et al., 2001). In particular, while the

neurons whose receptive field cover the stimulus location will be activated by the bottom-up signal at first, this signal will be combined with the corollary discharge in extrastriate cortex and then, via the SC to neurons whose receptive field will overlap with the stimulus region after the eye movement.

Convergent and forward predictive remapping

In their seminal study, Duhamel et al., (1992) reported that a set of LIP neurons predictively shift their receptive fields from their current location to their future retinotopic location prior to a saccade. This type of predictive remapping was termed *forward remapping*, since RF locations are shifted parallel to the saccade vector, as has been observed in several studies (Walker et al., 1995; Umeno & Goldberg, 2001; Nakamura & Colby, 2002). However, another type of predictive remapping has been proposed, which is termed *convergent remapping*, suggesting that the receptive fields shift toward the saccade target location rather than their postsaccadic location (Tolias et al., 2001; Zirnsak et al., 2014). Due to limitations in the experimental paradigms, forward and convergent remapping are sometimes difficult to distinguish. In particular, in many previous studies the test stimulus often constituted the saccade target, and in this case forward and convergent remapping theories make indistinguishable predictions.

In our current study, when the test stimulus was presented outside the saccade target location (Experiment 2 and 3), we still observed a robust forward pre-saccadic remapping effect. This result is in line with a previous electrophysiological study in V4 (Neupane et al., 2016b). In contrast, convergent remapping has been reported in FEF (Zirnsak et al., 2014). We speculate that the convergent remapping in FEF, which is a non-visual area, may not be functionally related to shifting of receptive fields but rather in anticipating and selecting relevant stimuli near the saccade target location, to facilitate processing of saccade targets. Conversely, for the visual system, maintaining stable representations of features across saccades is critical for seamless visually guided behaviors, which may be enabled by forward remapping. However, even though we provide evidence for forward remapping, no direct evidence against convergent remapping was observed in our experiments. Therefore, it is possible that forward and convergent remapping could occur concurrently. In addition, recent evidence suggests that these two types of remapping may have different time courses, with forward remapping preceding convergent

remapping (Neupane et al., 2016a). Therefore, although we find evidence for forward remapping in our study, it is possible that convergent remapping would dominate at later time points.

Slopes of psychometric functions

In Experiment 1 (**Figure 2.2**), the slopes of the psychometric functions for the initial fixation (IF) position are shallower at early time bins (before saccade) than at late time bins (after saccade). This may reflect worse discriminability due to adaptation. While discrimination performance can be improved if an adaptor is oriented orthogonally to the orientation of a test stimulus, discrimination is typically impaired if the orientation of an adaptor differs from the orientation of a test stimulus by 7° to 45° (Regan & Beverley, 1985; Schwartz et al., 2007). In line with this explanation, an opposite pattern of slope changes was found in Experiment 3 in which we used peripheral adaptors.

CONCLUSION

We found strong support for predictive remapping of the orientation feature of a test stimulus that was presented shortly before saccade onset. This pre-saccadic remapping also occurred for stimuli that were not saccade targets, and had the characteristics of a 'forward remapping' process that operates across the whole visual field. Thereby, forward predictive feature remapping may constitute an important mechanism for mediating visual stability.

CHAPTER 3

VISUAL WORKING MEMORY REPRESENTATIONS IN
VISUAL AND PARIETAL CORTEX DO NOT REMAP
AFTER EYE MOVEMENTS

ABSTRACT

It has been suggested that our visual system does not only process stimuli that are directly available to our eyes, but also has a role in maintaining information in VWM over a period of seconds. It remains unclear however what happens to VWM representations in the visual system when we make saccades. Here, we tested the hypothesis that VWM representations are remapped within the visual system after making saccades. We directly compared the content of VWM for saccade and no-saccade conditions using MVPA of delay-related activity measured with fMRI. We found that when participants did not make a saccade, VWM representations were robustly present in contralateral early visual cortex. When making a saccade, VWM representations degraded in contralateral V1-V3 after the saccade shifted the location of the remembered grating to the opposite visual field. However, contrary to our hypothesis we found no evidence for the representations of the remembered grating at the saccadic target location in the opposite visual field, suggesting that there is no evidence for remapping of VWM in early visual cortex. Interestingly, IPS showed persistent VWM representations in both the saccade and no-saccade condition. Together, our results indicate that VWM representations in early visual cortex are not remapped across eye movements, potentially limiting the role of early visual cortex in VWM storage.

This chapter has been posted as a preprint:

INTRODUCTION

Research in the past decade has suggested that our visual system may not only process incoming information, but also be relevant for maintaining internal representations of previously observed visual stimuli, i.e. visual working memory (VWM). The ability to maintain information that is no longer in view is critical for reasoning about and mentally manipulating visual information despite temporal discontinuous in visual inputs that occur for example during eye movements, occlusions, and object motion (Curtis & D'Esposito, 2003; Lorenc et al., 2018; Serences, 2016).

VWM information has been observed both in early sensory areas (Albers et al., 2013; Ester et al., 2009; Harrison & Tong, 2009; Sreenivasan et al., 2014), as well as higher-order parietal (Bettencourt & Xu, 2016; Christophel et al., 2015; Ester et al., 2015), and prefrontal regions (Goldman-Rakic 1995; Durstewitz et al. 2000; reviewed in Riley & Constantinidis, 2016). Moreover, VWM representations in early visual cortex have also been found to be spatially specific, maintained in a retinotopic manner, at least in V1 and V2 (Pratte and Tong 2014; although see Ester et al. 2009). Crucially however, in these previous studies, participants were instructed to maintain fixation while remembering a visual stimulus during a retention period. While this is a common approach to investigate VWM in a lab environment, it is arguably quite different from real-world settings that are marked by multiple eye movements per second. Humans perform about three saccadic eye movements per second in order to guide the fovea toward regions of interest in the visual field (e.g., Summerfield et al., 2008; Kok et al., 2012; Richter et al., 2018). Previous research has indicated that both stimulus features and attentional pointers are remapped across eye movement to aid visual stability (He et al., 2018; Melcher, 2007; Rolfs et al., 2011). It is currently unclear however, whether VWM is also remapped within the visual system after making saccades.

One possibility is that VWM representations are dynamically remapped and follow the shift of the retinotopic location caused by eye movements. In this case, the cortical location representing the VWM would be updated after an eye-movement. Alternatively, if VWM does not remap, working memory information might be maintained across multiple brain regions following eye movements. On this account, after every eye movement, the up-to-date feature of

3

the stimulus (e.g., the latest location of the stimuli) would be integrated with the previous working memory information.

Here, we tested the potential remapping of VWM in the early visual system, by presenting participants with an orientated grating in either the left or right visual field. The grating orientation had to be maintained for a subsequent retention period, while we measured blood oxygenation level-dependent (BOLD) signals with functional magnetic resonance imaging (fMRI). Using multivariate pattern analysis (MVPA), we attempted to decode the remembered orientation in both the contralateral and the ipsilateral hemispheres during trials in which participants performed either a saccade or maintained fixation during the working memory period.

To preview, we found a contralateral VWM representation in the early visual system. This VWM representation degraded when participants made a saccade and was not remapped to ipsilateral visual cortex. In contrast, VWM representations in IPS persisted after saccades. These findings suggest a limited role of the early visual system in VWM.

MATERIALS AND METHODS

Data and code availability

All data and code used for stimulus presentation and analysis is freely available on the Donders Repository (https://data.donders.ru.nl/login/reviewer-77603154/28KfrmSvRmvGnYdOkGqdQQf MufTI7W29jY686hMMaro).

Participants

Thirty-four healthy participants (18 females, mean age 24.3 years, ranging from 19 to 33 years) with normal or corrected-to-normal vision were recruited from the institute's subject pool in exchange for either monetary compensation or study credits. This sample size of N = 34 included subjects ensured 80% power to detect an effect size of at least Cohen's d $\geq$ 0.5. All participants were naive with respect to the purposes of the study. The experiments were approved by the Radboud University Institutional Review Board and were carried out in accordance with the guidelines expressed in the Declaration of Helsinki. Written informed consent was obtained from all participants prior to the start of the study. Only participants who completed the entire experimental protocol (i.e., the behavioral experiment and the two fMRI sessions) were included in the final analysis. Data from six participants were excluded: one participant didn't complete the fMRI sessions due to discomfort, one participant failed to follow the instructions (i.e., fixate and saccade) during experiment, four participants had excessive head motion (motion cutoff = 1 mm).

Stimuli

Stimuli were programmed in MATLAB (v2016a, The MathWorks, Inc., Natick, MA) using the Psychtoolbox (Brainard, 1997). The circular sinusoidal grating stimulus subtended 10° and was centered with a small jitter (0.3°) on the screen center. The grating was full contrast, with a spatial frequency of 1 cycles/degree, a random phase and an orientation of either 25° or 115° (with a small jitter of 3°) from the horizontal axis. The contrasts of the edges of the grating were linearly attenuated over the distance from 4.5° to 5.0° radius. Two filled dots (0.5°, one green, one black) were presented at the periphery of the screen (6° left or right away from the center of the screen), which were served as the fixation dot and saccade target in the task. In the behavioral training

session, stimuli were presented on a 24-inch flat-panel display (BenQ XL2420T, 1,920 x 1,080 resolution, 60 Hz refresh rate). In the fMRI sessions, stimuli were displayed on a rear-projection screen using an EIKI LC-XL100L (EIKI, Rancho Santa Margarita, CA) multimedia projector (1,024 x 768 resolution, 60 Hz refresh rate).

Experimental design

Behavioral training procedure. Prior to the fMRI scan sessions, all participants completed a one-hour behavioral training session to familiarize themselves with the fMRI main task and to establish their individual orientation discrimination threshold, which served as an initial orientation difference of the gratings in the following fMRI sessions. The experimental design of the behavioral training task was exactly the same as during the fMRI main task, except that the delay period and the inter-trial interval (ITI) were shortened to 3 s to reduce the experimental time. Participants completed two to three blocks of 56 trials until a stable orientation discrimination threshold was obtained, during which the eye movements were continuously monitored by an Eyelink 1000 plus eye tracker. In addition, participants were familiarized with the localizer tasks and the retinotopic mapping procedures that were used in the fMRI session at the end of the behavior session.

fMRI main task. The experimental design (**Figure 3.1a**) was adapted from a well-known delayed orientation discrimination task used before (Harrison & Tong, 2009). Each trial began with two filled dots (one green, one black) that were presented at the periphery of the screen (2 s). Participants were asked to fixate at the green dot through the trial. Two oriented gratings were flashed sequentially at the center of the screen (which could be in the left or right visual field of the participants, depending on the location of the green fixation dot) for 200 ms, respectively, with an inter-stimulus interval of 400 ms, and followed by a retro-cue (400 ms, "1" or "2") to indicate which orientation of the grating should be remembered during the following delay period. The sequence of the orientations (25° and 115°) were randomly chosen on each trial. On 10 out of 28 trials (No-saccade condition) in each run, the two dots did not swap their locations, which indicated to participants that they needed to keep their fixation at the initial fixation location during the 10 s delay period. On the remaining 18 trials (Saccade condition) in the run, the green dot was shifted to the opposite side of the screen at the beginning of the delay

period (2 s after the offset of the retro-cue). This instructed participants to move their eyes to the opposite location of the screen and maintain their fixation at the new position for the remaining 8 s. A probe grating was presented at the screen center after the delay period and participants were required to make a judgement of whether the probe orientation was rotated clockwise or count-clockwise relative to the grating they memorized during the delay period. Finally, feedback was provided and a black fixation dot instructed participants to move their eyes to the center of the screen in preparation for the next trial. Trials were separated by an ITI of 9.6 s. The central fixation dot changed its color from black to gray at the last second of the ITI to indicate that the next trial was going to start.

In order to incentivize participants to form spatially specific visual working memories, four catch trials were included in each run. Stimuli and timing of the catch trials were identical to the main trials, except for the following changes. During the presentation of the probe in the catch trial, the probe was horizontally shifted 1.2° to the left or right with respect to the location of the sample gratings. Participants were instructed to not respond when the location of the probe grating did not match with the sample gratings. The rationale of this was that it forced participants to memorize the orientation stimulus at its original location in order to successfully perform the task, resulting in a spatially specific VWM representation.

Each run comprised 28 trials, consisting of 10 no-saccade trials (including 2 catch trials), 18 saccade trials (including 2 catch trials). We chose these trial numbers because the saccade trials were of primary interest and we therefore wanted to have maximal sensitivity for this condition. The order of trials was a pseudo-randomized within each run. Each trial lasted 26.4 s, consisting of a 16.8 s task period and a 9.6 s ITI. Each run lasted 12.32 min and started with 6 s of fixation that was discarded from the analysis.

Staircase procedure

The staircase procedure was used to ensure equal task difficulty across participants and to equate task difficulty levels across no-saccade and saccade conditions within participants. In the behavioral training session, immediately after the delay period, participants were asked to compare the tilted orientation between the probe and the internal remembered grating. The staircase procedure estimated the difference between probe and remembered

grating that ensured 75% performance, using QUEST (Prins & Kingdom, 2018; Watson & Pelli, 1983). A maximum orientation difference of 20° between the probe and remembered grating was enforced. The staircase was initiated with an orientation difference of 10° and dynamically adapted according to participants' performance on previous trial until a stable threshold was acquired. This threshold was used as a seed in the following fMRI sessions and the same staircase procedure was also used during scanning.

Eye tracking

Eye position was monitored with an MR-compatible Eyelink 1000 (SR Research Ltd., Ottawa, Canada) eye tracker. Only the left eye was recorded in the scanner. Pupil and corneal reflection were sampled at 1000 Hz and analyzed offline to ensure that participants fixated at the correct location. The eye tracker was calibrated at the beginning of each session and repeated between runs if necessary. In 10 out of 192 runs, the eye tracker signal was lost during scanning due to subjects' head motion or technical problems. During these runs, the experimenter monitored the eye position online via the live video feed from the camera. All participants were trained on the fixation task and to perform saccades in the behavioral training session prior to the scanning session.

fMRI parameters

Functional and anatomical images were carried out with a 3T Siemens Prisma fit MRI system (Siemens, Erlangen, Germany), using a 32-channel headcoil. Functional images were acquired using a whole brain T2*-weighted multiband-4 sequence (TR/TE = 1,200/39 ms, voxel size 2.4x2.4x2.4 mm, 56 transversal slices, 65° flip angle, A/P phase encoding direction, FOV = 210 mm, BW = 2030 Hz/Px). Anatomical images were acquired using a T1-weighted magnetization prepared rapid gradient echo (MP-RAGE) sequence (TR/TE = 2,300/3.03ms, voxel size 1x1x1 mm, 192 transversal slices, 8° flip angle).

fMRI preprocessing

fMRI data were preprocessed using FSL (FMRIB Software Library; Oxford, UK; www.fmrib.ox.ac.uk/fsl; Smith et al. 2004, RRID:SCR_002823), including motion correction (six-parameter affine transform), temporal high-pass filtering (100 s) and Savitzky–Golay low-pass

filter (time window length = 11 TRs, polynomial order = 3; Savitzky & Golay, 1964) for each run separately. No spatial smoothing and slice timing correction was performed. All univariate and multivariate analyses were performed in native subject space with custom python code using Nibabel [https://doi.org/10.5281/zenodo.1464282], Scipy (Millman & Aivazis, 2011; Oliphant, 2007) and scikit-learn (Pedregosa et al., 2011).

Functional localizers

In addition to the main experiment, participants underwent two localizer runs, which were used to select voxels that maximally responded to stimuli presented in the contralateral hemifield in both the univariate and multivariate analysis. The same grating stimulus parameter were used in localizer runs as those in the main experiment. Participants fixated at the left or right green dot and the grating was presented at the center of screen for 16 s, with a frequency of 4 Hz. Throughout the localizer, participant had to fixate at the green dot and monitor a sequence of rapidly changing letters just above fixation, to which they had to respond by button press whenever a target letter ("X" or "Z") occurred in a stream of non-target letters ("A", "H", "R", "N", "T", "V", "U", "Y"). Letters were presented at a frequency of 2 Hz. When the green dot shifted from the left to the right side of the screen (or vice versa) at the end of the trial, participants had to move their eyes to follow the fixation dot. Each trial was separated by a 2 s ITI in which only the fixation cross was presented, to give participants enough time to saccade and stabilize their eyes in the new position. Two blocks of 20 trials (10 trials per visual field: left or right) were collected.

Images of the localizer runs were also preprocessed following the same procedure as the main tasks. Onsets and duration of the localizer blocks were convolved with a double gamma haemodynamic response function (HRF) and fitted using a general linear model in left and right hemisphere separately. For each participant a two-sided t-contrast was calculated contrasting between left and right hemispheres. Resulting statistical maps were thresholded at $Z > 3.1$ and a corrected cluster significance threshold of $p < 0.05$.

Retinotopic mapping of early visual areas (V1 – V3)

Early visual areas (V1, V2, and V3) for each participant were identified using two

retinotopic mapping blocks based on the standard traveling-wave method using rotating wedges (DeYoe et al., 1996; Engel et al., 1997; Wandell et al., 2007), consisting of a clockwise and a counterclockwise-rotating run. Participants were instructed to fixate at the center of the screen and fulfill rapid letter detection task (exact same as that in localizer runs). The BOLD responses to the wedges were used to estimate the polar angle of the visual field representation.

Regions of interest (ROIs)

Early visual areas (V1 - V3) and the intraparietal sulcus (IPS0 - IPS5) within each hemisphere were independently chosen as the ROIs in our analyses. For the ROI of the early visual areas, we first used Freesurfer (http://surfer.nmr.mgh.harvard.edu/, Fischl et al., 2002) to define the gray–white matter boundary and perform cortical surface reconstruction. The borders of the early visual areas V1 - V3 were delineated based on retinotopic maps. The ROI of the intraparietal sulcus was defined based on anatomical probability maps of retinotopic areas in the intraparietal sulcus (IPS0 - IPS5) from the Probabilistic atlases (Wang et al., 2015). Finally, all surface-based ROIs were backward-transformed into participant's native space. Next, the visually active voxels corresponding to the grating that was positioned at the left and right visual field was identified based on statistical activation maps from the functional localizer runs. Two types of ROI were defined in the decoding analyses: contralateral ROIs and ipsilateral ROIs. For instance, when decoding the orientation of the grating that was initially presented at participant's right visual field, regardless of the no-saccade and saccade condition, the left hemisphere would be labeled as the contralateral ROIs, while the right hemisphere would be labeled as the ipsilateral ROIs (see **Figure 3.1b**) and vice versa. Finally, we selected the 150 most active voxels across visual areas V1, V2, V3, as well as 250 most active voxels across the combined early visual cortex (V1 - V3) and the entire intraparietal sulcus (IPS0 - IPS5) to perform the decoding analyses, separately.

Univariate fMRI analyses

To estimate the BOLD response of each hemisphere in each condition, we selected the same voxels as those used for decoding. We separately modeled the onset of each trial for each hemisphere and for no-saccade and saccade condition within each run to fit voxel-wise general linear models (GLM) using FSL FEAT. An additional nuisance regressor of 24 motion

regressors (FSL's standard + extended motion parameters) were also added to the GLM. To quantify BOLD activity during the trial, contrasts between left and right hemisphere regressors for each condition were created. Multiple-comparison correction was performed using Gaussian random-field based cluster thresholding. The significance level was set at the cluster-forming threshold of z > 3.1 (i.e., $p < 0.001$, two-sided) and a cluster significance threshold of $p < 0.05$. All fMRI data were transformed from MRI signal intensity to units of percent signal change, calculated relative to the average level of activity for each voxel across the first volume of each trial within each run. BOLD activity over time were statistically tested using nonparametric cluster-based permutation t test (10,000 permutations; two-sided $p < 0.05$; cluster formation threshold $p < 0.05$) (Maris & Oostenveld, 2007).

Multivariate fMRI analyses

We used multivariate pattern analyses (MVPA) to determine whether the pattern of activity in each ROI and each hemisphere contained orientation information, as implemented in Scikit-learn 0.20.3 (Pedregosa et al., 2011). To this end, linear support vector machines (SVMs) were trained to discriminate between the two grating orientations based on the pattern of BOLD activity over voxels. In this study we used classification distance as an indication of the amount of orientation information being maintained in each hemisphere. To calculate the classification distance, we measured the distance of each sample to the separating hyperplane that was trained by a linear SVM with a positive/negative sign (the sign indicates the class). We then averaged the distance within each class and calculated the absolute distance between these two classes. While this approach can give us a binary predicted label (25° or 115°), which can be used to calculate classification accuracy, it additionally allows one to review the confidence of this classification and provide a continuous metric of the decoding performance. In each ROI, the larger the classification distance, the more confident the classifier is in determining the stimulus class based on the BOLD activity pattern, and hence the more orientation information is contained within the pattern of BOLD activity.

When training and testing within the main experiment we averaged the BOLD activity over time points 7.2 - 10.8 s after the onset of the delay period. This time period was selected to be as far from the onset of the two gratings at the beginning of the trial as possible, and therefore

not reflect activity elicited by the stimuli, but also prior to the onset of the probe stimulus. These time series were then normalized on a voxel-by-voxel and run-by-run basis for each voxel using a z-scored transformation and sorted into one of sixteen bins based on four factors: hemisphere (left or right hemisphere), orientation (25° or 115°), stimulus location (left or right hemifield) and saccade condition (saccade or no-saccade). A leave-one-run-out cross-validation procedure was used to train the classifier where we trained in 7 ("training" dataset) out of 8 runs and tested on the remaining run ("test" dataset) for each hemisphere, stimulus location and saccade condition pair, separately. Within the independent "training" and "test" dataset, activation patterns comprising the mean response of each voxel during 25° or 115° trials were calculated. Finally, the decoding distances in each corresponding stimulus location and hemisphere pair were collapsed into the contralateral (i.e., left hemifield and right hemisphere, right hemifield and left hemisphere) or ipsilateral (i.e., left hemifield and left hemisphere, right hemifield and right hemisphere) hemisphere condition.

Bayesian analyses

In order to further evaluate all the statistical tests, we performed the Bayesian equivalents of the above outlined analyses. JASP 0.10.2 (JASP Team, 2019, RRID:SCR_015823) was used to perform all Bayesian analyses, using default settings. Thus, for Bayesian t-tests a Cauchy prior width of 0.707 was chosen. Qualitative interpretations of Bayes Factors are based on criteria by Lee & Wagenmakers (2014).

RESULTS

Our primary goal was to investigate whether VWM representations in early visual cortex (V1-V3) are remapped after eye movements. We used MVPA (Haynes & Rees, 2006; Kamitani & Tong, 2005; Norman et al., 2006) to determine whether the information in VWM that was initially represented in the contralateral hemisphere (corresponding to the stimulus location) was remapped to the opposite (ipsilateral) hemisphere following an eye movement to the opposite visual field during the retention period. 34 participants performed a delayed orientation discrimination task, in which they initially fixated at the peripheral fixation dot while passively viewing two successive grating stimulus orientations (25° and 115°) in one visual field, followed by a cue and a delay period. Importantly, in 18 out of 28 trials (*saccade condition*) in each run, participants were asked to saccade to the opposite side of the screen during the delay period, while in the remaining 10 trials (*no-saccade condition*) in the same run, participants maintained fixation at the initial side through the entire trial. A probe grating was presented at the end of the trial (**Figure 3.1a, b**).

In order to encourage participants to memorize the grating in its original location, we also included catch trials in which the probe grating was horizontally shifted 1.2° with respect to the location of the sample gratings. Participants were instructed to discriminate the orientation between the probe and the memorized grating only when they were presented at the same location (see Methods for details). This experimental design was chosen to encourage participants to maintain both the orientation and location of the presented grating. Indeed, behavioral data showed that participants successfully withheld their response (i.e. correct rejection rate) at a rate of 63.6% (SD 18.37) and 62.87% (SD 19.58) in both no-saccade and saccade conditions when the probe was presented at a displaced location, and no difference was found between the two conditions ($t_{(33)}$ = 0.257, p = 0.7989, Cohen's d = 0.039; BF_{10} = 0.189), suggesting that participants remembered the orientation in a spatially specific way.

Behavioural data further confirmed that participants could successfully discriminate small differences between the cued grating and the probe grating (**Figure 3.1c**, mean discrimination threshold, no-saccade condition: 8.63°, SD 5.07; saccade condition: 8.89°, SD 4.55) at an accuracy of 82.1% (SD 5.05) and 81.1% (SD 4.43) in both no-saccade and saccade

trials. Notably, there was no difference in accuracy between trials with and without a saccade ($t_{(33)}$ = 1.125, p = 0.2687, Cohen's d = 0.193; BF_{10} = 0.328), and no difference in the mean discrimination threshold ($t_{(33)}$ = 0.66, p = 0.514, Cohen's d = 0.113; BF_{10} = 0.225), indicating that the VWM performance was not impaired by the eye movement during the delay period.

A univariate BOLD analysis showed that the presentation of the grating stimuli induced stronger BOLD activity in contralateral than ipsilateral early visual areas (cluster permutation test, p = 0.0001). As expected, probe presentation at the end of the trial led to a BOLD activity increase in the contralateral hemisphere during no-saccade trials and a BOLD activity increase in the ipsilateral hemisphere, corresponding to the updated stimulus location after the eye movement, in the saccade condition (**Figure 3.1d**). Taken together, these results suggest that participants engaged successfully in the task.
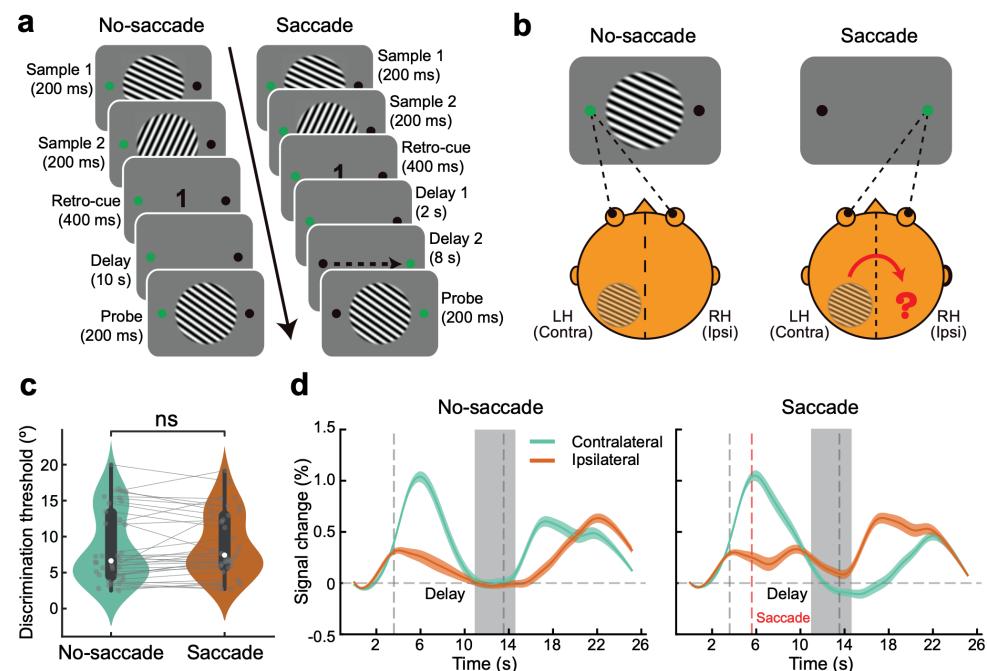
**Figure 3.1. Experimental paradigm, behavioral performance and BOLD activity in the early visual cortex. (a)** Participants performed a delayed orientation discrimination task. At the start of each trial, two dots were presented at the periphery of the screen and participants were instructed to fixate at the green dot. Two orientated gratings (25° and 115°) were successively flashed in the center of the screen, followed

by a retro-cue (1 or 2) that indicated which grating to remember in the following delay period. Crucially, during a 10 s delay period, if the green dot shifted to the opposite side of the screen (*saccade condition*), participants had to make an eye movement to the opposite side and maintained at the new location through the following time period (the dashed arrow is for illustration only, not present in the actual test). Conversely, in the no-saccade condition, the green dot did not change its position and participants maintained fixation at the initial side throughout the entire trial. After the delay period a probe was presented, and participants indicated whether the probe was tilted clockwise or counterclockwise relative to the remembered grating. **(b)** Illustration of the experimental design probing remapping. In the no-saccade condition (left), the remembered grating presented in right visual field is initially represented in the left (contralateral) early visual cortex. In the saccade condition (right), after participants saccade from the left to the right side of the screen, we set out to examine whether VWM contents that initially generated in contralateral (left) early visual cortex transfer to the ipsilateral (right) visual cortex. **(c)** there was no difference in the mean discrimination threshold between trials with and without a saccade, demonstrating that the VWM performance was not impaired by the eye movement during the delay period. Grey dots with connecting lines denote individual participants. Colors are estimated densities, white dots are group medians, boxes are quartiles and whiskers are 1.5 interquartile range. **(d)** Group averaged (N = 34) BOLD time course in contralateral and ipsilateral early visual areas (V1 – V3). In the no-saccade condition, the presentation of grating stimuli evoked a higher BOLD response in contralateral than in ipsilateral early visual areas. In the saccade condition, while the BOLD activity was still higher in contralateral relative to ipsilateral early visual areas after presentation of the grating stimuli, the pattern inverted after presentation of the probe – BOLD activity became higher in ipsilateral than in contralateral early visual areas. The first vertical dashed gray line represents the onset of the gratings, while the second vertical dashed gray line indicates the onset of the probe. The vertical dashed red line in saccade condition indicates the onset of the saccade. The vertical gray bar represents the delay period (7.2 s - 10.8 s after onset of maintenance) that selected for multivariate analysis. BOLD activity data was interpolated and smoothed for display only, all statistical tests were applied before data interpolation. Shaded areas denote SEM.

In order to evaluate the potential remapping of VWM in early visual cortex, we assessed whether the patterns of activation in both hemispheres, contralateral and ipsilateral to the item location, contained the remembered orientation information during the delay period (**Figure 3.1d**, gray region). A leave-one-run-out cross-validation approach was used to train the classifier to discriminate the grating orientation (25° vs. 115°) within the working memory period and test on the left-out run. We used classification distance to measure the amount of orientation information present in the activity patterns (Dijkstra et al., 2019; Linde-Domingo et al., 2019). This approach results in a binary prediction (25° or 115°), but additionally yields a continuous metric of the decoding performance that can be seen as the confidence of the classification (see Methods for additional details).

No remapping of VWM in early visual cortex following eye movements.

During the no-saccade condition, activity patterns in the early visual areas (V1 - V3) contralateral to the grating location contained information about the maintained orientation during the delay period (7.2 s - 10.8 s after onset of maintenance) (**Figure 3.2**, dark green bar; $t_{(33)}$ = 3.652, p = 0.0009, Cohen's d = 0.63; BF_{10} = 35.369). There was also weak evidence for some orientation information in the ipsilateral hemisphere of V1 - V3 (**Figure 3.2**, dark orange bar; $t_{(33)}$ = 2.192, p = 0.0356, Cohen's d = 0.38; BF_{10} = 1.501), and no compelling evidence for a difference between the contralateral and ipsilateral hemisphere of V1 - V3 ($t_{(33)}$ = 1.669, p = 0.1047, Cohen's d = 0.32; BF_{10} = 0.642). The same pattern was also visible when inspecting the early visual areas separately (**Supplementary Figure 3.1**). However, in the saccade trials, in which participants made an eye movement that shifted the location of the remembered grating to the opposite visual field during the delay period, the classifier was not able to distinguish between grating orientations in V1 – V3 contralateral to the item location (**Figure 3.2**, light green bar; $t_{(33)}$ = 0.03, p = 0.9765, Cohen's d = 0.005; BF_{10} = 0.184), and similarly there was no compelling evidence for orientation information in ipsilateral V1-V3 (**Figure 3.2**, light orange bar; $t_{(33)}$ = 1.905, p = 0.0655, Cohen's d = 0.327; BF_{10} = 0.92). Again, there was no difference in orientation information between the contralateral and ipsilateral hemisphere of V1 – V3 ($t_{(33)}$ = 1.722, p = 0.09438, Cohen's d = 0.286; BF_{10} = 0.694). Crucially, there was a significant degradation of orientation information in the contralateral hemisphere of the early visual cortex after an eye movement ($t_{(33)}$ = 2.748, p = 0.0096, Cohen's d = 0.478; BF_{10} = 4.452).
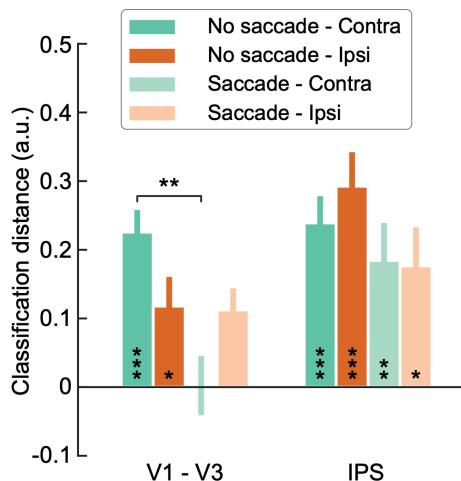
Figure 3.2. Orientation classification performance during the delay period in early visual cortex and intraparietal sulcus (IPS) using a leave-one-run-out cross-validation approach. In the combined early visual cortex (V1 – V3), both the contralateral and the ipsilateral early visual areas contained orientation information during the delay period in no-saccade condition. In the saccade condition, however, the orientation information significantly degraded in the contralateral hemispheres. Nevertheless, orientation information in the ipsilateral hemisphere after an eye movement was not higher than that before the saccade, suggesting no remapping of VWM in the early visual areas. In the IPS, the classifier could select the remembered orientation in both the contralateral and the ipsilateral hemisphere in the no-saccade trials, in line with the findings in early visual cortex. In the saccade condition, after the eye movement there was still a reliable orientation information in both the contralateral and ipsilateral IPS, suggesting a consistent VWM representation in the IPS. Error bars denote SEM. *No saccade – Contra*: No saccade condition, contralateral hemisphere; *No saccade – Ipsi*: No saccade condition, ipsilateral hemisphere; *Saccade – Contra*: Saccade condition, contralateral hemisphere; *Saccade – Ipsi*: Saccade condition, ipsilateral hemisphere. *$p < 0.05$; **$p < 0.01$; ***$p < 0.001$.

Although orientation information in the contralateral hemisphere was degraded after the saccade, the remapping hypothesis of VWM predicts that orientation information should become stronger in the ipsilateral hemisphere after the eye movement. However, in contrast to this hypothesis, there was no difference in terms of orientation information in the ipsilateral hemisphere after the eye movement compared to when no saccade was made ($t_{(33)} = 0.072$, $p = 0.9431$, Cohen's $d = 0.017$; $BF_{10} = 0.184$). Therefore, these results indicate that there is no remapping of VWM following eye movements in the early visual areas.

Persistent VWM representations after an eye movement in the IPS.

Our findings revealed that VWM representations in early visual cortex during maintenance were not remapped following eye movements. Bettencourt & Xu (2016) have recently shown that while remembered orientation information was degraded by irrelevant distractors in early visual cortex, VWM information remained available in the superior intraparietal sulcus (IPS). We sought to test whether we could observe similar results in our study. To this end, we also applied the leave-one-run-out cross-validation method to IPS. First, we found that both the contralateral (**Figure 3.2**, dark green bar; $t_{(33)} = 4.451$, $p = 0.0001$, Cohen's $d = 0.775$; $BF_{10} = 272.079$) and ipsilateral IPS (**Figure 3.2**, dark orange bar; $t_{(33)} = 5.075$, $p < 0.0001$, Cohen's $d = 0.883$; $BF_{10} = 1444.41$) contained information about the remembered orientation in no-saccade trials during delay period, as also observed in early visual cortex. However, in contrast to the early visual cortex, the remembered grating orientation could still be decoded from both the contralateral (**Figure 3.2**, light green bar; $t_{(33)} = 3.13$, $p = 0.0036$, Cohen's $d = 0.545$; $BF_{10} = 10.276$) and ipsilateral (**Figure 3.2,** light orange bar; $t_{(33)} = 2.6$, $p = 0.0138$, Cohen's $d = 0.453$; $BF_{10} = 3.281$) IPS after an eye movement, indicating a persistent VWM representations in IPS. These results also provided a neural evidence for supporting the preserved behavioral performance after a saccade.

Finally, in order to ensure that the results are not dependent on the a priori but arbitrarily chosen mask sizes of the ROIs, we repeated the analyses for ROIs of sizes ranging from 20 to 250 voxels in step of 10 voxels in the areas V1, V2 and V3, or ranging from 50 to 500 voxels in step of 20 voxels in the combined V1 – V3 and IPS (**Supplementary Figure 3.2**). Results were qualitatively identical to those mentioned above (**Figure 3.2** and **Supplementary Figure 3.1**) for almost entire range of ROI sizes, indicating that our results do not depend on an arbitrary ROI size but represent a robust pattern within the areas.

DISCUSSION

In the current study, we investigated whether VWM representations are remapped following eye movements and whether VWM information persists in the early visual cortex and parietal cortex after the execution of a saccade. We found robust encoding of maintained orientation information in the contralateral hemisphere of early visual cortex. However, this information significantly degraded upon making a saccade to the opposite hemifield and did not remap to the ipsilateral hemisphere in early visual cortex. This suggests that there is no robust representation of VWM representations across eye movements in the early visual cortex nor remapping of VWM representations. Additionally, although VWM representations in early visual cortex were impaired by the saccade during the retention period, this orientation information remained reliably present in the IPS even after execution of a saccade. These findings show that early visual cortex is susceptible to interference of eye movements during a working memory period, while IPS appears less sensitive to this interference.

Spatially specific encoding of VWM information in early visual cortex?

The issue of how VWM information is stored in early visual cortex has been debated previously. While some researchers observed a retinotopically specific encoding of items into VWM (Pratte & Tong, 2014), Ester and colleagues (2009) observed a non-spatially specific coding of VWM in early visual cortex. In their study, they could decode the orientation information in early visual areas both contralateral and ipsilateral to the stimulus location when participants were instructed to remember the orientation presented only in one visual hemifield. However, although the remembered grating was always located in one of the hemifields, participants could potentially use a strategy in which they memorized the orientation of the grating perifoveally instead of at its original location (Williams et al., 2008). Thus, it is unclear whether their result reflected the true effect of the spatially global representations or was caused by the lack of relevance of the spatial dimension in their task. To incentivize participants to form a spatially specific visual working memory, we inserted catch trials, in which the probe grating and the remembered grating were horizontally offset by 1.2 visual degree in each run. Participants were instructed to respond only when the probe location matched the location of the initially presented grating. Therefore, participants had to maintain the orientation of the gratings at the

presented location in order to be able to successfully complete the task. Behavioral results confirmed that participants indeed remembered the orientation stimuli in a spatially specific way. Decoding performance in the early visual cortex (i.e., V1 – V3) showed a numerically larger amount of orientation information in contralateral than ipsilateral cortex, echoing earlier results (Pratte & Tong, 2014) and suggesting a spatially specific code. However, this difference was not statistically reliable, and Bayesian analyses showed anecdotal evidence for a lack of difference (BF_{10} = 0.642). Thus, while our results may tentatively suggest some degree of retinotopic specificity of VWM encoding, our data preclude any strong conclusion.

No remapping of VWM following eye movements.

Attentional or feature based remapping of visual input just prior to a saccade has been well established from a variety of studies and is thought to maintain visual stability across eye movements. For instance, Rolfs et al. (2011) found that attention is predictively remapped to the future retinotopic location of an upcoming target, even before the execution of the eye movement. In the current experiment, we asked whether memory traces would also be updated with eye movements. However, we found no evidence that visual working memory representations were remapped following eye movements. At least two reasons should be emphasized to address the discrepancy in remapping between attention and VWM. First, to survive in a multifaceted and dynamically changing world, our attention needs to be selectively shifted to the most important stimuli that are goal-relevant. In order to be competent for such a complicated task, remapping of attention may be a crucial mechanism to prepare information in advance. In contrast, the main function of working memory is to temporarily retain information available for processing. While attention could be flexibly remapped to different locations to extract information, storing working memory information in one or several stationary regions could be potentially an efficient way for retrieval. Second, in line with the arguments of 'activity-silent' models of WM when compared to the persistent activity models of WM (Stokes, 2015; Wolff et al., 2017), remapping of VWM after each eye movement could also be energetically expensive, especially if VWM is maintaining an up-to-date information of the external environment. Therefore, a stationary working memory representation could be an ideal way for ecologically maintaining and manipulating information in the brain.
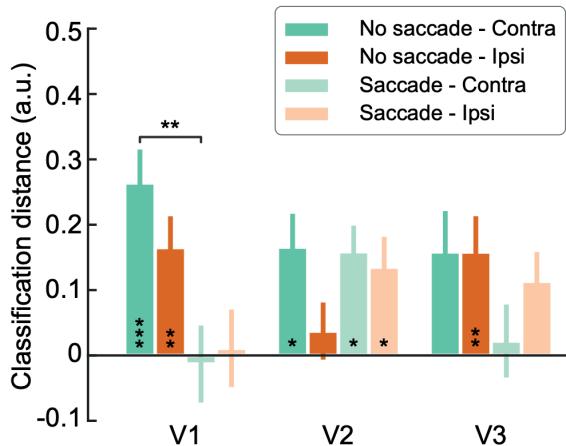
Parietal cortex may subserve VWM representations after saccades.

In recent years, the parietal cortex has been repeatedly implicated in VWM maintenance (Bettencourt & Xu, 2016; Christophel et al., 2015; Ester et al., 2015; Todd & Marois, 2004), alongside the involvement of sensory areas (Emrich et al., 2013; Harrison & Tong, 2009; Rademaker et al., 2019; Serences et al., 2009). Our results indicate that the early visual cortex is susceptible to the interference of eye movements during the delay period, potentially limiting the role of the early visual cortex in VWM. Similarly, Bettencourt and Xu (2016) observed that VWM representations in early visual cortex were destroyed by the presentation of distractors, while superior IPS exhibited persistent activity that was not impaired by the presentation of intervening distractor stimuli. In our experiment, the eye movements during the delay period potentially may also generate distracting new input to the visual system, which could disturb the VWM representations. Intriguingly, while VWM representations in early visual cortex were degraded following the eye movement, these representations were still maintained in IPS. Behaviorally, participants' memory performance was indistinguishable between the saccade and no saccade trials. Therefore, it could be that the preserved behavioral performance we observed is supported by these IPS representations, rather than the early visual cortex representations. In a more recent study, Lorenc et al. (2018) found that the VWM information could be reliably maintained only in early visual cortex without distractors. However, these early visual cortex representations seem to transfer to the IPS representations when distractors were presented, which suggesting a flexible coding of VWM between the early visual cortex and the IPS depending on the task demands. This shows that VWM information maintained in visual cortex is susceptible to interference, in line with the idea that the early visual cortex may only play a limited role in VWM storage.

3
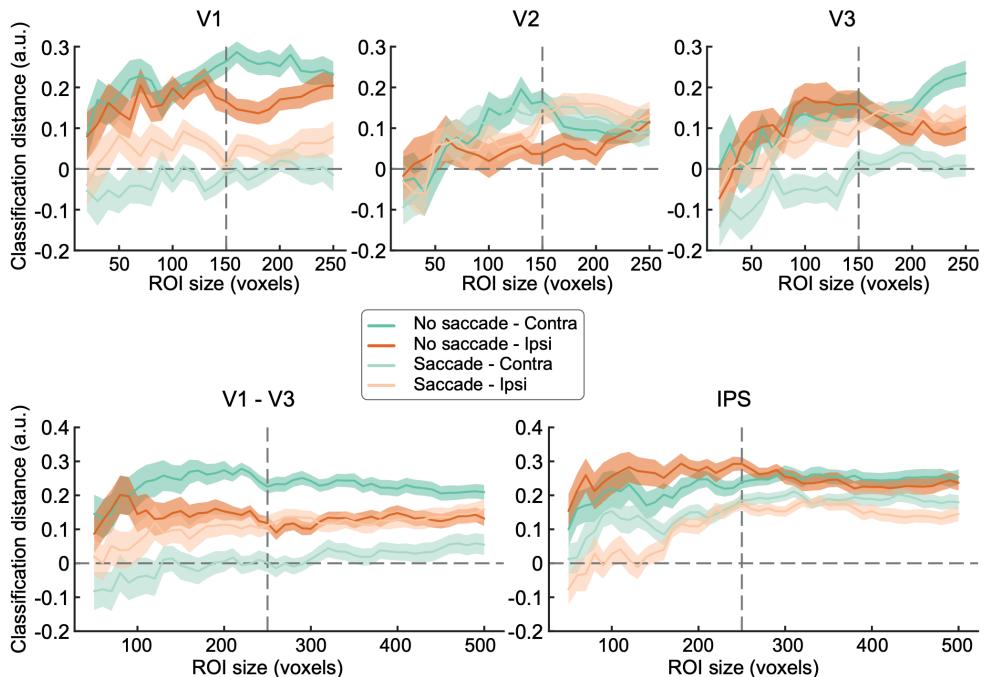
CONCLUSION

In conclusion, our results indicate that VWM representations in early visual cortex are degraded and not remapped after eye movements, but stably represented in parietal cortex. These results suggest a limited role of early visual cortex in VWM storage.

SUPPLEMENTARY MATERIALS

Supplementary Figure 3.1. Orientation classification performance during the delay period in early visual areas separately. Same analysis as in **Figure 3.2** but performed in V1, V2 and V3 individually. The same pattern was observed as in **Figure 3.2**. Specifically, in no-saccade trials, orientation information was present in the contralateral hemisphere of V1 ($t_{(33)}$ = 3.701, p = 0.0008, Cohen's d = 0.64; BF_{10} = 39.988), V2 ($t_{(33)}$ = 2.460, p = 0.0193, Cohen's d = 0.43; BF_{10} = 2.48), and V3 ($t_{(33)}$ = 1.892, p = 0.0673, Cohen's d = 0.33; BF_{10} = 0.901), and also in the ipsilateral hemisphere of V1($t_{(33)}$ = 2.883, p = 0.0069, Cohen's d = 0.502; BF_{10} = 5.945) and V3 ($t_{(33)}$ = 3.147, p = 0.0035, Cohen's d = 0.548; BF_{10} = 10.688), but not V2 ($t_{(33)}$ = 0.612, p = 0.5447, Cohen's d = 0.107; BF_{10} = 0.219). In saccade trials, however, the classifier was not able to distinguish between grating orientations in the contralateral hemisphere of the V1 ($t_{(33)}$ = -0.174, p = 0.8627, Cohen's d = 0.03; BF_{10} = 0.186) and V3 ($t_{(33)}$ = 0.313, p = 0.7562, Cohen's d = 0.054; BF_{10} = 0.192), but not V2 ($t_{(33)}$ = 2.542, p = 0.0159, Cohen's d = 0.443; BF_{10} = 2.917), while the orientation information remained stable in the ipsilateral hemisphere of the V2 ($t_{(33)}$ = 2.306, p = 0.0276, Cohen's d = 0.395; BF_{10} = 1.848) and V3 ($t_{(33)}$ = 2.028, p = 0.0507, Cohen's d = 0.348; BF_{10} = 1.128), but not V1 ($t_{(33)}$ = 0.132, p = 0.8959, Cohen's d = 0.023; BF_{10} = 0.185). The orientation information in the contralateral hemisphere of the V1 was significantly degraded by an eye movement ($t_{(33)}$ = 2.765, p = 0.0093, Cohen's d = 0.647; BF_{10} = 4.612). Error bars denote SEM. *No saccade – Contra*: No saccade condition, contralateral hemisphere; *No saccade – Ipsi*: No saccade condition, ipsilateral hemisphere; *Saccade – Contra*: Saccade condition, contralateral hemisphere; *Saccade – Ipsi*: Saccade condition, ipsilateral hemisphere. *p < 0.05; **p < 0.01; ***p < 0.001.

Supplementary Figure 3.2. Orientation classification performance during the delay period over a range of ROI sizes using a leave-one-run-out cross-validation method. Same analysis as in **Figure 3.2** but performed over a wide range of ROI sizes. In areas V1, V2, and V3, we rerun the analysis for ROIs of sizes ranging from 20 to 250 voxels in step of 10 voxels, while in areas V1 – V3 and IPS, the analysis was repeated for ROIs of sizes ranging from 50 to 500 voxels in step of 20 voxels. The dashed vertical line is at the predefined ROI of 150 voxels in areas V1, V2, and V3, or 250 voxels in areas combined V1 – V3 and IPS. The same pattern of effects was found for almost entire range of ROIs. Interestingly, in the combined V1 – V3, while WM information in the contralateral hemisphere was reduced after an eye movement (dark green line vs. light green line), it was persistently presented in the ipsilateral hemisphere for trials with and without a saccade (dark orange line vs. light orange line) over all range of ROIs. In IPS, however, no matter in the saccade or no-saccade condition, both the contralateral and ipsilateral hemispheres showed consistent orientation information over the range of ROIs, suggesting a robust VWM representation in this region.

Area	No saccade		Saccade	
	Contralateral	Ipsilateral	Contralateral	Ipsilateral
V1	0.264*** (t = 3.701, p = 0.0008; BF10 = 39.988)	0.165** (t = 2.883, p = 0.0069; BF_{10} = 5.945)	-0.013 (t = -0.174, p = 0.8627; BF_{10} = 0.186)	0.011 (t =0.132, p =0.8959; $BF_{1}0$ =0.185)
V2	0.166* (t = 2.460, p = 0.0193; BF_{10} = 2.48)	0.037 (t = 0.612, p = 0.5447; BF_{10} = 0.219)	0.159* (t = 2.542, p = 0.0159; BF_{10} = 2.917)	0.135* (t = 2.306, p = 0.0276; BF_{10} = 1.848)
V3	0.158 (t = 1.892, p = 0.0673; BF_{10} = 0.901)	0.158** (t = 3.147, p = 0.0035; BF_{10} = 10.688)	0.022 (t = 0.313, p = 0.7562; BF_{10} = 0.192)	0.114 (t = 2.028, p = 0.0507; BF_{10} = 1.128)
V1 – V3	0.226*** (t = 3.652, p = 0.0009; BF10 = 35.369)	0.118* (t = 2.192, p = 0.0356; BF_{10} = 1.501)	0.002 (t = 0.03, p = 0.9765; BF_{10} = 0.184)	0.112 (t = 1.905, p = 0.0655; BF_{10} = 0.92)
IPS	0.239*** (t = 4.451, p = 0.0001; BF_{10} = 272.079)	0.293*** (t = 5.075, p = 0.0000; BF_{10} = 1444.41)	0.184** (t = 3.13, p = 0.0036; BF_{10} = 10.276)	0.177* (t = 2.6, p = 0.0138; BF_{10} = 3.281)

Supplementary Table 3.1. Decoding distance over 7.2 – 10.8 seconds after the onset of the delay period for each ROI and post-hoc t-test of significant differences (see Figure 3.2). Dark grey cells indicate that there was a significant effect of saccade and hemisphere condition in that ROI, light grey cells represent the effect only reached a marginal significance, while cells indicate that there was no significant effect in that ROI. *p < 0.05; **p < 0.01; ***p < 0.001.

CHAPTER 4

ACTIVITY SUPPRESSION FOLLOWING STATISTICAL
LEARNING OF SPATIAL CONTEXT THROUGHOUT THE
VENTRAL VISUAL STREAM

ABSTRACT

Both spatial and temporal context play an important role in visual perception and behavior. Humans can extract statistical regularities from these contexts to help processing the present and to construct expectations about the future. Numerous studies have found reduced neural responses to expected stimuli compared to unexpected stimuli. However, most of these concerned expectations derived from temporal (sequential) regularities. Thus, little is known about the neural consequences of the statistical learning of spatial regularities. In the current fMRI study, thirty-three human volunteers were exposed to object stimuli that could be expected or surprising both in terms of their spatial and temporal context. We found a reliable modulation of neural responses by spatial context. Specifically, neural responses to stimuli in expected compared to unexpected spatial contexts were suppressed throughout the ventral visual stream. Surprisingly, we observed no additional modulation by temporal context. These results suggest that spatial context may be a more powerful modulator of neural responses than temporal context within the visual system.

INTRODUCTION

Humans are exquisitely sensitive to visual statistical regularities. Indeed, knowledge of both spatial and temporal context can facilitate visual perception and perceptual decision-making (Bar, 2004). For instance, in the case of spatial context, a foreground object is more easily identified when it appears on congruent backgrounds, compared to when it appears on incongruent backgrounds (Davenport & Potter, 2004). Facilitatory effects of temporal context have also been shown, for instance during exposure to successively presented stimuli, with faster and more accurate responses to expected compared to unexpected stimuli (Bertels et al., 2012; Hunt & Aslin, 2001; Richter & de Lange, 2019). At the same time neural responses have been shown to be modulated by temporal context, with a marked suppression of sensory responses to expected compared to unexpected stimuli, reported in humans (den Ouden et al., 2009; Egner et al., 2010; Richter et al., 2018; Richter & de Lange, 2019; Summerfield et al., 2008) and non-human primates (Freedman et al., 2006; Kaposvari et al., 2018; Meyer & Olson, 2011). However, little is known about the modulation of neural responses by spatial context. Human fMRI studies suggest that a similar network of (sub-)cortical areas is involved in spatial context learning as during learning of temporal sequences (Karuza et al., 2017). Thus, while the learning process of temporal and spatial learning may share characteristics, the consequences for sensory processing following the acquisition of spatial regularities remain unknown. Also, it is unclear if and how spatial and temporal context interact in terms of modulating sensory processing.

In the current study, we set out to concurrently examine the neural and behavioral consequences of spatial and temporal contextual expectations following statistical learning. To this end, participants were exposed to leading image pairs, consisting of two images presented left and right of fixation, which predicted the identity of trailing image pairs, thus rendering the trailing images expected based on the temporal context. Moreover, the simultaneously presented images were also predictive of each other, thus generating a predictable spatial context (see **Figure 4.1c**). Blood oxygenation level-dependent (BOLD) signals were recorded with functional magnetic resonance imaging (fMRI), while participants monitored the images for occasional target images (i.e., flipped object image) that occurred at unpredictable moments.

To preview our results, we show that spatial context strongly modulates sensory processing throughout key areas of the ventral visual stream, with pronounced reductions in neural responses to stimuli predicted by spatial context, compared to stimuli occurring in unexpected contexts. By comparison, there was no robust evidence for a modulation of neural responses by temporal context. The expectation suppression by spatial context occurred in similar cortical areas as implicated in previous studies that investigated temporal contextual regularities (Richter & de Lange, 2019). Combined our results suggest that spatial context is a stronger modulator of sensory processing than temporal context, but modulates the same neural network that we previously have found to be modulated by temporal context.

MATERIALS AND METHODS

Data and code availability

All data and code used for stimulus presentation and analysis is freely available on the Donders Repository (https://data.donders.ru.nl/login/reviewer-96936509/CX_hgbzoqZJ_Ok_yNk1ZugyXx0eRyfzu6w-wfhgOiXl).

Participants

Thirty-three healthy, right-handed participants (13 females, aged 22.36 ± 2.38 years, mean ± SD) were recruited in exchange for monetary compensation (100 Yuan/hour). All participants reported normal or corrected-to-normal vision and were prescreened for MRI compatibility, had no history of epilepsy or cardiac problems. The experiments reported here were approved by the Institutional Review Board of Psychological Sciences at Hangzhou Normal University and were carried out in accordance with the guidelines expressed in the Declaration of Helsinki. Written informed consent was obtained from all participants. Data from two participants were excluded. Of these two exclusions, one participant's behavioral performance of the post-scanning task was at chance level, while the other participant showed excessive head motion (i.e., a number of relatively head motion events exceeding 1 mm notably above the group mean).

Stimuli

The object images were a selection of stimuli from Brady et al. (2008), and also previously used by Richter and de Lange (2019). A subset of 48 full color object stimuli, comprised of 24 electronic objects and 24 non-electronic objects were shown during the present study. For each participant, 24 objects (12 electronics and 12 non-electronics) were pseudo-randomly selected, of which 6 (including 3 electronics) were pseudo-randomly assigned as left leading images, 6 (including 3 electronics) were appointed as right leading images, another 6 (including 3 electronics) served as left trailing images while the remaining 6 (including 3 electronics) acted as right trailing images. Therefore, each specific image could occur in any position or condition (left or right, leading or trailing), thereby minimizing potential biases by specific features of individual object stimuli. Image size was 5° x 5° visual angle presented on a mid-gray background. Stimuli

and their association remained the same during the behavioral learning session, MRI scanning and a post-scanning object categorization task. During the behavioral learning session and post-scanning test, object stimuli were presented on an LCD screen (ASUS VG278q, 1920 x 1080 pixel resolution, 60 Hz refresh rate). During MRI scanning, stimuli were displayed on a rear-projection MRI-compatible screen (SAMRTEC SA-9900 projector, 1024 x 768 pixel resolution, 60 Hz refresh rate), visible using an adjustable mirror mounted on the head coil.

Experimental design

Each participant completed two sessions on two consecutive days. The first session comprised a behavioral learning task while the second session included an fMRI task and a post-scanning object categorization task. While the stimuli and their associations were identical during both sessions, different tasks were employed.

Day one - Learning session. Each trial began with a black fixation dot (diameter = 0.4° visual angle) in the center of the screen, participants were asked to maintain fixation on the fixation dot throughout the trial. Two leading images were presented 1.5° visual angle left and right from the central fixation dot for 500 ms, immediately followed by two trailing images, without ISI, at the same locations for 500 ms (**Figure 4.1a**). Participants were required to count the pairs of same category objects (electronic vs. non-electronic) shown during the leading and trailing images and respond within 2000 ms after trailing image onset by pressing one of three response buttons (corresponding to none, one, or both; see *Pair counting task* below for details). Finally, feedback was presented for 500 ms, followed by a 1000 - 2000 ms ITI. 24 object images (12 electronics and 12 non-electronics) were pseudo-randomly preselected per participant from a pool of images, 12 of which were pseudo-randomly combined into pairs, forming a total of 6 leading image pairs (i.e., the first two images on a trial), while the remaining 6 pairs were used as trailing image pairs (i.e., the second two images on a trial). Crucially, during the learning session, the leading image pair was perfectly predictive of the identity of the trailing image pair [P(trailing pair | leading pair) = 1]. At the same time, the left and right images within both the leading and trailing image pairs were 100% predictive of one another (i.e., pairs always occurred together). Thus resulting in deterministic association in both spatial (co-occurrence) and temporal (sequence) contexts during learning session (see the most left

panel in **Figure 4.1c**). During the learning session each participant performed 5 blocks, with each block comprised of 216 trials, resulting in a total of 180 trials per pair during learning session. The learning session took approximately 60 minutes.

Day two – fMRI session. One day after the learning session, participants performed the fMRI session. This session started with one additional block identical to the behavioral learning session, including 216 trials, to renew the learned associations before MRI scanning. During MRI scanning, participants first performed 36 practice trials during acquisition of the anatomical image. The fMRI session was similar to the behavioral learning session, except for the following three modifications. First, a longer ITI of 2000 – 6000 ms (mean = 3000 ms) was used. Second, instead of counting pairs of the same category, participants were required to detect oddball images. Oddballs were the same object images, as shown before, but flipped upside-down, occurring on 10% of trials. Participants were instructed to respond to these target images by pressing a button as quickly as possible, while no response was required during trials without an oddball image. Crucially, whether an image was upside-down was completely randomized and could not be predicted on the basis of the statistical regularities that were present in the image sequences. Third, while the association between images remained the same as during the behavioral learning session, in the fMRI session also unexpected image pairs were shown. In particular, the transition matrices shown in **Figure 4.1b**, determined how often images were presented together. In 50% of trials, a leading image pair was followed by its expected trailing image pair, identical to the learning session, thus constituting the expected condition. For instance, L_{L1} (leading image, left 1) and L_{R1} (leading image, right 1) served as leading image pair for T_{L1} (trailing image, left 1) and T_{R1} (trailing image, right 1). In the other half of trials, one of the three unexpected conditions (temporally unexpected context, spatially unexpected context, both temporally and spatially unexpected context) occurred with equal possibilities, resulting in 16.67% per unexpected condition. Specifically, for the temporal unexpected context (**Figure 4.1c** left middle panel), after presenting a leading image pair, one of the other five unmatched trailing image pairs would occur. Thus, while the two images within both the leading and trailing image pair were still expected (i.e., no spatial expectation violation), the temporal sequence of images was unexpected. For example, in this condition L_{L1} and L_{R1} were followed by T_{L2} and T_{R2}. For the spatially unexpected context (**Figure 4.1c** right middle panel), each leading image was

followed by its expected trailing image (e.g., $L_{L1} \rightarrow T_{L1}$ and $L_{R2} \rightarrow T_{R2}$). However, the two images presented during both the leading and trailing image period were not usually paired; e.g., L_{L1} x $L_{R2} \rightarrow T_{L1}$ x T_{R2}). Thus, in this condition spatial context expectations were violated, while temporal context was expected, thus constituting the spatially unexpected condition. In a final condition, both, spatial and temporal context were violated (**Figure 4.1c** most right panel). In particular, all four images shown during this condition did not appeared together in the learning session. Crucially, the expectation status only depended on the usual association between the leading image pair and trailing image pair, rather than the frequency or identity of an object image per se. In other words, each object image occurred as expected object and in each unexpected condition. Therefore, all images occurred equally often throughout the experiment, ruling out potential confounds of stimulus frequency or familiarity. Feedback on behavioral performance (accuracy) was provided after each run.

During MRI scanning, each run consisted of 108 trials, including 54 expected trials, 18 temporal context violation trials, 18 spatial context violation trials and 18 trials where both spatial and temporal context were violated. The order of trials was randomized within each run. In total each participant performed 5 runs. Each run lasted ~12 minutes with 5 null events of 12 s that were evenly distributed across the run, which also served as brief resting periods. The first 8 s of fixation was discarded from analysis. Finally, after MRI scanning, a pair counting task, identical to the learning session was performed outside of the MRI scanner room, which took approximately 20 minutes (see *Pair counting task* below for details).

4
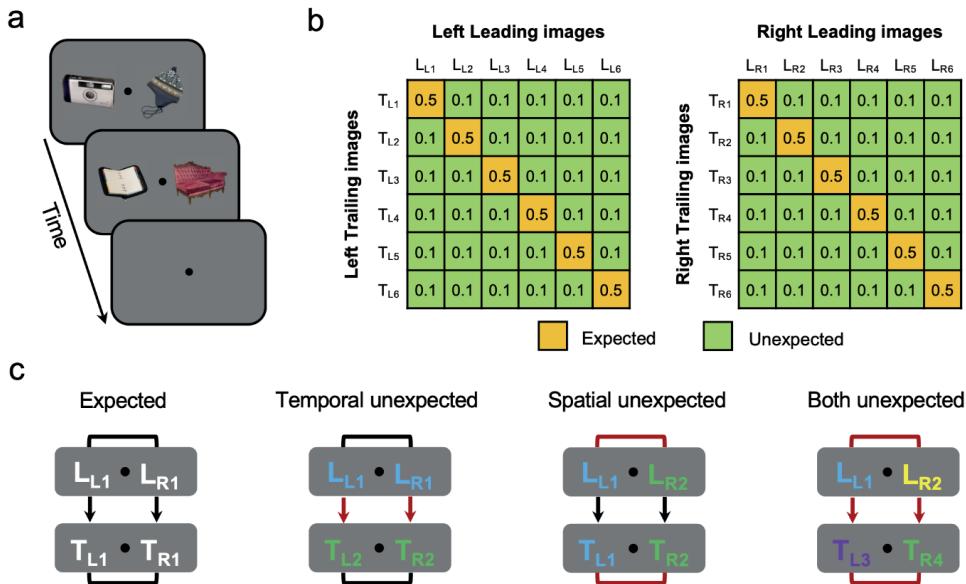
Figure 4.1. Experimental paradigm and design. (a) Experimental paradigm in both the behavioral learning and fMRI session. A trial starts with a 500 ms presentation of two leading images, presented 1.5° left and right from the central fixation dot. The two trailing images are immediately followed by the leading images, without ISI, at the same locations, also shown for 500 ms. Participants were asked to detect an infrequently presented upside-down version of the images (~10% of trials). Trailing images were followed by a 2 - 6 s (mean 3 s) ITI period. **(b)** Shown are the image transition matrices determining the statistical regularities between leading and trailing images during MRI scanning. On the left, L_{L1} to L_{L6} represent the six leading images presented on the left of the fixation dot, while T_{L1} to T_{L6} represent the associated six left trailing images. Similarly, L_{R1} to L_{R6} represent the six right leading images, while T_{R1} to T_{R6} represent the six right trailing images. Yellow cells indicate image pairs that are expected by temporal context, while green denotes unexpected image pairs. Numbers represent the probability of that cell during MRI scanning. Crucially, the left and right images were also associated with each other, constituting the spatial context. For instance, L_{L1} was associated with L_{R1}, and T_{L1} was associated with T_{R1}. In this case, L_{L1}, L_{R1}, T_{L1} and T_{R1} composed two image pairs that were expected in both the temporal and spatial contexts (see **Figure 4.1c**, 'Expected'). **(c)** Illustration of the four expectation conditions during MRI scanning. Black lines indicate expected associations, while red lines indicate unexpected pairings. *Expected condition*: the matched image configuration that was shown during the behavioral learning session. *Temporally unexpected context*: both the two leading images (L_{L1} and L_{R1}) and two trailing images (T_{L2} and T_{R2}) were expected in terms of spatial context (same as the expected condition), the temporal association was violated (i.e., $L_{L1} \rightarrow T_{L2}$ and $L_{R1} \rightarrow T_{R2}$). *Spatially unexpected context*: while the leading image reliably predicted the identity of the trailing image on both the left ($L_{L1} \rightarrow T_{L1}$) and right ($L_{R2} \rightarrow T_{R2}$) side independently, thus retaining the expected temporal context, image pairs were not associated in terms of spatial context, neither during the leading images nor during the two trailing images (e.g., L_{L1} and L_{R2} occurring together). *Both unexpected*: shown were four images that do not appeared together in the expected condition. Therefore, the expectation violations occurred in both the temporal and spatial contexts.

Functional localizer. Following the main task runs during the fMRI session, two functional localizer runs were scanned. These localizer runs were used to define object-selective LOC, and to select voxels that were maximally responsive to the relevant object images. For each participant, the same 12 trailing images that were previously seen in the main task runs and their phase-scrambled version were presented during the localizer. Images were presented at the left and right from the center of screen, corresponding to the location where the stimuli were shown during the main task runs. Each image was shown for 11 s, alternating between the left and right side. Images flashed with a frequency of 2 Hz (300 ms on, 200 ms off). Throughout the localizer, participants were instructed to fixate the fixation dot, while monitoring for an unpredictable dimming of the stimulus (dimming period = 300 ms). Participants responded as quickly as possible by pressing a button. In each run, 4 null events of 11 s were evenly inserted, and each trailing image and its phase-scrambled version was presented two times. The order of trials was fully randomized, except for excluding direct repetitions of the same image. Each participant completed two localizer runs, with each run lasting 9.53 minutes. In total each image and its phase-scrambled version was presented 4 times.

Pair counting task. Because the oddball detection performed during fMRI scanning does not relate to the underlying statistical regularities, and therefore does not indicate whether statistical regularities were indeed learned, an additional pair counting task was performed after fMRI scanning. In this task, participants were asked to count the number of pairs of the same object category shown on each trial. Participants were further instructed to respond as quickly and accurately as possible. Thus, this task was the same as the task performed during the behavioral learning session, except that the three unexpected conditions were also included. The rationale of this task was to gauge the learning of the object pairs (i.e., statistical regularities) in terms of both temporal and spatial context. Participants could benefit from the knowledge of the associations between the image pairs, as both knowledge about the co-occurrence and temporal sequence would allow for faster responses. Therefore, the performance difference (e.g., accuracy and reaction time) between the expected condition and each unexpected condition could be considered as an indication for the learning of the underlying statistical regularities. In total, participants performed 360 trials split into 2 blocks, including 180 expected trials, 60 temporally unexpected context trials, 60 spatially unexpected context trials and 60

trials in which both spatial and temporal context were unexpected. The pair counting task took approximately 20 minutes.

fMRI parameters

Functional and anatomical images were acquired on a 3.0T GE MRI-750 system (GE Medical Systems, Waukesha, WI, USA) at Hangzhou Normal University, using a standard 8-channel headcoil. Functional images were acquired in a sequential (Bottom/Up) order using a T2*-weighted gradient-echo EPI pulse sequence (TR/TE = 2000/30 ms, voxel size 2.5 x 2.5 x 2.3 mm, 0.2 mm slice space, 36 transversal slices, 75° flip angle, FOV = 240 mm^2). Anatomical images were acquired using a T1-weighted inversion prepared 3D spoiled gradient echo sequence (IR-SPGR) (inversion time = 450 ms, TR/TE = 8.2/3.1ms, FOV = 256 x 256 mm^2, voxel size 1 x 1 x 1 mm, 176 transversal slices, 8° flip angle, parallel acceleration = 2).

Data analysis

Behavioral data analysis

Behavioral data from the pair counting task was analyzed in terms of response accuracy and RT. RT was calculated relative to the onset of the trailing image objects. Only trials with correct responses were included in RT analysis. Additionally, we excluded trials with RTs shorter than 200 ms (0.82%) or more than three standard deviations above the subject's mean response time (0.49%). RT and accuracy data for expected and unexpected trailing image trials were averaged separately per participant and across subjects subjected to a paired t test. The effect size was calculated in terms of Cohen's d_z for all paired t-test, while partial eta-squared (η2) was used for indicating effect sizes in the repeated measures ANOVA (Lakens, 2013).

fMRI data preprocessing

fMRI data preprocessing was performed using FSL 6.0.1 (FMRIB Software Library; Oxford, UK; www.fmrib.ox.ac.uk/fsl; Smith et al., 2004, RRID:SCR_002823). The preprocessing pipeline included brain extraction (BET), motion correction (MCFLIRT), slice timing correction (Regular up), temporal high-pass filtering (128 s), and spatial smoothing for univariate analyses (Gaussian kernel with FWHM of 5 mm). Functional images were registered to the anatomical image using FSL FLIRT (BBR) and to the MNI152 T1 2 mm template brain (linear registration

with 12 degrees of freedom). Registration to the MNI152 template brain was only applied for whole-brain analyses, while all ROI analyses were performed in each participant's native space in order to minimize data interpolation.

Whole brain analysis

To estimate the BOLD response to expected and unexpected stimuli across the entire brain, FSL FEAT was used to fit voxel-wise general linear models (GLM) to each participant's run data in an event-related approach. In the first level GLMs, expected and three unexpected image object trials were modeled as four separate regressors with a duration of one second (the combined duration of leading and trailing image pairs), and convolved with a double gamma hemodynamic response function. An additional nuisance regressor for oddball trials (upside-down images) was added. Additionally, first-order temporal derivatives for the five regressors, and 24 motion regressors (FSL's standard + extended motion parameters) were also added to the GLM. To quantify expectation suppression, we contrasted each unexpected regressor and the expected regressor (e.g., spatial context expectation suppression = $BOLD_{Spatially\ unexpected\ context}$ – $BOLD_{Expected\ context}$). Data were combined across runs using FSL's fixed effect analysis. For the across-participants whole-brain analysis, FSL's mixed effect model (FLAME 1) was used. Multiple-comparison correction was performed using Gaussian random-field based cluster thresholding. The significance level was set at a cluster-forming threshold of $z > 3.1$ (i.e., $p < 0.001$, two-sided) and a cluster significance threshold of $p < 0.05$.

Regions of interest (ROIs) analysis

ROI analyses were conducted in each participant's native space. Primary visual cortex (V1), object-selective lateral occipital complex (LOC), and temporal occipital fusiform cortex (TOFC) were chosen as the three ROIs (see *ROI definition* below) for analysis, based on two previous studies that used a highly similar experimental setup (Richter et al., 2018; Richter & de Lange, 2019). The mean parameter estimates were extracted from each ROI for the expected and unexpected conditions separately. For each ROI, these data were submitted to a one-way repeated measures ANOVA with the different levels of expectation (expected context, temporally unexpected context, spatially unexpected context, both unexpected contexts) as four levels.

ROI definition. All ROIs were defined using independent data from the localizer runs. Specifically, V1 was defined based on each participant's anatomical image, using Freesurfer 6.0 to define the gray–white matter boundary and perform cortical surface reconstruction (recon-all; Dale et al., 1999; RRID:SCR_001847). The resulting surface-based ROI of V1 was then transformed into the participant's native space and merged into one bilateral mask. Object selective LOC was defined as bilateral clusters, within anatomical LOC, showing a significant preference for intact compared to scrambled object stimuli during the localizer run (Haushofer et al., 2008; Kourtzi & Kanwisher, 2001). To achieve this, intact objects and scrambled objects were modeled as two separate regressors in each participant's localizer data. The temporal derivatives of all regressors and the 24 motion regressors were also added to fit the data. Finally, the contrast of interest, objects minus scrambles, was constrained to anatomical LOC. In order to create the TOFC ROI mask, the anatomical temporal-occipital fusiform cortex mask from the Harvard-Oxford cortical atlas (RRID:SCR_001476), distributed with FSL, was further constrained to voxels showing a significant conjunction inference of expectation suppression on the group level in Richter et al. (2018) and Richter and de Lange (2019). The resulting mask was then transformed from MNI space to each participant's native space using FSL FLIRT. Finally, the 200 most active voxels in each of the three ROI masks were selected for further statistical analyses. To this end, the contrast interest between the left and right hemisphere in V1 (including both the intact and scrambled images) was calculated, while in LOC and TOFC, the contrast interest between the intact images and the scrambled images was calculated based on the localizer data. The resulting z-map of this contrast was then averaged across runs. Finally, we selected the 200 most responsive voxel from this contrast. In order to verify that our results did not depend on the a priori defined, but arbitrary number of voxels in the ROI masks, we repeated all ROI analyses with masks ranging from 50 to 500 voxels in steps of 50 voxels.

Bayesian analysis

In order to further evaluate any non-significant results, and arbitrate between an absence of evidence and evidence for the absence of an effect, the Bayesian equivalents of the above outlined analyses were additionally performed. JASP 0.10.2 (JASP Team, 2019, RRID:SCR_015823) was used to perform all Bayesian analyses, using default settings. Thus, for Bayesian t-tests a Cauchy prior width of 0.707 was chosen. Qualitative interpretations of Bayes Factors are based on criteria by Lee and Wagenmakers (2014).

RESULTS

We exposed participants to statistical regularities by presenting two successive object image pairs in which the leading image pairs predicted the identity of the trailing image pairs with 100% reliability. Therefore, the identities of the image pairs were also fixed in terms of the spatial context; i.e., simultaneously shown left and right images always occurred together. Subsequently, in the MRI scanner, participants were shown the same object image pairs (expected), but additional expectation violations were introduced. In particular, either the temporal context was violated, or the spatial context was broken, or a combination of both expectation violations (both unexpected).

Violations of spatial context strongly modulate sensory processing throughout the ventral visual stream

We first investigated the consequences of violating perceptual expectations by contrasting between each unexpected condition and the expected condition within our a prior defined ROIs (**Figure 4.2a**): primary visual cortex (V1), object-selective lateral occipital complex (LOC), and temporal occipital fusiform cortex (TOFC). In both LOC and TOFC, we observed a significant difference in BOLD responses depending on whether the stimulus was unexpected or expected (LOC: $F_{(3, 96)} = 11.654$, $p = 1.4e\text{-}6$, η2 $= 0.267$; TOFC: $F_{(3, 96)} = 12.915$, $p = 3.7e\text{-}7$, η2 $= 0.288$). In particular, spatially unexpected stimuli elicited a larger response than expected stimuli (LOC: $t_{(32)} = 5.186$, $p = 1.2e\text{-}5$, Cohen's $d_z = 0.903$; TOFC: $t_{(32)} = 3.0$, $p = 0.0052$, Cohen's $d_z = 0.522$), as did stimuli when both spatial and temporal expectations were violated (LOC: $t_{(32)} = 6.292$, $p = 4.7e\text{-}7$, Cohen's $d_z = 1.095$; TOFC: $t_{(32)} = 6.059$, $p = 9.2e\text{-}7$, Cohen's $d_z = 1.055$).
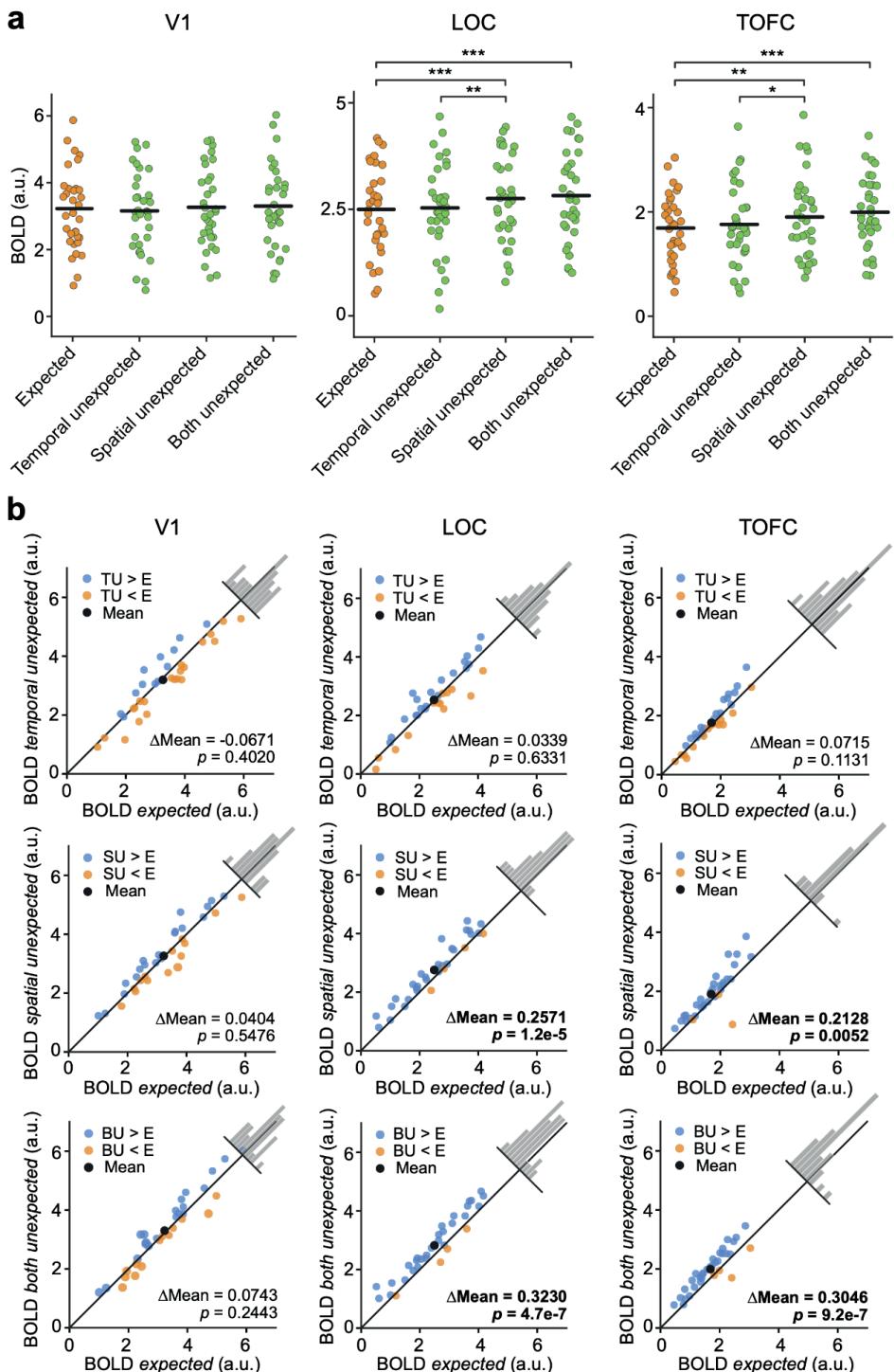
Figure 4.2. Expectation suppression within V1, LOC and TOFC. **(a)** Parameter estimates for responses to expected and unexpected images pairs. In both LOC and TOFC, BOLD responses to spatial and both, spatially and temporally unexpected image pairs were significantly stronger than to expected image pairs. Responses to spatially unexpected context were also significantly stronger than the responses to temporally unexpected context. No reliable difference was found between BOLD responses to all four conditions in V1. Each dot denotes an individual participant and the black line is the mean across participants. *$p < 0.05$, **$p < 0.01$, ***$p < 0.001$. **(b)** BOLD responses evoked by each unexpected and expected context within V1 (left column), LOC (middle column) and TOFC (right column). The upper row represents the BOLD contrast between the temporally unexpected context and expected context. The middle row represents the BOLD contrast between the spatially unexpected context and expected context. The bottom row represents the BOLD contrast between the context where both, spatial and temporal context are violated. Blue and yellow dots represent individual participants. Blue indicates expectation suppression (unexpected > expected), yellow indicates expectation enhancement (unexpected < expected), and black indicates the mean of all subjects. ΔMean is equal to the difference of BOLD response between the unexpected and expected condition. The inset histogram shows the distribution of deviations from the unity line.

However, we did not find a reliable modulation of response by temporal context violations in either the LOC or TOFC (LOC: $t_{(32)} = 0.482$, $p = 0.6331$, Cohen's $d_z = 0.084$; TOFC: $t_{(32)} = 1.629$, $p = 0.1131$, Cohen's $d_z = 0.284$). The absence of the temporal contextual expectation effect was further supported by the lack of a difference in BOLD responses between the conditions in which either only spatial context was unexpected and both spatial and temporal context were unexpected (LOC: $t_{(32)} = 1.103$, $p = 0.2781$, Cohen's $d_z = 0.192$; TOFC: $t_{(32)} = 1.830$, $p = 0.0765$, Cohen's $d_z = 0.319$). Indeed, Bayesian analyses showed that there was a moderate support for the absence of an effect of temporal context ($BF_{10} < 1/3$) in LOC (temporally unexpected context vs. expected context: $BF_{10} = 0.207$; spatially unexpected context vs. both unexpected: $BF_{10} = 0.325$). However, there was only anecdotal evidence for the absence of the temporal context effect in TOFC (temporally unexpected context vs. expected context: $BF_{10} = 0.613$; spatially unexpected context vs. both unexpected: $BF_{10} = 0.825$). In addition, the difference between the temporal and spatial context effect was confirmed by a larger BOLD response to spatially unexpected than temporally unexpected contextual stimuli (LOC: $t_{(32)} = 2.870$, $p = 0.0072$, Cohen's $d_z = 0.50$; TOFC: $t_{(32)} = 2.575$, $p = 0.0149$, Cohen's $d_z = 0.448$). Thus, these results suggest that expectations derived from spatial, but not temporal, statistical regularities strongly modulate sensory processing in intermediate (LOC) and higher visual areas (TOFC).

Perhaps surprisingly, we did not find any reliable differences between all four expectation conditions in V1 ($F_{(3, 96)}$ = 1.202, p = 0.3131, η2 = 0.036). Indeed, in V1, Bayesian analyses yielded moderate evidence for the absence of a modulation of neural responses by temporal and spatial context violations (temporally unexpected context vs. expected context: BF_{10} = 0.26; spatially unexpected context vs. expected context: BF_{10} = 0.221), and anecdotal support for the absent of an effect when both spatial and temporal context were simultaneously violated (both unexpected context vs. expected context: BF_{10} = 0.354).

To ensure that these results were not dependent on the a prior but arbitrarily chosen mask sizes of the ROIs, we repeated the analyses for ROIs of sizes ranging from 50 to 500 voxels in step of 50 voxels. Results, summarized in **Supplementary Figure 4.1**, were qualitatively identical to those mentioned above (**Figure 4.2a**) for all ROI sizes within all three ROIs (V1, LOC, TOFC), indicating that our results do not depend on ROI size but well represent results within the ROIs.

4
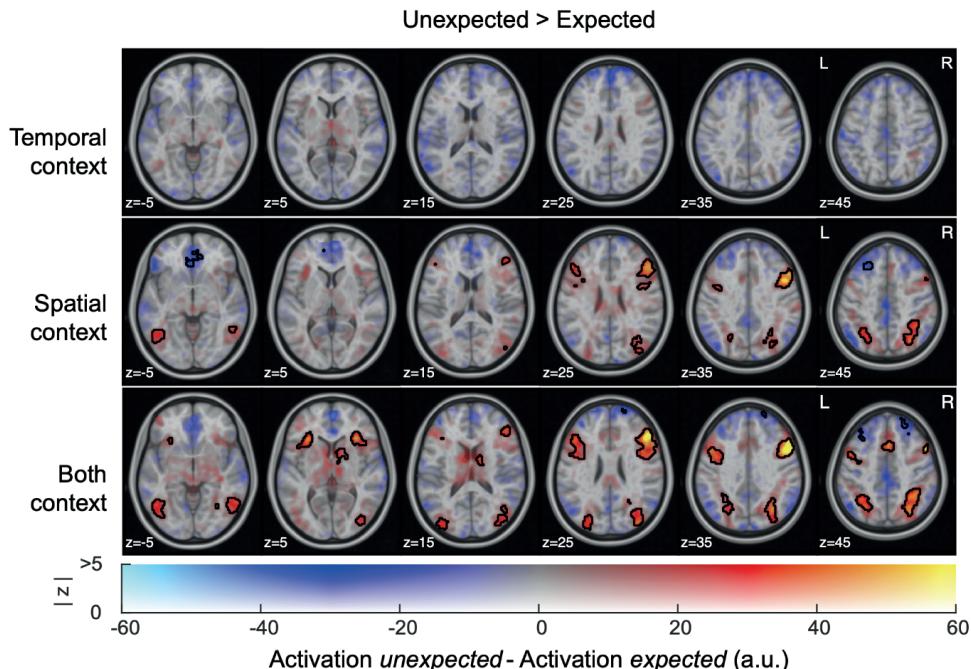
Figure 4.3. Expectation suppression across cortex for each of the three unexpected conditions. Displayed are parameter estimates for unexpected minus expected image pairs overlaid onto the MNI152 2 mm anatomical template. Color represents the unthresholded parameter estimates: red-yellow clusters denote expectation suppression, blue-cyan clusters indicate expectation enhancement; opacity indicates the z statistics of the contrast. Black contours outline statistically significant clusters (Gaussian random field cluster corrected). No significant clusters were found when contrasting between the temporally unexpected context and expected context (upper row). However, for both the spatial expectation violation (middle row) and both, spatial and temporal context violation (bottom row) significant clusters showing expectation suppression were observed in parts of the ventral visual stream (LOC, TOFC), as well as frontal gyrus, anterior insular and superior parietal lobule.

A whole-brain analysis was also performed to investigate the effects of both the temporal context and spatial context outside of our predefined ROIs. Results are illustrated in **Figure 4.3**. While there were significant clusters (black contours) of expectation suppression across the ventral visual stream compared to the conditions in which spatial or both contexts were unexpected (middle and bottom row), there was no evidence for activity differences with the temporally unexpected context (upper row). Moreover, outside the ventral visual stream, additional clusters of expectation suppression were evident. These clusters included bilateral

middle frontal gyrus, superior and inferior frontal gyrus, precentral gyrus, paracingulate gyrus, bilateral frontal operculum and anterior insular, as well as the bilateral superior parietal lobule. Similar to the ventral visual stream, these non-sensory clusters showed reduced BOLD responses for expected object image pairs compared to spatially and spatio-temporally unexpected contexts. There was no significant modulation of activity by temporal contextual expectations anywhere in the whole brain analysis.

Expectations facilitate object categorization

In addition to the neural effects of expectations, we also examined whether behavioral benefits of expectations were evident. During a post-scanning object categorization task, participants were asked to count the pairs of same category objects shown during the leading and trailing image pairs. In order to fulfill this task, as quickly and accurately as possible, participants could benefit from the knowledge of the underlying statistical regularities – both in terms of co-occurrence (spatial) and sequence (temporal) prediction. In line with our hypothesis, RTs and accuracy of responses (**Figure 4.4**) were affected by expectations (RT: $F_{(3, 96)}$ = 95.754, p = 9.5e-29, η2 = 0.75; accuracy: $F_{(3, 96)}$ = 83.556, p = 1.2e-26, η2 = 0.723). Specifically, participants were faster and more accurate in response to expected objects compared to objects in all unexpected conditions (RT: Temporally unexpected context vs. Expected context: ΔMean = 159 ms, p = 1.2e-10, Cohen's d_z = 1.624; Spatially unexpected context vs. Expected context: ΔMean = 293 ms, p = 1.2e-15, Cohen's d_z = 2.433; Both unexpected context vs. Expected context: ΔMean = 281 ms, p = 2.6e-13, Cohen's d_z = 2.076; accuracy: Temporally unexpected context vs. Expected context: ΔMean = 17%, p = 1.02e-8, Cohen's d_z = 1.332; Spatially unexpected context vs. Expected context: ΔMean = 28%, p = 2.7e-12, Cohen's d_z = 1.894; Both unexpected context vs. Expected context: ΔMean = 27%, p = 2.3e-12, Cohen's d_z = 1.909). Mirroring the results of the neural data, spatial context expectations affected RTs and accuracy more strongly than temporal context expectations (RT: $t_{(32)}$ = 8.117, p = 2.9e-9, Cohen's d_z = 1.424; accuracy: $t_{(32)}$ = 6.713, p = 1.4e-7, Cohen's d_z = 1.413). In short, behavioral performance benefitted from both temporal and spatial context expectations, and more strongly from spatial than temporal context.
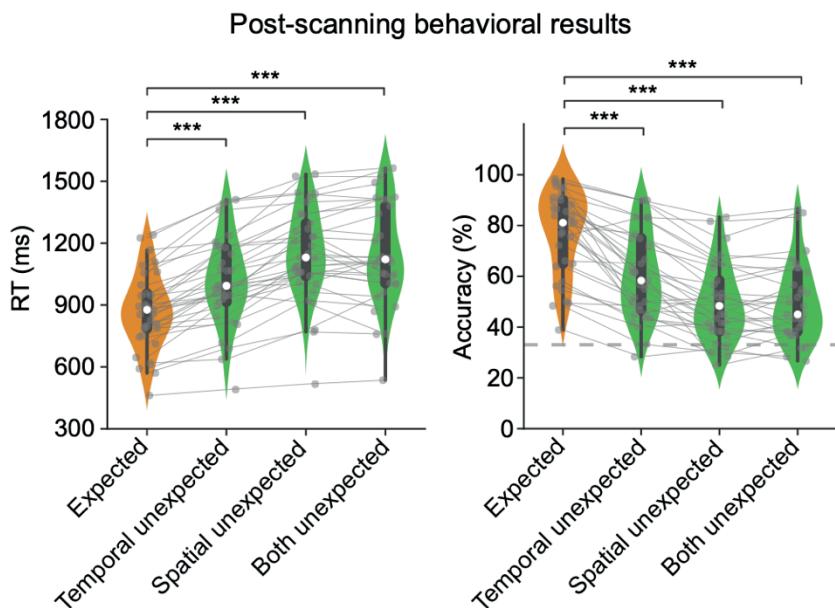
Figure 4.4. Behavioral data indicate statistical learning. Reaction time (left) and accuracy (right) are plotted for expected and unexpected conditions, respectively. Behavioral responses in the expected condition are significantly faster and more accurate than in the unexpected conditions. Dashed horizontal gray line indicates chance level accuracy (33.33%). Gray dots with connecting lines represent individual participants. White dots, boxes and whiskers represent between-subject medians, quartiles and 1.5 interquartile ranges, respectively. ***$p < 0.001$.

Spatial and temporal context violations modulate neural responses in similar cortical areas
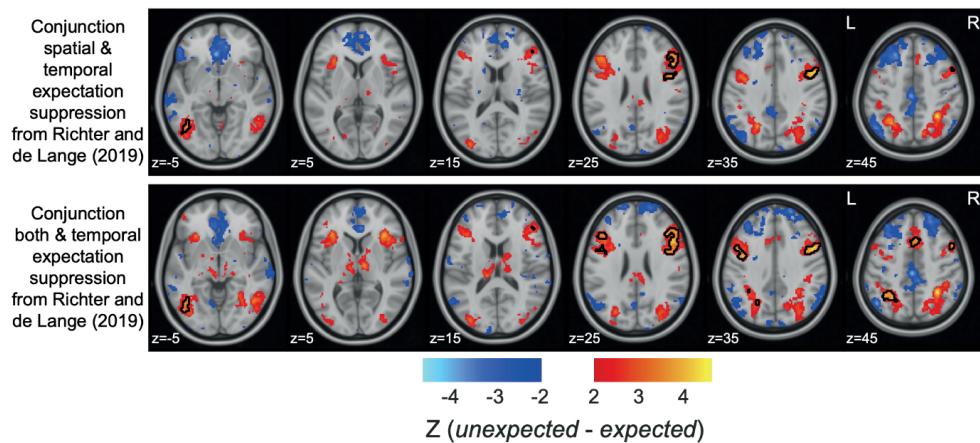

Figure 4.5 Displayed are z statistics of the contrast between unexpected and expected of a conjunction inference between data from the spatial (top) and both contexts violation (bottom) and data from a temporal context violation effect from Richter and de Lange (2019). Significant overlaps in expectation suppression include clusters in parts of the ventral visual stream, middle and inferior frontal gyrus, and precentral gyrus. This overlap suggests analogous underlying neural modulations for temporal and spatial context violations.

Given the behavioral effect of temporal context violations, and the prevalence of expectation suppression reported in previous studies investigating temporal context violations, it is suprising that we did not find evidence of temporal expectation effects in the present data. It is possible that experimental design choices contributed to this absence, as we will discuss later (see Discussion). Interestingly however, a qualitative inspection of the spatial pattern of the here reported spatial expectation suppression effect suggests a substiantial overlap with temporal expectation suppression shown in previous studies. In an explorative analysis, we formalized this assessment by conducing a conjunction analysis. In this conjunction, we analyzed the overlap in expectation suppression between previously reported temporal expectation suppression from Richter and de Lange (2019) and the present spatial and combined (spatial and temporal) expectation violation. Results illustrated in **Figure 4.5**, show clusters of expectation suppression that overlap between the temporal context and spatial context violations (top row), as well as the combined spatial and temporal context violation (bottom row), throughout parts of the ventral visual stream, and several non-sensory areas, including middle and inferior frontal gyrus,

precentral gyrus. Thus, spatial context violations, as observed here, and temporal context violations, as reported by Richter and de Lange (2019), are observed in a highly similar neural network.

DISCUSSION

Both spatial and temporal context play an important role in visual perception and behavior. The present study investigated the neural consequences of spatial and temporal context violations across the ventral visual stream. To this end, we exposed participants to two forms of statistical regularities, making stimuli predictable in terms of spatial context (co-occurrence of stimuli at specific locations) and temporal context (specific temporal sequence of stimuli). Image transitions were not task relevant during fMRI scanning, and thus the observed neural modulations by spatial and temporal context are not dependent on task-relevance of the underlying statistical regularities. We found a reliable and wide-spread activity modulation in the ventral visual stream as a function of spatial context. In other words, when stimuli frequently co-occurred neural responses were suppressed compared to the response to the same stimulus co-occurring with another stimulus, even though all stimuli were equally familiar and always occurred at the same spatial position. Contrary to previous studies (e.g., Summerfield et al., 2008; Alink et al., 2010; Kok et al., 2012; Richter et al., 2018; Richter and de Lange, 2019), we did not find evidence for a modulation of neural responses by temporal context (i.e., predictability of stimulus sequence).

Behavioral facilitation by spatial and temporal context

Our data showed a substantial and robust facilitation of behavioral responses by both spatial and temporal contexts. During a post-scanning test, requiring participants to count stimulus pairs of the same category (i.e., both electronic, or both non-electronic stimuli), knowledge of spatial and temporal contexts strongly benefited behavioral performance (**Figure 4.4**). Specifically, responses were faster and more accurately to stimuli presented in a spatially and temporally expected context, and the violation of either context increased RTs and decreased response accuracy – with larger decrements for spatial context violations. Thus, our data show that participants can learn and benefit from both spatial and temporal statistical regularities simultaneously, supporting and extending conclusions from previous studies (e.g., Hunt and Aslin, 2001; Conway and Christiansen, 2009; Richter et al., 2018; Richter and de Lange, 2019).

Spatial context modulates sensory processing throughout the ventral visual stream

Our results show that sensory responses, in object selective visual areas (LOC and TOFC; Kourtzi and Kanwisher, 2001; Richter and de Lange, 2019), to object stimulus pairs are suppressed, if stimuli occur in expected spatial context compared to unexpected spatial context. In other words, stimuli that frequently co-occur evoke reduced sensory responses than the same stimuli in less frequently co-occurring configurations, even though the frequency of the individual stimuli are equal (thereby excluding potentially confounding effects of stimulus frequency or familiarity). This observation matches key characteristics of expectation suppression, a phenomenon previously described in terms of suppressed sensory responses to expected compared to unexpected stimuli by virtue of temporal context; i.e., a leading image predicting the identity of a trailing image (Brady and Oliva, 2008; Meyer and Olson, 2011; Richter et al., 2018; Richter and de Lange, 2019). Indeed, using a conjunction analysis we showed that here the observed spatial context suppression is evident in similar cortical areas as previously reported temporal context suppression (Gheysen et al., 2011; Turk-Browne et al., 2009, 2010). Interestingly, this overlap in cortical regions showing expectation suppression was not just limited to object selective visual cortex, but also included several non-sensory areas, such as inferior frontal gyrus. Hence, these results suggest that spatial and temporal contexts can have similar modulatory effects on neural processing, thereby implying that the neural mechanism underlying contextual prediction effects may be independent of the type of context. In agreement with this suggestion, Karuza et al. (2017) reported similar neural modulations, and correlations of these modulations with behavior, during learning of spatial regularities, as previous studies reported for statistical learning of temporal (sequence) regularity (Turk-Browne et al., 2009). Thus, combined the available data suggest that the neural architecture and computations underlying different types of context predictions may largely overlap, evident in both behavioral and neural responses.

No modulation of neural responses by temporal context

While the present data showed a modulation of neural responses by spatial context, we failed to find any reliable modulation by temporal context. Given the multitude of previous

studies reporting modulations of sensory processing by temporal context (Abla et al., 2008; Abla & Okanoya, 2008; Cunillera et al., 2009; Gheysen et al., 2010; Karuza et al., 2013; McNealy et al., 2006; Meyer & Olson, 2011; Plante et al., 2015; Richter et al., 2018; Richter & de Lange, 2019; Tobia, Iacovella, Davis, et al., 2012; Tobia, Iacovella, & Hasson, 2012; Tremblay et al., 2013; Turk-Browne et al., 2009, 2010), the absence of a modulation in the present data is surprising. In the following we will discuss some potential reasons for the absence of a modulation by temporal context in the present data.

First, we consider modality specific constraints. Vision is particularly apt to handle simultaneous inputs and the spatial structure between these simultaneous stimuli, while audition on the other hand shows a remarkable sensitivity to the temporal structure of inputs (Conway & Christiansen, 2009; Kubovy, 1988; Saffran, 2002). Indeed, such modality specific constraints can affect the manner in which stimuli are perceived (Mahar et al., 1994; Repp & Penel, 2002), maintained in working memory (Collier & Logan, 2000; Penney, 1989) and learned (Conway & Christiansen, 2009; Handel & Buffardi, 1969; Saffran, 2002). Thus, it is plausible that similar modality specific biases affect statistical learning. Accordingly, previous studies support this interpretation by showing that statistical learning in the non-preferred mode of processing (e.g., temporal context during statistical learning of visual stimuli) was negatively affected by reducing stimulus duration, while learning in the preferred mode (spatial context) was not (Conway & Christiansen, 2009). The presentation duration in the present experiment may have indeed been fast, given the low behavioral performance during the post-scanning test; i.e., the performance near chance level for the unexpected conditions suggest a strong dependence on statistical regularities to successfully perform the task. Thus, modality specific constraints may imply a significantly larger sensitivity to spatial compared to temporal statistical regularities.

However, while the above account may predict larger effects of spatial compared to temporal context on neural processing, this alone does not explain the absence of any modulation by temporal context. Indeed, if we take the absence of a temporal modulation at face value, it suggests that as a result of the modality specific bias towards spatial regularity in vision, spatial expectations may overwrite temporal ones. The rationale is that, during a temporal context violation, spatial context was preserved (expected). Hence, if vision is biased towards spatial
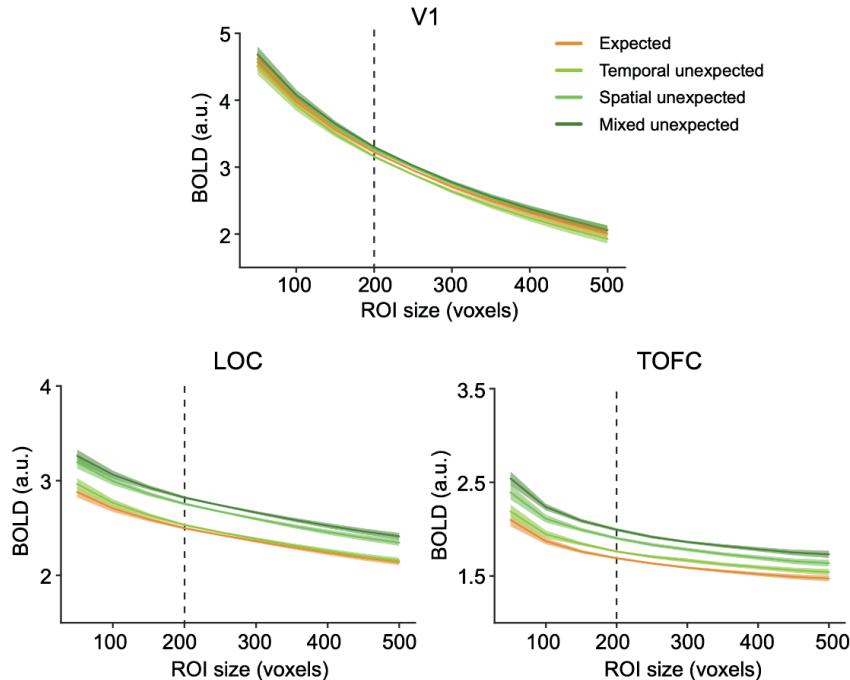
over temporal information, as argued above, it is possible that the confirmation of spatial context took precedence over the violation of temporal context. Therefore, the prediction violation of temporal context may not be evident, if spatial context is preserved. Computationally speaking, on a predictive coding account, a possible interpretation is that the prediction necessary to evoke temporal expectation suppression, may not have been instantiated (Friston, 2005; Rao & Ballard, 1999).

That said, we do not believe that a concurrent neural modulation by spatial and temporal predictions are categorically impossible. Indeed, as previously noted, our behavioral results do show a modulation by both temporal and spatial contexts. However, the concurrent predictions may depend on task-specific parameters. During MRI scanning participants performed a detection task of unpredictable oddballs, hence making predictions task-irrelevant. Thus, the observed expectation suppression likely constitutes an automatic process, reflecting an automatic instantiation of the associated spatial context prior. Actively attending the predictive structure, particularly the temporal context may result in an activation of both spatial and temporal priors, as evident during the post-scanning behavioral test (counting of same category stimuli). In sum, one possible interpretation of the present results is that automatic predictions occurred only for the predominant mode of processing, in the case of vision spatial contexts, and/or overwrote predictions in non-preferred modes (i.e., here temporal context). While further work is necessary to empirically assess this explanation, it does account well for the previous and present results.
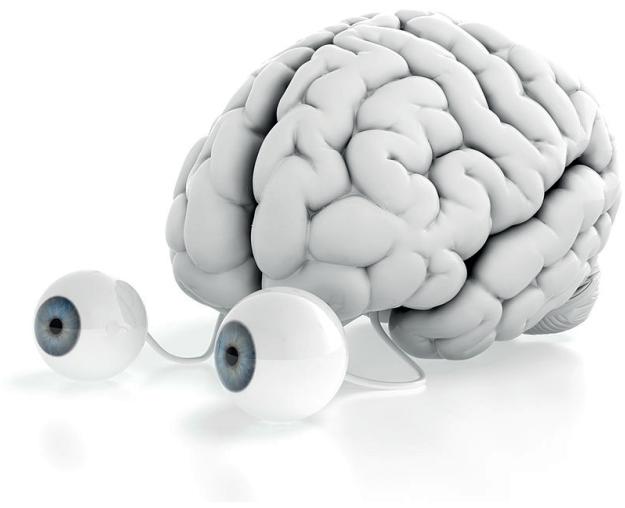
CONCLUSION

In conclusion, our data suggest that temporal and spatial statistical regularities can be simultaneously acquired, even without explicit instruction to learn. Subsequently, expectations based on temporal and spatial contexts can facilitate behavioral responses, leading to faster and more accurate responses. However, when statistical regularities are task-irrelevant, spatial context predictions may dominate over temporal context. The net result of this spatial dominance is a strong activity modulation by spatial context, but not by temporal context.

4

SUPPLEMENTARY MATERIALS

Supplementary Figure 4.1. The differences of the BOLD responses between each unexpected condition and the expected condition in our a prior defined ROIs (V1, LOC and TOFC) are stable over a range of ROI sizes. The dashed vertical line is at the predefined ROI of 200 voxels. Same analysis as in **Figure 4.2a**, but performed over a wide range of ROI sizes, from 50 to 500 voxels, with steps of 50. Obviously, BOLD responses gradually decreased with the increase of the mask size of the ROI in all areas. However, the spatial and both unexpected image pairs elicited significantly stronger BOLD responses than expected image pairs in LOC and TOFC regions (all $t_{(32)} > 2.169$, all $p < 0.0377$, all Cohen's dz > 0.3776). No significant difference between the temporally unexpected and expected image pairs within all three ROI regions (all $t_{(32)} < 1.913$, all $p > 0.0647$, all Cohen's dz < 0.333). The shaded areas denote within-subject SEM.

CHAPTER 5

GENERAL DISCUSSION

In this thesis, I investigated how different forms of predictability are exploited by the visual system to facilitate visual perception. Specifically, I focused on predictive saccadic remapping and prior (spatial and temporal) context. To this end, several classical techniques in neuroscience were used, including psychophysics, eye tracking and fMRI. In this section, I will first summarize the key findings of these studies and then discuss their relevance for our understanding of how predictions shape visual processing in the brain.

Overview of key findings

Chapter 2 deals with predictions of visual input in anticipation of eye movements. Even though we all experience our perception as stable and continuous, this is actually not true for our visual inputs. Every time we move our eyes, the image of objects in the world shifts its position on the retina. Previous research has discovered that predictive remapping could be a mechanism contributing to visual stability. However, there is still an intensive debate regarding whether and how feature information is remapped prior to saccades. In the current three psychophysical experiments, we found robust evidence for predictive remapping of feature information just before the onset of an eye movement. Crucially, we observed remapped feature information for the test stimulus (a visual stimulus briefly presented prior to saccade onset), but no remapping of adaptation – a previously seen adaptor and its consequences (Experiment 1). Additionally, in order to resolve the discrepancy between forward and convergent remapping, we put the test stimulus not exactly at the saccadic target location but above it. Again, we observed presaccadic remapping of feature information, providing evidence for the forward remapping hypothesis.

In **Chapter 3**, I set out to investigate whether predictive remapping also occurs for VWM, where stimuli are not present within our visual field. On the one hand, WM contents are dynamically stored and therefore might be remapped following eye movements. On the other hand, WM information might not require remapping in order to incorporate the latest inputs. Instead, after every eye movement, the up-to-date stimulus features could be integrated into the previous WM information. In this chapter, I used MVPA of delay-related activity measured with fMRI to directly compare the content of VWM between saccade and no-saccade conditions. We found robust encoding of VWM information in the contralateral early visual cortex when participants did not make a saccade. This information in the contralateral early visual cortex

degraded significantly after the saccade shifted the location of the remembered grating to the opposite visual field. However, we did not find evidence for the remapping of VWM in early visual cortex. Additionally, given that eye movements during the delay period can be considered as a distractor, VWM information in early visual areas could be impaired in the saccade condition. Indeed, we found that VWM contents in early visual cortex were degraded by the saccade in the retention period. In contrast, IPS always showed persistent VWM representations in both the saccade and no-saccade condition, pointing to a limited role of early visual cortex in VWM storage.

In **Chapter 4**, I focused on a different form of predictability, namely prior context. Although there is a vast body of studies demonstrating expectation suppression for sequential stimuli, few studies have shed light on the neural mechanism of expectation suppression for spatial context. In this chapter, I adopted a statistical learning paradigm that included both spatial and temporal expectation violations. We found a reliable and widespread suppression of neural responses to spatially expected compared to unexpected stimuli, which can be considered as the neural signature of spatial context expectations. Surprisingly, we did not find neural evidence supporting temporal context expectations. However, after running a conjunction analysis between our spatial expectation suppression and a robust temporal expectation suppression from a previous study (Richter & de Lange, 2019), we found extensive significant clusters throughout most of the ventral visual stream and in several non-sensory areas. This suggests that the same brain regions play a comparable role in spatial as well as temporal processing in humans.

Feature remapping in visual perception

The question whether feature information is remapped across eye movements has been previously debated extensively. Rolfs and colleagues (2011) found that when participants were planning two successive saccades, their behavioral performance was significantly enhanced at the future retinotopic location of the second target, even before the execution of the first eye movement. In their experimental paradigm, each target orientation was immediately followed by a strong mask, making target detection very difficult. Hence, the task could only be solved by deploying attention toward the target location. Therefore, Rolfs and colleagues concluded that

the predictive remapping process prior to a saccade only occurred for the attentional pointer and not for the feature information. Later, the concept of predictive remapping of the attentional pointer was further elaborated (Rolfs, 2015): before the onset of an eye movement, the priority map (including LIP, FEF, SC), consisting of the attentional pointer, is updated. The updated map sends a feedback signal to the post-saccadic retinal location of the target in early visual areas. This predictively increases the activity of neurons that will process the target location after the eye movement and thus facilitates visual processing for the saccadic target. However, a number of studies have shown that feature information could also be involved in trans-saccadic remapping, in addition to the attentional pointers (Demeyer et al., 2009, 2010; Eccelpoel et al., 2008; Edwards et al., 2017; Gordon et al., 2008; Harrison & Bex, 2014; He et al., 2017; Wijdenes et al., 2015; Sligte et al., 2017; Zimmermann et al., 2013, 2017; Zirnsak et al., 2011). This is also in line with our findings in **Chapter 2**.

Although our results are consistent with many existing studies supporting the feature remapping hypothesis, our design allowed us to extend the scope of this hypothesis. We found that the remapped feature did not originate from the adaptation effect generated by the adaptor, but rather from the test stimulus that was briefly presented before the saccade. In our experiments, the adaptor had disappeared long before the onset of the eye movement. Therefore, the absence of adaptor remapping makes sense as a stimulus no longer present in the visual field is useless for visual perception. Additionally, the adaptation effect, which is caused by the long presentation of the adaptor, might be due to a reduction in the excitability of the adapted neurons. It is also unlikely that such a reduction of neuronal excitability can be 'remapped' by the planning of a saccade. Finally, we found that what is remapped are the test stimuli, which are briefly presented before saccade onset. Furthermore, after using more fine-grained time bins before saccade onset to examine the remapping of feature information, we found that feature information did not change significantly up to at least 80 ms before saccade onset. However, a dramatic change occurred in the 50 ms before saccade onset, in line with the idea that predictive feature remapping occurs very close to saccade onset.

What is the underlying neural mechanism for feature remapping within the visual system? How does our brain redirect the feature information to the correct retinotopic locations

even before the onset of an eye movement? In line with the idea of attention remapping, we propose that feature remapping might also be driven by feedback signals from higher brain areas to early visual cortex. However, this process might not involve the so-called priority map, that plays a key role in the attention remapping hypothesis. Instead, corollary discharge might be important as activity elicited by the test stimulus could be remapped under the guidance of corollary discharge signals (Rao & Ballard, 1999; Sommer & Wurtz, 2006). Corollary discharge refers to the idea that when the motor system generates a movement command for muscles, a copy or corollary of this command is also sent to other brain regions to inform them about the upcoming movement. These other regions might include early sensory areas, such as V1 or V2. During the preparation of a saccade, early visual areas encode the visual features of the stimuli. These areas will be activated first and so their signal with the feature information is then transferred to higher areas (i.e., SC) along with the corollary discharge signal. Since the corollary discharge signal contains information about the onset and target location of the upcoming eye movement (Fries, 1984; Tolias et al., 2001), the feature information can be correctly distributed to the future retinotopic locations of the stimuli in visual cortex by feedback signals.

The difference in remapping between perception and visual working memory

Before discussing the difference in remapping between perception and VWM, I first want to introduce the neural signature of VWM. In the very beginning of this field, researchers only took persistent neural activity as a signature of VWM (Fuster & Alexander, 1971; Pasternak & Greenlee, 2005). Persistent activity can somewhat reveal that the content of WM was encoded in a specific region during the delay period. However, it is not necessarily a signature of WM as this region might just have an influence on storage taking place in other areas. Therefore, a neural signal encoding WM content needs to have at least two properties: first, it should be specific to the memorized content. In other words, different memory contents should lead to different patterns of activity, also referred to as stimulus selectivity. Second, stimulus-selective activity should be present over extended delays in the absence of the stimulus, meaning there is persistent activity. Importantly, persistent activity does not mean that a single selective neuron is firing throughout the entire delay period. Instead, it implies that the activity of a neural population encodes stimulus-specific information at any point during the delay (Christophel et al., 2017).

Multivariate pattern analysis (MVPA; Haxby et al., 2001; Kamitani and Tong, 2005; Haynes and Rees, 2006; Kriegeskorte et al., 2006) is a powerful approach to detect content-specific activity during the delay, as it can provide more information about representational content in a region compared to univariate analyses (Mur et al., 2009). Using this method, I found that WM information was maintained both in early visual areas and in parietal cortex. However, after participants made a saccade during the delay period, WM contents were impaired in early visual cortex but not in parietal areas. This result is consistent with previous findings (Bettencourt & Xu, 2016). Furthermore, although lots of studies found predictive remapping of attention or feature information around the time of an eye movement during perception, there is no evidence supporting the existence of WM remapping.

Here, I propose at least three reasons for the difference in remapping between perception and VWM. First, they have different functions. While attention needs to be selectively shifted to the areas we are most interested in and thus can quickly extract information from the target location, the key function of working memory is to temporarily maintain information for future processing. During visual perception, the most interesting target is usually not at our fovea. Thus, we need to keep moving our eyes to direct the fovea to that location. In order to successfully avoid discrete perception during eye movements and to keep track of the stimuli before and after a saccade, predictive remapping seems to be necessary. In contrast, although we often move our eyes during a WM period, it is not necessary to update the WM storage location along with each eye movement. Instead, remembering the information in several stationary regions can be beneficial for a precise memory.

Second, as suggested by activity-silent models of working memory (Stokes, 2015; Wolff et al., 2017), WM maintenance is not always accompanied by an unbroken chain of persistent delay activity. Indeed, recent studies found that there is a relatively silent period during the delay, which is more efficient in terms of energy compared to persistent WM activity. In line with the idea of an energy-saving coding format, VWM should not be remapped after every eye movement. The core purpose of remapping is to update information timely. We can imagine that it would be very expensive in terms of energy, if WM contents were remapped from one region to another following every eye movement. Therefore, a stationary WM representation could be

ideal for an efficient maintenance of information in the brain.

Third, there is only weak evidence for spatially specific encoding of VWM information, which would be necessary for VWM remapping to be feasible. If VWM indeed needs to be updated after every eye movement, then it should be stored in a spatially specific format corresponding to the external stimulus location. This would allow for successful remapping from the current to the future representation region. While some studies found retinotopic encoding of items into VWM (Pratte & Tong, 2014), Ester and colleagues (2009) observed spatially non-specific coding of VWM in early visual cortex. The question of how VWM information is stored is still extensively debated. In our study (**Chapter 3**), we found more WM information in the contralateral than in the ipsilateral cortex, but this difference was not statistically reliable. Thus, there is still no strong evidence supporting the retinotopic specificity of VWM encoding, which would be necessary for VWM remapping.

5

One may now wonder how our brain can update mnemonic information when moving our eyes, without this information being remapped after eye movements. To the best of my knowledge, no study has shed light on this question. Here, I propose a hypothesis termed index-updating model to answer this question. Our brain can track different WM information simply through indexing the marker of each event, even when the actual storage location is not updated after every saccade. If we think of our brain as a computer, WM is like the cache memory lying in between the CPU (i.e., higher cognitive processing) and the main memory (i.e., long-term memory). The data (i.e., WM contents) might be stored in several distributed regions and therefore no remapping occurs after a saccade. However, higher brain areas are still able to link and index each piece of WM information by updating the marker of that information. The marker could be a unique identifier or symbol that is associated with specific data. It would be easier to manage WM contents by updating the marker of the WM instead of updating the WM itself. If this is the case, the marker and the WM might be stored in two discrete brain regions. Therefore, finding no evidence for WM remapping after eye movements does not necessarily mean that our brain is unable to discriminate and update WM information.

Spatial context in predictions

So far, I discussed visual predictions of future visual input or memory (i.e., predictive remapping) in **Chapter 2** and **3**. Essentially, remapping effects can be considered as predictions based on temporal context. Before moving our eyes, we always predict the upcoming saccade vector (e.g., direction, length) to facilitate information transfer between the current and future locations. In **Chapter 4**, I investigated the effects of another form of predictability on visual processing, namely prior context. Knowledge of both spatial and temporal contexts can independently facilitate visual perception (Bar, 2004). Different sensory systems also have different biases to these priors. For instance, the visual system is biased toward spatial priors, whereas the auditory system is biased toward temporal priors. This is in line with their general sensitivities, with vision being adept at handling spatial stimuli while audition is powerful at dealing with temporal inputs (Conway & Christiansen, 2009; Kubovy, 1988). Although the modulation of neural responses by temporal context has been investigated, little is known about the modulation of neural activity by spatial context, except for a few behavioral studies (Conway & Christiansen, 2009; Fiser & Aslin, 2001, 2005). In the conventional paradigms in the field of statistical learning, researchers present successive stimuli in a temporal order, where the trailing stimulus can be predicted from the leading stimulus. Violated predictions allow researchers to directly examine the effects of unexpected temporal context. However, what happens if one of the co-occurring stimuli is replaced by a novel stimulus, resulting in a violation of the expected spatial context? I aimed to answer this question in **Chapter 4**.

We found a reliable and wide-spread expectation suppression effect for spatial context, but surprisingly there was no evidence for a reduced neural response caused by temporal context expectations (i.e., predictability of stimulus sequence). This is different compared to many existing studies . One of the most obvious reasons is that we tested both spatial and temporal context within one paradigm. Hence, there could be mutual interference. In other words, the absence of a neural response modulation by temporal context could be induced by a bias in statistical learning towards spatial context. Indeed, as mentioned above, previous studies have shown that visual statistical learning is more adept at processing stimuli that are presented simultaneously (i.e., spatial context) compared to sequentially (i.e., temporal context). This is due to modality constraints biasing vision to readily handle spatial inputs while audition is good at processing

temporal inputs (Conway & Christiansen, 2009; Kubovy, 1988; Saffran, 2002). Furthermore, beyond the realm of statistical learning but consistent with the findings on modality constraints, many researchers have demonstrated that modality constraints can also affect the way in which stimuli are perceived (Mahar et al., 1994; Repp & Penel, 2002), maintained in working memory (Collier & Logan, 2000; Penney, 1989), or learned (Conway & Christiansen, 2009; Handel & Buffardi, 1969; Saffran, 2002). Therefore, the most efficient processing combination in terms of statistical learning should be either visual-spatial or auditory-temporal. Additionally, our findings also hint at expectation suppression in the visual system being modulated by attention (Richter and de Lange, 2019). More specifically, prior context only exerts an influence on stimuli that are in the focus of attention, while there is no modulation of neural responses when attention is drawn away from the object stimuli. For our study, this means that predictive processing could be gated by attention if vision is biased toward spatial context: most attention is deployed to the spatial context with little attention on the temporal context, resulting in the absence of temporal context expectations.

Another interesting and even broader question, going beyond the modality constraint of expectations, concerns the debate about domain generality versus domain specificity (Frost et al., 2019). Domain generality of statistical learning refers to a unitary learning system (e.g., human) that executes similar computations across stimuli and these computations can also be observed across domains (Saffran & Thiessen, 2008) and species (Toro & Trobalón, 2005). Domain specificity indicates that the learning process is constrained to a specific modality or even to a specific stimulus (Frost et al., 2015). Although statistical learning performance in a given modality is relatively stable within an individual (Siegelman et al., 2017), it does not reliably predict the ability to learn regularities in another modality. For example, Conway and Christiansen (2006) showed that learning two grammars can happen without interference as long as they are implemented in two different modalities. In the same vein, transfer of learning has been shown to be very limited across modalities (e.g., Redington and Chater, 1996; Tunney and Altmann, 1999). Our findings are in line with the idea of domain specificity. Although we found modulations of neural responses by spatial and temporal contexts within similar cortical areas, no transfer of learning was observed between these two contexts.

In contrast to the viewpoint of domain specificity, recent evidence suggests that the hippocampus plays a central role for all statistical learning computations. Admittedly, this is in line with the idea of domain generality (Schapiro et al., 2014, 2017; Turk-Browne & Scholl, 2009). For instance, Schapiro et al. (2014) reported the case of an amnestic patient with hippocampal damage, who showed no statistical learning abilities. This argues for the necessity of the medial temporal lobe system for statistical learning. However, in a later study, Covington et al. (2018) showed above chance performance in some statistical learning task variants for patients with hippocampal damage. Thus, the domain generality of statistical learning still remains an open question.

Concluding remarks

Predictions have a profound impact on the way we perceive the world and strongly facilitate many cognitive processes. However, there are many different forms of predictability that can be implemented in different ways. In this thesis, I investigated the effects of two different forms of predictability on visual perception. One was predictions of future inputs in anticipation of an eye movement. Here, I found that predictive remapping occurred for physical stimuli presented in the visual field, but no similar effects were observed for VWM. This points toward our visual system being dynamic and adaptive in predictive processing of visual information. The second form of predictability was prior context and here the results showed a reliable modulation of neural responses by spatial but not by temporal context. While predictive processing can subserve visual perception in varied ways, it can also be biased for different sensory modalities. Nevertheless, analogous neural mechanisms may still underlie temporal and spatial context expectations: similar brain regions were activated for both temporal and spatial context violations. One particularly interesting question for future research is how all these different forms of predictions (e.g., predictive remapping and prior context) interact in sensory processing. I hope that the work presented in this thesis can contribute to the research on predictions and stimulates additional interest in better understanding this topic.

REFERENCES

1. Abla, D., Katahira, K., & Okanoya, K. (2008). On-line Assessment of Statistical Learning by Event-related Potentials. Journal of Cognitive Neuroscience, 20(6), 952–964. https://doi.org/10.1162/jocn.2008.20058

2. Abla, D., & Okanoya, K. (2008). Statistical segmentation of tone sequences activates the left inferior frontal cortex: A near-infrared spectroscopy study. Neuropsychologia, 46(11), 2787–2795. https://doi.org/10.1016/j.neuropsychologia.2008.05.012

3. Adam, K. C. S., & Serences, J. T. (2019). Working Memory: Flexible but Finite. Neuron, 103(2), 184–185. https://doi.org/10.1016/j.neuron.2019.06.025

4. Albers, A. M., Kok, P., Toni, I., Dijkerman, H. C., & de Lange, F. P. (2013). Shared Representations for Working Memory and Mental Imagery in Early Visual Cortex. Current Biology, 23(15), 1427–1431. https://doi.org/10.1016/j.cub.2013.05.065

5. Alink, A., Schwiedrzik, C., Kohler, A., Singer, W., & Muckli, L. (2010). Stimulus Predictability Reduces Responses in Primary Visual Cortex. The Journal of Neuroscience, 30(8), 2960–2966. https://doi.org/10.1523/jneurosci.3730-10.2010

6. Bar, M. (2004). Visual objects in context. Nature Reviews Neuroscience, 5(8), 617–629. https://doi.org/10.1038/nrn1476

7. Bertels, J., Franco, A., & Destrebecqz, A. (2012). How implicit is visual statistical learning? Journal of Experimental Psychology: Learning, Memory, and Cognition, 38(5), 1425–1431. https://doi.org/10.1037/a0027210

8. Bettencourt, K. C., & Xu, Y. (2016). Decoding the content of visual short-term memory under distraction in occipital and parietal areas. Nature Neuroscience, 19(1), 150–157. https://doi.org/10.1038/nn.4174

9. Biber, U., & Ilg, U. J. (2011). Visual Stability and the Motion Aftereffect: A Psychophysical Study Revealing Spatial Updating. PLOS ONE, 6(1), e16265. https://doi.org/10.1371/journal.pone.0016265

10. Brady, T. F., Konkle, T., Alvarez, G. A., & Oliva, A. (2008). Visual long-term memory has a massive storage capacity for object details. Proceedings of the National Academy of Sciences, 105(38), 14325–14329. https://doi.org/10.1073/pnas.0803390105

11. Brady, T. F., & Oliva, A. (2008). Statistical learning using real-world scenes: Extracting categorical regularities without conscious intent. Psychological Science, 19(7), 678–685. https://doi.org/10.1111/j.1467-9280.2008.02142.x

12. Brainard, D. H. (1997). The Psychophysics Toolbox. Spatial Vision, 10(4), 433–436. https://doi.org/10.1163/156856897X00357

13. Button, K. S., Ioannidis, J. P. A., Mokrysz, C., Nosek, B. A., Flint, J., Robinson, E. S. J., & Munafò, M. R. (2013). Power failure: Why small sample size undermines the reliability of neuroscience. Nature Reviews Neuroscience, 14(5), 365–376. https://doi.org/10.1038/nrn3475

14. Cavanagh, P., Hunt, A. R., Afraz, A., & Rolfs, M. (2010a). Visual stability based on remapping of attention pointers. Trends in Cognitive Sciences, 14(4), 147–153. https://doi.org/10.1016/j.tics.2010.01.007

15. Cavanagh, P., Hunt, A. R., Afraz, A., & Rolfs, M. (2010b). Visual stability based on remapping of attention pointers. Trends in Cognitive Sciences, 14(4), 147–153. https://doi.org/10.1016/j.tics.2010.01.007

16. Cha, O., & Chong, S. C. (2013). The background is remapped across saccades. Experimental Brain Research, 232(2), 609–618. https://doi.org/10.1007/s00221-013-3769-9

17. Chalk, M., Seitz, A. R., & Seriès, P. (2010). Rapidly learned stimulus expectations alter perception of motion. Journal of Vision, 10(8), 2–2. https://doi.org/10.1167/10.8.2

18. Christophel, T. B., Cichy, R. M., Hebart, M. N., & Haynes, J.-D. (2015). Parietal and early visual cortices encode working memory content across mental transformations. NeuroImage, 106, 198–206. https://doi.org/10.1016/j.neuroimage.2014.11.018

19. Christophel, T. B., Klink, P. C., Spitzer, B., Roelfsema, P. R., & Haynes, J.-D. (2017). The

Distributed Nature of Working Memory. Trends in Cognitive Sciences, 21(2), 111–124. https://doi.org/10.1016/j.tics.2016.12.007

20. Clark, A. (2013). Whatever next? Predictive brains, situated agents, and the future of cognitive science. Behavioral and Brain Sciences, 36(3), 181–204. https://doi.org/10.1017/S0140525X12000477

21. Colby, C. L. (1996). A neurophysiological distinction between attention and intention. In T. Inui & J. L. McClelland (Eds.), Attention and performance 16: Information integration in perception and communication (pp. 157–177). The MIT Press.

22. Collier, G. L., & Logan, G. (2000). Modality differences in short-term memory for rhythms. Memory & Cognition, 28(4), 529–538. https://doi.org/10.3758/BF03201243

23. Conway, C. M., & Christiansen, M. H. (2006). Statistical Learning Within and Between Modalities: Pitting Abstract Against Stimulus-Specific Representations. Psychological Science. https://doi.org/10.1111/j.1467-9280.2006.01801.x

24. Conway, C. M., & Christiansen, M. H. (2009). Seeing and hearing in space and time: Effects of modality and presentation rate on implicit statistical learning. European Journal of Cognitive Psychology, 21(4), 561–580. https://doi.org/10.1080/09541440802097951

25. Covington, N. V., Brown-Schmidt, S., & Duff, M. C. (2018). The necessity of the hippocampus for statistical learning. Journal of Cognitive Neuroscience, 30(5), 680–697. https://doi.org/10.1162/jocn_a_01228

26. Cunillera, T., Càmara, E., Toro, J. M., Marco-Pallares, J., Sebastián-Galles, N., Ortiz, H., Pujol, J., & Rodríguez-Fornells, A. (2009). Time course and functional neuroanatomy of speech segmentation in adults. NeuroImage, 48(3), 541–553. https://doi.org/10.1016/j.neuroimage.2009.06.069

27. Curtis, C. E., & D'Esposito, M. (2003). Persistent activity in the prefrontal cortex during working memory. Trends in Cognitive Sciences, 7(9), 415–423. https://doi.org/10.1016/S1364-6613(03)00197-9

28. Dale, A. M., Fischl, B., & Sereno, M. I. (1999). Cortical Surface-Based Analysis: I. Segmentation and Surface Reconstruction. NeuroImage, 9(2), 179–194. https://doi.org/10.1006/nimg.1998.0395

29. Davenport, J. L., & Potter, M. C. (2004). Scene Consistency in Object and Background Perception. Psychological Science, 15(8), 559–564. https://doi.org/10.1111/j.0956-7976.2004.00719.x

30. de Lange, F. P., Heilbron, M., & Kok, P. (2018). How Do Expectations Shape Perception? Trends in Cognitive Sciences, 22(9), 764–779. https://doi.org/10.1016/j.tics.2018.06.002

31. Demeyer, M., De Graef, P., Wagemans, J., & Verfaillie, K. (2009). Transsaccadic identification of highly similar artificial shapes. Journal of Vision, 9(4), 28.1-14. https://doi.org/10.1167/9.4.28

32. Demeyer, M., De Graef, P., Wagemans, J., & Verfaillie, K. (2010). Parametric integration of visual form across saccades. Vision Research, 50(13), 1225–1234. https://doi.org/10.1016/j.visres.2010.04.008

33. Demeyer, M., Graef, P. D., Verfaillie, K., & Wagemans, J. (2011). Perceptual Grouping of Object Contours Survives Saccades. PLOS ONE, 6(6), e21257. https://doi.org/10.1371/journal.pone.0021257

34. den Ouden, H. E. M., Friston, K. J., Daw, N. D., McIntosh, A. R., & Stephan, K. E. (2009). A Dual Role for Prediction Error in Associative Learning. Cerebral Cortex, 19(5), 1175–1185. https://doi.org/10.1093/cercor/bhn161

35. DeYoe, E. A., Carman, G. J., Bandettini, P., Glickman, S., Wieser, J., Cox, R., Miller, D., & Neitz, J. (1996). Mapping striate and extrastriate visual areas in human cerebral cortex. Proceedings of the National Academy of Sciences, 93(6), 2382–2386. https://doi.org/10.1073/pnas.93.6.2382

36. Dijkstra, N., Ambrogioni, L., & Gerven, M. A. J. van. (2019). Neural dynamics of perceptual inference and its reversal during imagery. BioRxiv, 781294. https://doi.org/10.1101/781294

37. Dorr, M., & Bex, P. J. (2013). Peri-Saccadic Natural Vision. The Journal of Neuroscience, 33(3), 1211–1217. https://doi.org/10.1523/JNEUROSCI.4344-12.2013

38. Duhamel, Colby, C. L., & Goldberg, M. E. (1992). The updating of the representation of visual space in parietal cortex by intended eye movements. Science, 255(5040), 90–92. https://doi.org/10.1126/science.1553535

39. Dunkley, B. T., Baltaretu, B., & Crawford, J. D. (2016). Trans-saccadic interactions in human parietal and occipital cortex during the retention and comparison of object orientation. Cortex, 82, 263–276. https://doi.org/10.1016/j.cortex.2016.06.012

40. Durstewitz, D., Seamans, J. K., & Sejnowski, T. J. (2000). Dopamine-Mediated Stabilization of Delay-Period Activity in a Network Model of Prefrontal Cortex. Journal of Neurophysiology, 83(3), 1733–1750. https://doi.org/10.1152/jn.2000.83.3.1733

41. Eccelpoel, C. V., Germeys, F., Graef, P. D., & Verfaillie, K. (2008). Coding of identity-diagnostic information in transsaccadic object perception. Journal of Vision, 8(14), 29–29. https://doi.org/10.1167/8.14.29

42. Edwards, G., VanRullen, R., & Cavanagh, P. (2017). Decoding trans-saccadic memory. Journal of Neuroscience, 0854–17. https://doi.org/10.1523/JNEUROSCI.0854-17.2017

43. Egner, T., Monti, J. M., & Summerfield, C. (2010). Expectation and Surprise Determine Neural Population Responses in the Ventral Visual Stream. Journal of Neuroscience, 30(49), 16601–16608. https://doi.org/10.1523/JNEUROSCI.2770-10.2010

44. Emrich, S. M., Riggall, A. C., LaRocque, J. J., & Postle, B. R. (2013). Distributed Patterns of Activity in Sensory Cortex Reflect the Precision of Multiple Items Maintained in Visual Short-Term Memory. Journal of Neuroscience, 33(15), 6516–6523. https://doi.org/10.1523/JNEUROSCI.5732-12.2013

45. Engel, S. A., Glover, G. H., & Wandell, B. A. (1997). Retinotopic organization in human visual cortex and the spatial precision of functional MRI. Cerebral Cortex, 7(2), 181–192. https://doi.org/10.1093/cercor/7.2.181

46. Ester, E. F., Serences, J. T., & Awh, E. (2009). Spatially Global Representations in Human Primary Visual Cortex during Working Memory Maintenance. Journal of Neuroscience, 29(48), 15258–15265. https://doi.org/10.1523/JNEUROSCI.4388-09.2009

47. Ester, E. F., Sprague, T. C., & Serences, J. T. (2015). Parietal and Frontal Cortex Encode Stimulus-Specific Mnemonic Representations during Visual Working Memory. Neuron, 87(4), 893–905. https://doi.org/10.1016/j.neuron.2015.07.013

48. Ezzati, A., Golzar, A., & Afraz, A. S. R. (2008). Topography of the motion aftereffect with and without eye movements. Journal of Vision, 8(14), 23–23. https://doi.org/10.1167/8.14.23

49. Fafrowicz, M., Marek, T., Karwowski, W., & Schmorrow, D. (2012). Neuroadaptive Systems: Theory and Applications. CRC Press.

50. Fairhall, S. L., Schwarzbach, J., Lingnau, A., Van Koningsbruggen, M. G., & Melcher, D. (2017). Spatiotopic updating across saccades revealed by spatially-specific fMRI adaptation. NeuroImage, 147, 339–345. https://doi.org/10.1016/j.neuroimage.2016.11.071

51. Fecteau, J. H., & Munoz, D. P. (2006). Salience, relevance, and firing: A priority map for target selection. Trends in Cognitive Sciences, 10(8), 382–390. https://doi.org/10.1016/j.tics.2006.06.011

52. Felleman, D. J., & Van Essen, D. C. (1991). Distributed Hierarchical Processing in the Primate Cerebral Cortex. Cerebral Cortex, 1(1), 1–47. https://doi.org/10.1093/cercor/1.1.1

53. Fischl, B., Salat, D. H., Busa, E., Albert, M., Dieterich, M., Haselgrove, C., van der Kouwe, A., Killiany, R., Kennedy, D., Klaveness, S., Montillo, A., Makris, N., Rosen, B., & Dale, A. M. (2002). Whole Brain Segmentation: Automated Labeling of Neuroanatomical Structures in the Human Brain. Neuron, 33(3), 341–355. https://doi.org/10.1016/S0896-6273(02)00569-X

54. Fiser, J., & Aslin, R. N. (2001). Unsupervised Statistical Learning of Higher-Order Spatial Structures from Visual Scenes. Psychological Science, 12(6), 499–504. https://doi.org/10.1111/1467-9280.00392

55. Fiser, J., & Aslin, R. N. (2005). Encoding Multielement Scenes: Statistical Learning of Visual

Feature Hierarchies. Journal of Experimental Psychology: General, 134(4), 521–537. https://doi.org/10.1037/0096-3445.134.4.521

56. Fracasso, A., Caramazza, A., & Melcher, D. (2010). Continuous perception of motion and shape across saccadic eye movements. Journal of Vision, 10(13), 14. https://doi.org/10.1167/10.13.14

57. Freedman, D. J., Riesenhuber, M., Poggio, T., & Miller, E. K. (2006). Experience-Dependent Sharpening of Visual Shape Selectivity in Inferior Temporal Cortex. Cerebral Cortex, 16(11), 1631–1644. https://doi.org/10.1093/cercor/bhj100

58. Fries, W. (1984). Cortical projections to the superior colliculus in the macaque monkey: A retrograde study using horseradish peroxidase. The Journal of Comparative Neurology, 230(1), 55–76. https://doi.org/10.1002/cne.902300106

59. Friston, K. (2005). A theory of cortical responses. Philosophical Transactions of the Royal Society of London. Series B, Biological Sciences, 360(1456), 815–836. https://doi.org/10.1098/rstb.2005.1622

60. Frost, R., Armstrong, B. C., & Christiansen, M. H. (2019). Statistical learning research: A critical review and possible new directions. Psychological Bulletin, 145(12), 1128–1153. https://doi.org/10.1037/bul0000210

61. Fuster, J. M., & Alexander, G. E. (1971). Neuron Activity Related to Short-Term Memory. Science, 173(3997), 652–654. https://doi.org/10.1126/science.173.3997.652

62. Ganmor, E., Landy, M. S., & Simoncelli, E. P. (2015). Near-optimal integration of orientation information across saccades. Journal of Vision, 15(16), 8–8. https://doi.org/10.1167/15.16.8

63. Gheysen, F., Van Opstal, F., Roggeman, C., Van Waelvelde, H., & Fias, W. (2010). Hippocampal contribution to early and later stages of implicit motor sequence learning. Experimental Brain Research, 202(4), 795–807. https://doi.org/10.1007/s00221-010-2186-6

64. Gheysen, F., Van Opstal, F., Roggeman, C., Van Waelvelde, H., & Fias, W. (2011). The Neural Basis of Implicit Perceptual Sequence Learning. Frontiers in Human Neuroscience,

5. https://doi.org/10.3389/fnhum.2011.00137

65. Girshick, A. R., Landy, M. S., & Simoncelli, E. P. (2011). Cardinal rules: Visual orientation perception reflects knowledge of environmental statistics. Nature Neuroscience, 14(7), 926–932. https://doi.org/10.1038/nn.2831

66. Goldberg, M. E., & Bruce, C. J. (1990). Primate frontal eye fields. III. Maintenance of a spatially accurate saccade signal. Journal of Neurophysiology, 64(2), 489–508. https://doi.org/10.1152/jn.1990.64.2.489

67. Goldman-Rakic, P. S. (1995). Cellular basis of working memory. Neuron, 14(3), 477–485. https://doi.org/10.1016/0896-6273(95)90304-6

68. Goodale, M. A. (1995). The cortical organization of visual perception and visuomotor control. In Visual cognition: An invitation to cognitive science, Vol. 2, 2nd ed (pp. 167–213). The MIT Press.

69. Gordon, R. D., Vollmer, S. D., & Frankl, M. L. (2008). Object continuity and the transsaccadic representation of form. Perception & Psychophysics, 70(4), 667–679. https://doi.org/10.3758/PP.70.4.667

70. Habtegiorgis, S. W., Rifai, K., Lappe, M., & Wahl, S. (2018). Experience-dependent long-term facilitation of skew adaptation. Journal of Vision, 18(9), 7. https://doi.org/10.1167/18.9.7

71. Handel, S., & Buffardi, L. (1969). Using Several Modalities to Perceive one Temporal Pattern. Quarterly Journal of Experimental Psychology, 21(3), 256–266. https://doi.org/10.1080/14640746908400220

72. Harrison, S. A., & Tong, F. (2009). Decoding reveals the contents of visual working memory in early visual areas. Nature, 458(7238), 632–635. https://doi.org/10.1038/nature07832

73. Harrison, W. J., & Bex, P. J. (2014). Integrating Retinotopic Features in Spatiotopic Coordinates. Journal of Neuroscience, 34(21), 7351–7360. https://doi.org/10.1523/JNEUROSCI.5252-13.2014

74. Harrison, W. J., Retell, J. D., Remington, R. W., & Mattingley, J. B. (2013). Visual Crowding at a Distance during Predictive Remapping. Current Biology, 23(9), 793–798. https://doi.org/10.1016/j.cub.2013.03.050

75. Haushofer, J., Livingstone, M. S., & Kanwisher, N. (2008). Multivariate Patterns in Object-Selective Cortex Dissociate Perceptual and Physical Shape Similarity. PLOS Biology, 6(7), e187. https://doi.org/10.1371/journal.pbio.0060187

76. Haxby, J. V., Gobbini, M. I., Furey, M. L., Ishai, A., Schouten, J. L., & Pietrini, P. (2001). Distributed and Overlapping Representations of Faces and Objects in Ventral Temporal Cortex. Science, 293(5539), 2425–2430. https://doi.org/10.1126/science.1063736

77. Hayhoe, M., Lachter, J., & Feldman, J. (1991). Integration of Form across Saccadic Eye Movements. Perception, 20(3), 393–402. https://doi.org/10.1068/p200393

78. Haynes, J.-D., & Rees, G. (2006). Neuroimaging: Decoding mental states from brain activity in humans. Nature Reviews Neuroscience, 7(7), 523–534. https://doi.org/10.1038/nrn1931

79. He, D., Mo, C., & Fang, F. (2017). Predictive feature remapping before saccadic eye movements. Journal of Vision, 17(5), 14–14. https://doi.org/10.1167/17.5.14

80. He, T., Fritsche, M., & de Lange, F. P. (2018). Predictive remapping of visual features beyond saccadic targets. Journal of Vision, 18(13), 20–20. https://doi.org/10.1167/18.13.20

81. Herwig, A., & Schneider, W. X. (2014). Predicting object features across saccades: Evidence from object recognition and visual search. Journal of Experimental Psychology: General, 143(5), 1903–1922. https://doi.org/10.1037/a0036781

82. Hubel, D. H., & Wiesel, T. N. (1977). Ferrier lecture—Functional architecture of macaque monkey visual cortex. Proceedings of the Royal Society of London. Series B. Biological Sciences, 198(1130), 1–59. https://doi.org/10.1098/rspb.1977.0085

83. Hübner, C., & Schütz, A. C. (2017). Numerosity estimation benefits from transsaccadic information integration. Journal of Vision, 17(13), 12–12. https://doi.org/10.1167/17.13.12

84. Hunt, A. R., & Cavanagh, P. (2011). Remapped visual masking. Journal of Vision, 11(1), 13–13. https://doi.org/10.1167/11.1.13

85. Hunt, R. H., & Aslin, R. N. (2001). Statistical learning in a serial reaction time task: Access to separable statistical cues by individual learners. Journal of Experimental Psychology: General, 130(4), 658–680. https://doi.org/10.1037/0096-3445.130.4.658

86. JASP Team. (2019). JASP (Version 0.10.2)[Computer software].

87. Jonikaitis, D., Szinte, M., Rolfs, M., & Cavanagh, P. (2013). Allocation of attention across saccades. Journal of Neurophysiology, 109(5), 1425–1434. https://doi.org/10.1152/jn.00656.2012

88. Kamitani, Y., & Tong, F. (2005). Decoding the visual and subjective contents of the human brain. Nature Neuroscience, 8(5), 679–685. https://doi.org/10.1038/nn1444

89. Kaposvari, P., Kumar, S., & Vogels, R. (2018). Statistical Learning Signals in Macaque Inferior Temporal Cortex. Cerebral Cortex, 28(1), 250–266. https://doi.org/10.1093/cercor/bhw374

90. Karuza, E. A., Emberson, L. L., Roser, M. E., Cole, D., Aslin, R. N., & Fiser, J. (2017). Neural signatures of spatial statistical learning: Characterizing the extraction of structure from complex visual scenes. Journal of Cognitive Neuroscience, 29(12), 1963–1976. https://doi.org/10.1162/jocn_a_01182

91. Karuza, E. A., Newport, E. L., Aslin, R. N., Starling, S. J., Tivarus, M. E., & Bavelier, D. (2013). The neural correlates of statistical learning in a word segmentation task: An fMRI study. Brain and Language, 127(1), 46–54. https://doi.org/10.1016/j.bandl.2012.11.007

92. Knapen, T., Rolfs, M., Wexler, M., & Cavanagh, P. (2010). The reference frame of the tilt aftereffect. Journal of Vision, 10(1), 8–8. https://doi.org/10.1167/10.1.8

93. Kok, P., Brouwer, G. J., Gerven, M. A. J. van, & de Lange, F. P. (2013). Prior Expectations Bias Sensory Representations in Visual Cortex. Journal of Neuroscience, 33(41), 16275–16284. https://doi.org/10.1523/JNEUROSCI.0742-13.2013

94. Kok, P., Jehee, J. F. M., & de Lange, F. P. (2012). Less Is More: Expectation Sharpens Representations in the Primary Visual Cortex. Neuron, 75(2), 265–270. https://doi.org/10.1016/j.neuron.2012.04.034

95. Koller, K., & Rafal, R. D. (2018). Saccade latency bias toward temporal hemifield: Evidence for role of retinotectal tract in mediating reflexive saccades. Neuropsychologia. https://doi.org/10.1016/j.neuropsychologia.2018.01.028

96. Kourtzi, Z., & Kanwisher, N. (2001). Representation of Perceived Object Shape by the Human Lateral Occipital Complex. Science, 293(5534), 1506–1509. https://doi.org/10.1126/science.1061133

97. Kriegeskorte, N., Goebel, R., & Bandettini, P. (2006). Information-based functional brain mapping. Proceedings of the National Academy of Sciences, 103(10), 3863–3868. https://doi.org/10.1073/pnas.0600244103

98. Kubovy, M. (1988). Should we resist the seductiveness of the space:time::vision:audition analogy? Journal of Experimental Psychology: Human Perception and Performance, 14(2), 318–320. https://doi.org/10.1037/0096-1523.14.2.318

99. Kumar, S., Kaposvari, P., & Vogels, R. (2017). Encoding of Predictable and Unpredictable Stimuli by Inferior Temporal Cortical Neurons. Journal of Cognitive Neuroscience, 29(8), 1445–1454. https://doi.org/10.1162/jocn_a_01135

100. Lakens, D. (2013). Calculating and reporting effect sizes to facilitate cumulative science: A practical primer for t-tests and ANOVAs. Frontiers in Psychology, 4. https://doi.org/10.3389/fpsyg.2013.00863

101. Lee, M. D., & Wagenmakers, E.-J. (2014). Bayesian Cognitive Modeling: A Practical Course. Cambridge University Press.

102. Lescroart, M. D., Kanwisher, N., & Golomb, J. D. (2016). No Evidence for Automatic Remapping of Stimulus Features or Location Found with fMRI. Frontiers in Systems Neuroscience, 10, 53. https://doi.org/10.3389/fnsys.2016.00053

103. Linde-Domingo, J., Treder, M. S., Kerrén, C., & Wimber, M. (2019). Evidence that neural information flow is reversed between object perception and object reconstruction from memory. Nature Communications, 10(1), 1–13. https://doi.org/10.1038/s41467-018-08080-2

104. Livingstone, M. S., & Hubel, D. (1988). Segregation of form, color, movement, and depth: Anatomy, physiology, and perception. Science, 240(4853), 740–749. https://doi.org/10.1126/science.3283936

105. Livingstone, M. S., & Hubel, D. H. (1987). Psychophysical evidence for separate channels for the perception of form, color, movement, and depth. The Journal of Neuroscience: The Official Journal of the Society for Neuroscience, 7(11), 3416–3468. https://doi.org/10.1523/JNEUROSCI.07-11-03416.1987

106. Lorenc, E. S., Sreenivasan, K. K., Nee, D. E., Vandenbroucke, A. R. E., & D'Esposito, M. (2018). Flexible Coding of Visual Working Memory Representations during Distraction. Journal of Neuroscience, 38(23), 5267–5276. https://doi.org/10.1523/JNEUROSCI.3061-17.2018

107. Mahar, D., Mackenzie, B., & McNicol, D. (1994). Modality-Specific Differences in the Processing of Spatially, Temporally, and Spatiotemporally Distributed Information. Perception, 23(11), 1369–1386. https://doi.org/10.1068/p231369

108. Maris, E., & Oostenveld, R. (2007). Nonparametric statistical testing of EEG- and MEG-data. Journal of Neuroscience Methods, 164(1), 177–190. https://doi.org/10.1016/j.jneumeth.2007.03.024

109. Maunsell, J. H., & Newsome, W. T. (1987). Visual processing in monkey extrastriate cortex. Annual Review of Neuroscience, 10, 363–401. https://doi.org/10.1146/annurev.ne.10.030187.002051

110. Mayo, J. P., & Sommer, M. A. (2010). Shifting attention to neurons. Trends in Cognitive Sciences, 14(9), 389. https://doi.org/10.1016/j.tics.2010.06.003

111. McNealy, K., Mazziotta, J. C., & Dapretto, M. (2006). Cracking the Language Code: Neural

Mechanisms Underlying Speech Parsing. Journal of Neuroscience, 26(29), 7629–7639. https://doi.org/10.1523/JNEUROSCI.5501-05.2006

112. Melcher, D. (2005). Spatiotopic Transfer of Visual-Form Adaptation across Saccadic Eye Movements. Current Biology, 15(19), 1745–1748. https://doi.org/10.1016/j.cub.2005.08.044

113. Melcher, D. (2007). Predictive remapping of visual features precedes saccadic eye movements. Nature Neuroscience, 10(7), 903–907. https://doi.org/10.1038/nn1917

114. Melcher, D. (2010). The missing link for attention pointers: Comment on Cavanagh et al. Trends in Cognitive Sciences, 14(11), 473. https://doi.org/10.1016/j.tics.2010.08.007

115. Melcher, D. (2011). Visual stability. Philosophical Transactions of the Royal Society of London B: Biological Sciences, 366(1564), 468–475. https://doi.org/10.1098/rstb.2010.0277

116. Melcher, D., & Morrone, M. C. (2003). Spatiotopic temporal integration of visual motion across saccadic eye movements. Nature Neuroscience, 6(8), 877–881. https://doi.org/10.1038/nn1098

117. Merriam, E. P., Genovese, C. R., & Colby, C. L. (2007). Remapping in Human Visual Cortex. Journal of Neurophysiology, 97(2), 1738–1755. https://doi.org/10.1152/jn.00189.2006

118. Meyer, T., & Olson, C. R. (2011). Statistical learning of visual transitions in monkey inferotemporal cortex. Proceedings of the National Academy of Sciences, 108(48), 19401–19406. https://doi.org/10.1073/pnas.1112895108

119. Millman, K. J., & Aivazis, M. (2011). Python for Scientists and Engineers. Computing in Science Engineering, 13(2), 9–12. https://doi.org/10.1109/MCSE.2011.36

120. Mishkin, M., & Ungerleider, L. G. (1982). Contribution of striate inputs to the visuospatial functions of parieto-preoccipital cortex in monkeys. Behavioural Brain Research, 6(1), 57–77. https://doi.org/10.1016/0166-4328(82)90081-X

121. Mishkin, M., Ungerleider, L. G., & Macko, K. A. (1983). Object vision and spatial vision: Two cortical pathways. Trends in Neurosciences, 6, 414–417. https://doi.org/10.1016/0166-

2236(83)90190-X

122. Mur, M., Bandettini, P. A., & Kriegeskorte, N. (2009). Revealing representational content with pattern-information fMRI—an introductory guide. Social Cognitive and Affective Neuroscience, 4(1), 101–109. https://doi.org/10.1093/scan/nsn044

123. Nakamura, K., & Colby, C. L. (2002). Updating of the visual representation in monkey striate and extrastriate cortex during saccades. Proceedings of the National Academy of Sciences, 99(6), 4026–4031. https://doi.org/10.1073/pnas.052379899

124. Nakashima, Y., & Sugita, Y. (2017). The reference frame of the tilt aftereffect measured by differential Pavlovian conditioning. Scientific Reports, 7, 40525. https://doi.org/10.1038/srep40525

125. Neupane, S., Guitton, D., & Pack, C. C. (2016a). Two distinct types of remapping in primate cortical area V4. Nature Communications, 7, 10402. https://doi.org/10.1038/ncomms10402

126. Neupane, S., Guitton, D., & Pack, C. C. (2016b). Dissociation of forward and convergent remapping in primate visual cortex. Current Biology, 26(12), R491–R492. https://doi.org/10.1016/j.cub.2016.04.050

127. Norman, K. A., Polyn, S. M., Detre, G. J., & Haxby, J. V. (2006). Beyond mind-reading: Multi-voxel pattern analysis of fMRI data. Trends in Cognitive Sciences, 10(9), 424–430. https://doi.org/10.1016/j.tics.2006.07.005

128. Oliphant, T. E. (2007). Python for Scientific Computing. Computing in Science Engineering, 9(3), 10–20. https://doi.org/10.1109/MCSE.2007.58

129. Oostwoud Wijdenes, L., Marshall, L., & Bays, P. M. (2015). Evidence for Optimal Integration of Visual Feature Representations across Saccades. The Journal of Neuroscience: The Official Journal of the Society for Neuroscience, 35(28), 10146–10153. https://doi.org/10.1523/JNEUROSCI.1040-15.2015

130. O'Regan, J. K., & Noë, A. (2001). A sensorimotor account of vision and visual consciousness. Behavioral and Brain Sciences, 24(05), 939–973. https://doi.org/10.1017/

S0140525X01000115

131. Paeye, C., Collins, T., & Cavanagh, P. (2017). Transsaccadic perceptual fusion. Journal of Vision, 17(1), 14–14. https://doi.org/10.1167/17.1.14

132. Pasternak, T., & Greenlee, M. W. (2005). Working memory in primate sensory systems. Nature Reviews Neuroscience, 6(2), 97–107. https://doi.org/10.1038/nrn1603

133. Pedregosa, F., Varoquaux, G., Gramfort, A., Michel, V., Thirion, B., Grisel, O., Blondel, M., Prettenhofer, P., Weiss, R., Dubourg, V., Vanderplas, J., Passos, A., Cournapeau, D., Brucher, M., Perrot, M., & Duchesnay, É. (2011). Scikit-learn: Machine Learning in Python. Journal of Machine Learning Research, 12(Oct), 2825–2830.

134. Pelli, D. G., & Cavanagh, P. (2013). Object Recognition: Visual Crowding from a Distance. Current Biology, 23(11), R478–R479. https://doi.org/10.1016/j.cub.2013.04.022

135. Penney, C. G. (1989). Modality effects and the structure of short-term verbal memory. Memory & Cognition, 17(4), 398–422. https://doi.org/10.3758/BF03202613

136. Plante, E., Patterson, D., Gómez, R., Almryde, K. R., White, M. G., & Asbjørnsen, A. E. (2015). The nature of the language input affects brain activation during learning from a natural language. Journal of Neurolinguistics, 36, 17–34. https://doi.org/10.1016/j.jneuroling.2015.04.005

137. Pratte, M. S., & Tong, F. (2014). Spatial specificity of working memory representations in the early visual cortex. Journal of Vision, 14(3), 22. https://doi.org/10.1167/14.3.22

138. Prime, S. L., Niemeier, M., & Crawford, J. D. (2006). Transsaccadic integration of visual features in a line intersection task. Experimental Brain Research, 169(4), 532–548. https://doi.org/10.1007/s00221-005-0164-1

139. Prime, S. L., Vesia, M., & Crawford, J. D. (2011). Cortical mechanisms for trans-saccadic memory and integration of multiple object features. Philosophical Transactions of the Royal Society B: Biological Sciences, 366(1564), 540–553. https://doi.org/10.1098/rstb.2010.0184

140. Prins, N., & Kingdom, F. A. A. (2018). Applying the Model-Comparison Approach to Test Specific Research Hypotheses in Psychophysical Research Using the Palamedes Toolbox. Frontiers in Psychology, 9, 1250. https://doi.org/10.3389/fpsyg.2018.01250

141. Puntiroli, M., Kerzel, D., & Born, S. (2015). Perceptual enhancement prior to intended and involuntary saccades. Journal of Vision, 15(4), 2–2. https://doi.org/10.1167/15.4.2

142. Rademaker, R. L., Chunharas, C., & Serences, J. T. (2019). Coexisting representations of sensory and mnemonic information in human visual cortex. Nature Neuroscience, 22(8), 1336–1344. https://doi.org/10.1038/s41593-019-0428-x

143. Rao, H. M., Mayo, J. P., & Sommer, M. A. (2016). Circuits for presaccadic visual remapping. Journal of Neurophysiology, 116(6), 2624–2636. https://doi.org/10.1152/jn.00182.2016

144. Rao, R. P. N., & Ballard, D. H. (1999). Predictive coding in the visual cortex: A functional interpretation of some extra-classical receptive-field effects. Nature Neuroscience, 2(1), 79–87. https://doi.org/10.1038/4580

145. Rayner, K. (1998). Eye movements in reading and information processing: 20 years of research. Psychological Bulletin, 124(3), 372–422. https://doi.org/10.1037/0033-2909.124.3.372

146. Redington, M., & Chater, N. (1996). Transfer in artificial grammar learning: A reevaluation. Journal of Experimental Psychology: General, 125(2), 123–138. https://doi.org/10.1037/0096-3445.125.2.123

147. Regan, D., & Beverley, K. I. (1985). Postadaptation orientation discrimination. Journal of the Optical Society of America. A, Optics and Image Science, 2(2), 147–155. https://doi.org/10.1364/JOSAA.2.000147

148. Repp, B. H., & Penel, A. (2002). Auditory dominance in temporal processing: New evidence from synchronization with simultaneous visual and auditory sequences. Journal of Experimental Psychology. Human Perception and Performance, 28(5), 1085–1099. https://doi.org/10.1037/0096-1523.28.5.1085

149. Richter, D., & de Lange, F. P. (2019). Statistical learning attenuates visual activity only for attended stimuli. eLife, 8, e47869. https://doi.org/10.7554/eLife.47869

150. Richter, D., Ekman, M., & de Lange, F. P. (2018). Suppressed Sensory Response to Predictable Object Stimuli throughout the Ventral Visual Stream. Journal of Neuroscience, 38(34), 7452–7461. https://doi.org/10.1523/JNEUROSCI.3421-17.2018

151. Riley, M. R., & Constantinidis, C. (2016). Role of Prefrontal Persistent Activity in Working Memory. Frontiers in Systems Neuroscience, 9, 181. https://doi.org/10.3389/fnsys.2015.00181

152. Robinson, D. A. (1964). The mechanics of human saccadic eye movement. The Journal of Physiology, 174(2), 245–264. https://doi.org/10.1113/jphysiol.1964.sp007485

153. Rolfs, M. (2015). Attention in Active Vision: A Perspective on Perceptual Continuity Across Saccades. Perception, 44(8–9), 900–919. https://doi.org/10.1177/0301006615594965

154. Rolfs, M., Jonikaitis, D., Deubel, H., & Cavanagh, P. (2011). Predictive remapping of attention across eye movements. Nature Neuroscience, 14(2), 252–256. https://doi.org/10.1038/nn.2711

155. Saffran, J. R. (2002). Constraints on Statistical Language Learning. Journal of Memory and Language, 47(1), 172–196. https://doi.org/10.1006/jmla.2001.2839

156. Saffran, J. R., & Thiessen, E. D. (2008). Domain-General Learning Capacities. In Blackwell Handbook of Language Development (pp. 68–86). John Wiley & Sons, Ltd. https://doi.org/10.1002/9780470757833.ch4

157. Savitzky, Abraham., & Golay, M. J. E. (1964). Smoothing and Differentiation of Data by Simplified Least Squares Procedures. Analytical Chemistry, 36(8), 1627–1639. https://doi.org/10.1021/ac60214a047

158. Schapiro, A. C., Gregory, E., Landau, B., McCloskey, M., & Turk-Browne, N. B. (2014). The necessity of the medial temporal lobe for statistical learning. Journal of Cognitive Neuroscience, 26(8), 1736–1747. https://doi.org/10.1162/jocn_a_00578

159. Schapiro, A. C., Turk-Browne, N. B., Botvinick, M. M., & Norman, K. A. (2017). Complementary learning systems within the hippocampus: A neural network modelling approach to reconciling episodic memory with statistical learning. Philosophical Transactions of the Royal Society of London. Series B, Biological Sciences, 372(1711). https://doi.org/10.1098/rstb.2016.0049

160. Schwartz, O., Hsu, A., & Dayan, P. (2007). Space and time in visual context. Nature Reviews Neuroscience, 8(7), 522–535. https://doi.org/10.1038/nrn2155

161. Serences, J. T. (2016). Neural mechanisms of information storage in visual short-term memory. Vision Research, 128, 53–67. https://doi.org/10.1016/j.visres.2016.09.010

162. Serences, J. T., Ester, E. F., Vogel, E. K., & Awh, E. (2009). Stimulus-Specific Delay Activity in Human Primary Visual Cortex. Psychological Science, 20(2), 207–214. https://doi.org/10.1111/j.1467-9280.2009.02276.x

163. Siegelman, N., Bogaerts, L., Christiansen, M. H., & Frost, R. (2017). Towards a theory of individual differences in statistical learning. Philosophical Transactions of the Royal Society B: Biological Sciences, 372(1711), 20160059. https://doi.org/10.1098/rstb.2016.0059

164. Simons, D. J., & Rensink, R. A. (2005). Change blindness: Past, present, and future. Trends in Cognitive Sciences, 9(1), 16–20. https://doi.org/10.1016/j.tics.2004.11.006

165. Sligte, I., Mulder, K., Zerr, P., Stigchel, S. V. der, Gayet, S., & Pinto, Y. (2017). Remapping high-capacity, pre-attentive, fragile sensory memory. Scientific Reports, 7(1), 15940. https://doi.org/10.1038/s41598-017-16156-0

166. Smith, S. M., Jenkinson, M., Woolrich, M. W., Beckmann, C. F., Behrens, T. E. J., Johansen-Berg, H., Bannister, P. R., De Luca, M., Drobnjak, I., Flitney, D. E., Niazy, R. K., Saunders, J., Vickers, J., Zhang, Y., De Stefano, N., Brady, J. M., & Matthews, P. M. (2004). Advances in functional and structural MR image analysis and implementation as FSL. NeuroImage, 23, S208–S219. https://doi.org/10.1016/j.neuroimage.2004.07.051

167. Snowden, R. J., Thompson, P., & Troscianko, T. (2011). Basic vision: An introduction to

visual perception. Oxford University Press.

168. Sommer, M. A., & Wurtz, R. H. (2006). Influence of the thalamus on spatial visual processing in frontal cortex. Nature, 444(7117), 374–377. https://doi.org/10.1038/nature05279

169. Sperry, R. W. (1950). Neural basis of the spontaneous optokinetic response produced by visual inversion. Journal of Comparative and Physiological Psychology, 43(6), 482–489. https://doi.org/10.1037/h0055479

170. Sreenivasan, K. K., Curtis, C. E., & D'Esposito, M. (2014). Revisiting the role of persistent neural activity during working memory. Trends in Cognitive Sciences, 18(2), 82–89. https://doi.org/10.1016/j.tics.2013.12.001

171. Sterzer, P., Frith, C., & Petrovic, P. (2008). Believing is seeing: Expectations alter visual awareness. Current Biology, 18(16), R697–R698. https://doi.org/10.1016/j.cub.2008.06.021

172. Stokes, M. G. (2015). 'Activity-silent' working memory in prefrontal cortex: A dynamic coding framework. Trends in Cognitive Sciences, 19(7), 394–405. https://doi.org/10.1016/j.tics.2015.05.004

173. Summerfield, C., & de Lange, F. P. (2014). Expectation in perceptual decision making: Neural and computational mechanisms. Nature Reviews Neuroscience, 15(11), nrn3838. https://doi.org/10.1038/nrn3838

174. Summerfield, C., & Egner, T. (2009). Expectation (and attention) in visual cognition. Trends in Cognitive Sciences, 13(9), 403–409. https://doi.org/10.1016/j.tics.2009.06.003

175. Summerfield, C., Trittschuh, E. H., Monti, J. M., Mesulam, M.-M., & Egner, T. (2008). Neural repetition suppression reflects fulfilled perceptual expectations. Nature Neuroscience, 11(9), 1004–1006. https://doi.org/10.1038/nn.2163

176. Tobia, M. J., Iacovella, V., Davis, B., & Hasson, U. (2012). Neural systems mediating recognition of changes in statistical regularities. NeuroImage, 63(3), 1730–1742. https://doi.org/10.1016/j.neuroimage.2012.08.017

177. Tobia, M. J., Iacovella, V., & Hasson, U. (2012). Multiple sensitivity profiles to diversity and transition structure in non-stationary input. NeuroImage, 60(2), 991–1005. https://doi.org/10.1016/j.neuroimage.2012.01.041

178. Todd, J. J., & Marois, R. (2004). Capacity limit of visual short-term memory in human posterior parietal cortex. Nature, 428(6984), 751–754. https://doi.org/10.1038/nature02466

179. Todorovic, A., Ede, F. van, Maris, E., & de Lange, F. P. (2011). Prior Expectation Mediates Neural Adaptation to Repeated Sounds in the Auditory Cortex: An MEG Study. Journal of Neuroscience, 31(25), 9118–9123. https://doi.org/10.1523/JNEUROSCI.1425-11.2011

180. Tolias, A. S., Moore, T., Smirnakis, S. M., Tehovnik, E. J., Siapas, A. G., & Schiller, P. H. (2001). Eye Movements Modulate Visual Receptive Fields of V4 Neurons. Neuron, 29(3), 757–767. https://doi.org/10.1016/S0896-6273(01)00250-1

181. Toro, J. M., & Trobalón, J. B. (2005). Statistical computations over a speech stream in a rodent. Perception & Psychophysics, 67(5), 867–875. https://doi.org/10.3758/bf03193539

182. Tremblay, P., Baroni, M., & Hasson, U. (2013). Processing of speech and non-speech sounds in the supratemporal plane: Auditory input preference does not predict sensitivity to statistical structure. NeuroImage, 66, 318–332. https://doi.org/10.1016/j.neuroimage.2012.10.055

183. Tunney, R. J., & Altmann, G. T. M. (1999). The transfer effect in artificial grammar learning: Reappraising the evidence on the transfer of sequential dependencies. Journal of Experimental Psychology: Learning, Memory, and Cognition, 25(5), 1322–1333. https://doi.org/10.1037/0278-7393.25.5.1322

184. Turk-Browne, N. B., & Scholl, B. J. (2009). Flexible visual statistical learning: Transfer across space and time. Journal of Experimental Psychology: Human Perception and Performance, 35(1), 195–202. https://doi.org/10.1037/0096-1523.35.1.195

185. Turk-Browne, N. B., Scholl, B. J., Chun, M. M., & Johnson, M. K. (2009). Neural evidence of statistical learning: Efficient detection of visual regularities without awareness. Journal of Cognitive Neuroscience, 21(10), 1934–1945. https://doi.org/10.1162/jocn.2009.21131

186. Turk-Browne, N. B., Scholl, B. J., Johnson, M. K., & Chun, M. M. (2010). Implicit perceptual anticipation triggered by statistical learning. The Journal of Neuroscience: The Official Journal of the Society for Neuroscience, 30(33), 11177–11187. https://doi.org/10.1523/JNEUROSCI.0858-10.2010

187. Umeno, M. M., & Goldberg, M. E. (1997). Spatial Processing in the Monkey Frontal Eye Field. I. Predictive Visual Responses. Journal of Neurophysiology, 78(3), 1373–1383. https://doi.org/10.1152/jn.1997.78.3.1373

188. Walker, M. F., Fitzgibbon, E. J., & Goldberg, M. E. (1995). Neurons in the monkey superior colliculus predict the visual result of impending saccadic eye movements. Journal of Neurophysiology, 73(5), 1988–2003. https://doi.org/10.1152/jn.1995.73.5.1988

189. Wandell, B. A., Dumoulin, S. O., & Brewer, A. A. (2007). Visual Field Maps in Human Cortex. Neuron, 56(2), 366–383. https://doi.org/10.1016/j.neuron.2007.10.012

190. Wang, L., Mruczek, R. E. B., Arcaro, M. J., & Kastner, S. (2015). Probabilistic Maps of Visual Topography in Human Cortex. Cerebral Cortex, 25(10), 3911–3931. https://doi.org/10.1093/cercor/bhu277

191. Watson, A. B., & Pelli, D. G. (1983). Quest: A Bayesian adaptive psychometric method. Perception & Psychophysics, 33(2), 113–120. https://doi.org/10.3758/BF03202828

192. Wenderoth, P., & Wiese, M. (2008). Retinotopic encoding of the direction aftereffect. Vision Research, 48(19), 1949–1954. https://doi.org/10.1016/j.visres.2008.06.013

193. Williams, M. A., Baker, C. I., Op de Beeck, H. P., Mok Shim, W., Dang, S., Triantafyllou, C., & Kanwisher, N. (2008). Feedback of visual object information to foveal retinotopic cortex. Nature Neuroscience, 11(12), 1439–1445. https://doi.org/10.1038/nn.2218

194. Wittenberg, M., Bremmer, F., & Wachtler, T. (2008). Perceptual evidence for saccadic updating of color stimuli. Journal of Vision, 8(14), 9–9. https://doi.org/10.1167/8.14.9

195. Wolf, C., & Schütz, A. C. (2015). Trans-saccadic integration of peripheral and foveal feature information is close to optimal. Journal of Vision, 15(16), 1–1. https://doi.org/10.1167/15.16.1

196. Wolfe, B. A., & Whitney, D. (2015). Saccadic remapping of object-selective information. Attention, Perception, & Psychophysics, 77(7), 2260–2269. https://doi.org/10.3758/s13414-015-0944-z

197. Wolff, M. J., Jochim, J., Akyürek, E. G., & Stokes, M. G. (2017). Dynamic hidden states underlying working-memory-guided behavior. Nature Neuroscience, 20(6), 864–871. https://doi.org/10.1038/nn.4546

198. Wurtz, R. H. (2008). Neuronal mechanisms of visual stability. Vision Research, 48(20), 2070–2089. https://doi.org/10.1016/j.visres.2008.03.021

199. Xu, Y. (2017). Reevaluating the Sensory Account of Visual Working Memory Storage. Trends in Cognitive Sciences, 21(10), 794–815. https://doi.org/10.1016/j.tics.2017.06.013

200. Xu, Y. (2018). Sensory Cortex Is Nonessential in Working Memory Storage. Trends in Cognitive Sciences, 22(3), 192–193. https://doi.org/10.1016/j.tics.2017.12.008

201. Zimmermann, E., Morrone, M. C., Fink, G. R., & Burr, D. (2013). Spatiotopic neural representations develop slowly across saccades. Current Biology, 23(5), R193–R194. https://doi.org/10.1016/j.cub.2013.01.065

202. Zimmermann, E., Weidner, R., Abdollahi, R. O., & Fink, G. R. (2016). Spatiotopic Adaptation in Visual Areas. The Journal of Neuroscience, 36(37), 9526–9534. https://doi.org/10.1523/JNEUROSCI.0052-16.2016

203. Zimmermann, E., Weidner, R., & Fink, G. R. (2017). Spatiotopic updating of visual feature information. Journal of Vision, 17(12), 6–6. https://doi.org/10.1167/17.12.6

204. Zirnsak, M., Gerhards, R. G. K., Kiani, R., Lappe, M., & Hamker, F. H. (2011). Anticipatory Saccade Target Processing and the Presaccadic Transfer of Visual Features. Journal of Neuroscience, 31(49), 17887–17891. https://doi.org/10.1523/JNEUROSCI.2465-11.2011

205. Zirnsak, M., & Moore, T. (2014). Saccades and shifting receptive fields: Anticipating consequences or selecting targets? Trends in Cognitive Sciences, 18(12), 621–628. https://doi.org/10.1016/j.tics.2014.10.002

206. Zirnsak, M., Steinmetz, N. A., Noudoost, B., Xu, K. Z., & Moore, T. (2014). Visual space is compressed in prefrontal cortex before eye movements. Nature, 507(7493), 504–507. https://doi.org/10.1038/nature13149

NEDERLANDSE SAMENVATTING

Visuele input is de meest essentiële informatie voor de mens. Terwijl andere dieren, zoals honden, vooral vertrouwen op hun reukzin, zijn mensen ongetwijfeld visuele wezens. Als we onze ogen openen worden we voortdurend gebombardeerd met een enorme hoeveelheid visuele informatie die van de ogen naar de hersenen stroomt. Wanneer we echter precies dezelfde fysieke visuele stimuli in de wereld ervaren, kunnen mensen deze toch waarnemen als verschillend. Hoewel de camera vaak wordt gezien als een metafoor voor het menselijk zicht, is er een essentieel verschil: onze visuele waarneming is selectief en subjectief, terwijl een camera dat niet is. Dit subjectieve karakter van visuele waarneming is zelfs een van de meest intrigerende facetten ervan. De visuele waarneming is dus niet alleen afhankelijk van de zintuiglijke input, maar ook van de interne toestand van de hersenen.

Voorspellingen zijn een belangrijke bron die de interne status van iemands hersenen bepaalt. Ze weerspiegelen voorkennis over wat er waarschijnlijk in de omgeving zal gebeuren. Als we bijvoorbeeld in een drukke straat op een vriend wachten, hebben we voorkennis over de kenmerken van de vriend. Dit soort voorkennis kan de visuele waarneming op veel verschillende manieren sterk moduleren. Omdat onze zintuiglijke informatie vaak inherent dubbelzinnig is als gevolg van occlusie, verschillende standpunten, etc., kunnen voorspellingen onze perceptie van de wereld beïnvloeden en zo ambigue informatie interpreteren. Zo kan de interpretatie van een gegeven waarneming ('Is dit een haardroger of een boor?') worden gestuurd door contextuele waarschijnlijkheden ('Ben ik in de badkamer of in de garage?').

Voorspellende verwerking is ook relevant in de context van oogbewegingen. Bij het voorbereiden van een snelle oogbeweging, ofwel saccade, naar een locatie waarin we geïnteresseerd zijn, moeten onze hersenen de vector van deze saccade (bijv. richting, lengte) al kennen voordat deze wordt uitgevoerd. Om de visuele stabiliteit over de saccades heen te ondersteunen wordt gebruik gemaakt van voorspellingen over de oogbeweging en het doelwit op basis van de perceptie van de toekomstige doelwitten. Ons brein wordt dan ook wel vergeleken met een 'voorspellingsmachine' die actief interne modellen construeert om binnenkomende visuele input te interpreteren met behulp van top-down voorspellingen. In dit proefschrift heb ik twee verschillende vormen van voorspelbaarheid onderzocht die door het visuele systeem worden

uitgebuit om de waarneming te ondersteunen. Ik zal me in het bijzonder richten op twee belangrijke onderzoeksgebieden: (1) voorspellende "remapping" over de oogbewegingen heen om de visuele stabiliteit te behouden; (2) voorafgaande context die voortkomt uit voorwaardelijke waarschijnlijkheden.

Hoofdstuk 2 gaat over voorspellingen van visuele input in afwachting van oogbewegingen. Hoewel we allemaal onze waarneming als stabiel en continu ervaren, geldt dit eigenlijk niet voor onze visuele input. Eerder onderzoek heeft uitgewezen dat voorspellende remapping een mechanisme zou kunnen zijn dat bijdraagt aan de visuele stabiliteit. Er is echter nog steeds een intensief debat gaande over de vraag of en hoe informatie over elementen van een stimulus (feature informatie) geremapt wordt voorafgaand aan de saccades. In dit project hebben we robuust bewijs gevonden voor het voorspellen van het remappen van functie-informatie vlak voor een oogbeweging. Belangrijk is dat we de geremapte feature informatie alleen hebben geobserveerd voor de stimulus die kort voor het begin van de saccade wordt gepresenteerd, maar geen remapping van de adaptatie - een eerder geziene adaptor en de gevolgen daarvan. Samen suggereren deze bevindingen dat voorspellende feature remapping belangrijk is voor het behalen van visuele stabiliteit.

Ook in hoofdstuk 3 heb ik het remappen onderzocht - niet van verwachte visuele input, maar van intern opgeslagen visuele werkgeheugen representaties. We hebben laten zien dat informatie van visuele objecten kan worden geremapt tussen oogposities. Het is echter nog onduidelijk of saccadische remapping ook optreedt voor stimuli die niet in ons visuele veld aanwezig zijn, maar die in het werkgeheugen worden opgeslagen. Dit is ook een veel voorkomende situatie in het dagelijks leven. Zo moeten we bijvoorbeeld het uiterlijk van een vriend in gedachten houden terwijl we onze ogen voortdurend naar verschillende locaties verplaatsen wanneer we de vriend op een station zoeken. We vonden informatie uit het werkgeheugen in zowel de vroege visuele cortex als de pariëtale cortex. Deze informatie in de vroege visuele cortex werd gedegradeerd door de oogbeweging tijdens de bewaarperiode. We hebben echter geen bewijs gevonden voor het overzetten van het werkgeheugen na deze saccade. Deze resultaten tonen aan dat het werkgeheugen in een stationele stijl wordt opgeslagen en dat de vroege visuele cortex geen optimaal gebied is voor opslag.

In hoofdstuk 4 heb ik me gericht op een andere vorm van voorspelbaarheid, namelijk de voorafgaande context. De context kan worden gedefinieerd zowel in de dimensie tijd (het rode licht wordt bijvoorbeeld gevolgd door het groene licht in een verkeerslicht) als de dimensies ruimte (een tafellamp staat bijvoorbeeld naast een computermonitor op het bureau). In dit hoofdstuk heb ik de effecten van ruimtelijke en temporele context op de waarneming onderzocht. Hoewel we al weten dat verwachtingen de neurale reacties in de hersenen kunnen moduleren - verwachte stimuli leiden tot een verzwakte neurale respons - is deze verwachtingsonderdrukking nog niet onderzocht op het neurale niveau voor ruimtelijke regelmatigheden. In dit hoofdstuk vonden we een betrouwbare en wijdverspreide onderdrukking van neurale reacties op ruimtelijk verwachte stimuli in vergelijking met onverwachte stimuli, wat kan worden beschouwd als de neurale handtekening van ruimtelijke contextverwachtingen. Daarnaast vonden we ook dat soortgelijke hersengebieden werden geactiveerd voor zowel temporele als ruimtelijke context schendingen, wat suggereert dat analoge neurale mechanismen ten grondslag liggen aan verwachtingen door temporele en ruimtelijke context.

Tot slot heb ik in hoofdstuk 5 alle empirische bevindingen samengevat en hun relevantie voor ons begrip van voorspellingen in de hersenen besproken. Het proefschrift eindigt met een algemene discussie over de implicaties van het gepresenteerde onderzoek.

ACKNOWLEDGEMENTS

How time flies! It feels like an instant that I already come to the end of my PhD journey. Doing a PhD is more like a marathon, which is full of difficulties and frustrations. However, I couldn't have wished for a better environment to do it in my current lab at Donders Institute. This project would not have been possible without the help of many invaluable people surrounding me. Here I would like to take this opportunity to express my sincere gratitude to all of them.

First and foremost, there are no proper words to convey my deep gratitude and respect for my supervisor, Prof. Floris de Lange. Floris, thanks for your encouragement and support no matter when I was caught in trouble, you are the most influential person in my academic career. You have inspired me to become an independent researcher and helped me realize the power of critical reasoning. I also really appreciate your easygoing but responsible personality, I never had a sense of distance between you and me, alternatively, I felt you always do your best to care for me and the other members in your group. If I say I was full of uncertainty about the future four years ago before I came to the Netherlands, now I can proudly say that I feel so lucky to meet with you, even from the first time I entered your office.

My sincere thanks must also go to the members of my daily supervisor and collaborators. Matthias E., thanks for your time to offer me valuable comments toward improving my work. You helped me open the door in the field of neuroscience, I am most grateful for you lending me your expertise to my scientific and technical problems. Annelinde, thanks for your sustained support both in and outside of academia, despite we only overlapped for a short time period, you always being there no matter how busy life was. Matthias F., thanks for your help during the first year of my PhD, thank you for your insightful discussions in my first PhD project, whenever I came to you, you never let me down. David, you are such a productive person, thanks for your substantial contribution to uplift the studies of my last PhD project, without your help, this project cannot move so quickly and smoothly. I am delighted to have worked with all of you and I look forward to working with you again.

Chuyao, we are old friends since the Master's programme in China, I'm grateful to meet you again in the same group in the Netherlands. Thanks for your discussion on the project as well as

fun during spare time, I hope you'll have a successful completion of your PhD next year. Kirsten, you are the most genius and highly motivated Master student that I have ever met. Thanks for your proofreading of the manuscript of this PhD thesis, I was deeply impressed by your carefulness and hardworking. I'm proud to have been your daily supervisor during your master's thesis. Ella, thank you for your proofreading of the Dutch summary, which magically making that raw, machine-translated text to be one that real humans can read and understand.

There is no way to express how much it meant to me to have been a member of Predictive Brain Lab. These brilliant friends and colleagues inspired me over the years: Benedikt, Ambra, Christoph, Ashley, Eelke, Alya, Kim, Alla, Floortje, Micha, Lieke, Mariya, Patricia, Joey, Karolis, Kirsten, Jorie, Alexis, Christian, Biao, Pim, Claudia, Erik, Annelinde, Anke Marit. All of your comments, questions as well as discussions in the group meeting deeply shaped my vision of doing science. While outside the science, I enjoyed the summer BBQ, Sinterklaas evening, group lunch and all other fun group activities.

Special thanks to my officemates Wei, Kristijan, Iva, Iris, Felix, Cagatay and Laura, who provided me with a friendly and inspiring environment to work and have fun. Wish you all the best.

To my neighborhood: Chunling, Lan, Manxia, Quan, Yanan, Fan, Shuang, Keyang, Ting, Han, Yulong, Yongxia, thanks for your chatting and happy dinner time. To my other friends and Chinese colleagues: Qi, Chao, Jinbiao, Chunan, Huan, Xiaochen, Bohan, Xiaojing, Rui, Xu, Xuyan, Zhen, Yuxi, Weibin, thanks for all of your supports in the past few years.

I am greatly indebted to my two ceremonial assistants – Chuyao and Ting – who made the last months of my PhD run safe and sound. This 4-year PhD journey would not have been possible without the financial support of China Scholarship Council (CSC), to whom I am sincerely grateful. The administrative staffs in the DCCN are memorable not only for their prompt support but also for kind care. I have especially benefited from the truly professional support from the technical groups.

The work presented in this thesis has been critically assessed and approved by an outstanding committee to whom I am more than grateful: Prof. Pieter Medendorp, Prof. Zhaoping Li, Prof. Stefan van der Stigchel. Hartelijk dank (Thank you)!

Mingmei, thank you for your firm support. You have said you will accompany me wherever I'll go, I could not imagine how I would finish the PhD journey without your companionship. I would also like to say a heartfelt thank you to my parents, elder sisters, grandparents and uncle. Thank you for all of your unconditional love and encouragement, which has been a great source of happiness to me during challenging times. Thank you for my parents' sacrifice in my education and research. Thank you for my grandparents for giving me wholehearted love without return, for believing in me when I didn't, and most importantly for instilling and nurturing a childhood dream of becoming a scientist deep in my heart.

CURRICULUM VITAE

Tao He was born on September 5th, 1991 in Suzhou, Anhui province, China. Although he originally intended to study clinical medicine and become a doctor in the future, fate played a small joke on him, he enrolled in the University and studied Psychology. In 2013, he obtained a Bachelor diploma (with distinction) at Fujian Medical University in China, with a major in Psychology. Although now he had the chance to work as a mental doctor, he realized cognitive neuroscience was more appealing to him. He then decided to study research master Clinical Cognitive Neuroscience supervised by Dr. Zhiguo Wang at Hangzhou Normal University. It was during this time that he opened the new door to neuroscience research and was fascinated by human visual perception study. He obtained his master's degree (with distinction) in 2016 and decided to apply for a PhD programme.

In the same year, he received a scholarship from China Scholarship Council (CSC) to pursue a PhD under the supervision of Prof. dr. Floris de Lange at the Donders Institute for Brain, Cognition and Behavior at Radboud University, the Netherlands. In his PhD project, he mainly focused on different forms of predictability on both visual perception and working memory using fMRI and eye-tracking. During this period, he additionally supervised master student, organized lab retreat and gave a talk on Donders Discussion. Currently, he is working as a postdoctoral researcher in the group of Prof. dr. Fang Fang at Peking University.

PUBLICATION LIST

- He, T., Fritsche M., & de Lange FP. (2018). Predictive remapping of visual features beyond saccadic targets. *Journal of Vision*, 18(13), 20-20.

- Ding, Y., Zhao, J., He, T., Tan, Y., Zheng, L., Zhang, X., & Wang, Z. (2016). Selective impairment of covert attention in Chinese dyslexic children. *Dyslexia*, 22(4), 362-378.

- Yan C., He T., Raymond M. Klein & Wang Z. (2016). Predictive remapping gives rise to inhibition of return in environment-centered coordinates. *Psychonomic Bulletin & Review*, 23(6): 1860-1866.

- Ding, Y., He, T., & Wang, Z. (2016). Inhibitory cueing effects following manual and saccadic responses to arrow cues. *Attention, Perception & Psychophysics*, 78(4): 1020–1029.

- He, T., Ding, Y., & Wang, Z. (2015). Environment- and eye-centered inhibitory cueing effects are both observed after a methodological confound is eliminated. *Scientific Reports*, 5, 16586.

- He, T., & Wang, Z. (2015). Spatiotopic, retinotopic, and object-centered reference frames of inhibition of return. *Journal of Psychological Science* (in Chinese), 38 (4): 813 - 821.

- He, T., Ekman M., Vandenbroucke A., & de Lange FP. Visual working memory representations in visual and parietal cortex do not remap after eye movements. *Under review*.

- He, T., Richter D., Wang Z., & de Lange FP. Suppression of predictable stimuli following statistical learning of spatial context throughout the ventral visual stream. *Under review*.

DONDERS GRADUATE SCHOOL FOR COGNITIVE NEUROSCIENCE

For a successful research Institute, it is vital to train the next generation of young scientists. To achieve this goal, the Donders Institute for Brain, Cognition and Behaviour established the Donders Graduate School for Cognitive Neuroscience (DGCN), which was officially recognized as a national graduate school in 2009. The Graduate School covers training at both Master's and PhD level and provides an excellent educational context fully aligned with the research programme of the Donders Institute.

The school successfully attracts highly talented national and international students in biology, physics, psycholinguistics, psychology, behavioral science, medicine and related disciplines. Selective admission and assessment centers guarantee the enrolment of the best and most motivated students.

The DGCN tracks the career of PhD graduates carefully. More than 50% of PhD alumni show a continuation in academia with postdoc positions at top institutes worldwide, e.g. Stanford University, University of Oxford, University of Cambridge, UCL London, MPI Leipzig, Hanyang University in South Korea, NTNU Norway, University of Illinois, North Western University, Northeastern University in Boston, ETH Zürich, University of Vienna etc.. Positions outside academia spread among the following sectors: specialists in a medical environment, mainly in genetics, geriatrics, psychiatry and neurology. Specialists in a psychological environment, e.g. as specialist in neuropsychology, psychological diagnostics or therapy. Positions in higher education as coordinators or lecturers. A smaller percentage enters business as research consultants, analysts or head of research and development. Fewer graduates stay in a research environment as lab coordinators, technical support or policy advisors. Upcoming possibilities are positions in the IT sector and management position in pharmaceutical industry. In general, the PhDs graduates almost invariably continue with high-quality positions that play an important role in our knowledge economy.

For more information on the DGCN as well as past and upcoming defenses please visit: http://www.ru.nl/donders/graduate-school/phd/

RESEARCH DATA MANAGEMENT

This research followed the applicable laws and ethical guidelines. Research Data Management was conducted according to the FAIR principles. The paragraphs below specify in detail how this was achieved.

Ethics

This thesis is based on the results of human studies, which were approved by the Radboud University Institutional Review Board and were carried out in accordance with the guidelines expressed in the Declaration of Helsinki.

Findable Accessible

The table below details where the data and research documentation for each chapter can be found on the Donders Repository (DR). All data archived as a Data Sharing Collection remain available for at least10 years after termination of the studies.

Chapter	DAC	RDC	DSC	DSC License
2	https://doi.org/ 10.34973/wj3k-xr87	https://doi.org/ 10.34973/p77s-fd94	https://doi.org/ 10.34973/3mdw-jn48	RU-DI-HD-1.0
3	https://doi.org/ 10.34973/z4p7-4949	https://doi.org/ 10.34973/n8dh-7848	https://doi.org/ 10.34973/mkym-qw38	RU-DI-HD-1.0
4	https://doi.org/ 10.34973/3few-mk06	https://doi.org/ 10.34973/jarn-y957	https://doi.org/ 10.34973/agh7-4919	RU-DI-NH-1.0

DAC = Data Acquisition Collection, RDC = Research Documentation Collection, DSC = Data Sharing Collection

The article of chapter 3 and 4 are still under review. The data are currently shared with the reviewers in a DSC and will be made publicly available, once the article has been published. It will then be shared under the RU-DI-HD-1.0 license as it contains potentially identifiable data. Informed consent was obtained on paper following the Centre procedure.

Interoperable, Reusable

The raw data are stored in the DAC in their original form. For RDC and DSC long-lived file formats (e.g. .csv, .tif,) have been used ensuring that data remains usable in the future. Results are reproducible by providing a description of the experimental setup, raw data (DAC and DSC), analysis scripts or pipelines (RDC and DSC).

Privacy

The privacy of the participants in this thesis has been warranted using random individual subject codes. Data in chapters 2, 3 and 4 are not identifiable and shared without restrictions. MRI data of chapter 3 and 4 is shared under the restricted license RU-DI-HD-1.0.